NASA Contractor Report 178064

NASA-CR-178064
19860018618

INITIAL DESIGN and EVALUATION of AUTOMATIC RESTRUCTURABLE FLIGHT CONTROL SYSTEM CONCEPTS

Jerold L. Weiss, Douglas P. Looze, John S. Eterno, and Daniel B. Grunberg

ALPHATECH, Inc.
Burlington, Massachusetts

June 1986

Prepared for
NASA Langley Research Center
Under Contract NAS1-17411

National Aeronautics and
Space Administration

Langley Research Center
Hampton, Virginia 23665

CONTENTS

CONTENTS (Continued)

FIGURES

FIGURES (Continued)

TABLES

LIST OF SYMBOLS

A	Generic System Matrix
A_a	System Matrix for B737 Application
$\overline{A}$	Stable Factorization of A
$\tilde{A}$	Augmented System Matrix
A_2	Constraint Matrix for Second Subproblem in Trim
A_F	Final System Matrix for FCS Design
A_{GLOB}	Global System Matrix for FCS Design
A_{LAT}	Lateral Axis System Matrix
A_{LON}	Longitudinal Axis System Matrix
A_o	Nominal System Matrix for Control Law Design
A_p	System Submatrix for Plant States
b	Elements of Constraints Corresponding to All Active Constraints
b_L	Elements of Constraints Corresponding to Lower Active Constraints
b_U	Elements of Constraints Corresponding to Upper Active Constraints
B	Generic Control Matrix
$\tilde{B}$	Augmented Control Matrix
B_a	Control Matrix for B737 Application
B_f	Nominal Value of $\overline{B}_f$
$\overline{B}_f$	Failed Control Effectiveness Matrix
B_F	Final Control Matrix for FCS Design
B_{GLOB}	Global Control Matrix for FCS Design

B_{LAT} Lateral Axis Control Matrix

B_{LON} Longitudinal Axis Control Matrix

B_{MIX} Collective/Differential Mixing Matrix

B_o Nominal Control Matrix for Control Law Design

B_p Control Submatrix for Plant States

C Generic Output Matrix

C_I System Submatrix for Integrator States

C_{LAT} Lateral Axis Output Matrix

C_{LON} Longitudinal Axis Output Matrix

C_o Square Root of State Weighting Matrix for Control Law Design

C_N New State Weights for Redesign

d Vector in Generic Least Squares Problem

$\overline{d}$ Modified Value of d

$\hat{d}$ Effective d Used in Uncertain Trim Problem

d_n Nominal Value of d

d_s Scaled Version of d

D Set of Optimal Solutions to Feasible Trim

D(s) Return Difference Matrix

$\overline{D}(s)$ Failed Return Difference

$\hat{D}(s)$ Weighted Return Difference Matrix

E Error Matrix

E(•) Expected Value

f_F Failed System Function

f_o Nominal System Function

F Set of Feasible Solutions to Trim Problem

F Matrix in Generic Least Squares Problem <=== (2)

$\bar{F}$	Partition of F Corresponding to Inactive Constraints
$\hat{F}$	Effective F Used in Uncertain Trim Problem
F_c	Partition of F Corresponding to All Active Constraints
F_L	Partition of F Corresponding to Lower Active Constrains
F_n	Nominal Value of F
F_s	Scaled Version of F
F_U	Partition of F Corresponding to Upper Active Constraints
g	Constant Part of Cost Used in Uncertain Trim Problem
G	Generic Control Gain Matrix
G_F	Control Gains After Failure
G_{GLOB}	Global Control Gain Matrix for FCS Design
G_I	Control Submatrix Corresponding to Integrator States
G_{LT}	Lateral Axis Gain Matrix
G_o	Nominal Control Gain Matrix
G_r	Control Submatrix Corresponding to Non-Integrated States
G_y	Control Submatrix Corresponding to Integrated States
h_F	Failed Output Function
h_o	Nominal Output Function
H	Hamiltonian
H(s)	Frequency Weighting Matrix
I_f	Index Set of Inactive Constraints
I_L	Index Set of Active Lower Constraints
I_U	Index set of Active Upper Constraints
J_1	Cost for Feasible Sub-Problem
J_2	Cost for Infeasible Sub-Problem
$\bar{J}_2$	Modified Value of J_2

K	Solution of Riccati Equation
K_L	Scaling Constant
K_s	Scaling Constant
K_U	Scaling Constant
$L_c(s)$	Weighted Loop Transfer Function Matrix
$L_o(s)$	Loop Transfer Function Matrix
$L(s)$	General Loop Transfer Function Matrix
$L_w(s)$	Weighted Loop Transfer Function Matrix
m	Generic Dimension of the Control Vector
M_I	Columns of C for Integrator States
M_p	Columns of C for Plant States
n	Generic Dimension of the State Vector
N	Square Root of R_N
N_o	Square Root of Nominal Control Weighting Matrix
p	Generic Dimension of the Output Vector
p	Roll Rate, rad/sec <=== (2)
P	Step Direction
P	Control Loop Weighting Matrix for Bandwidth Constraints <=== (2)
P	Permutation Matrix for Nominal Control System Design <=== (3)
q	Pitch Rate, rad/sec
Q	Generic State Weighting Matrix
Q_F	Covariance of ΔF in Trim Problem
Q_F	Final State Weight Matrix for FCS Design <=== (2)
Q_{GLOB}	Global State Weighting Matrix for FCS Design
Q_I	State Weights for Integrator States
Q_{LAT}	Lateral Axis State Weights

Q_{LON}	Longitudinal Axis State Weights
Q_o	Nominal State Weights
Q_p	State Weights for Plant States
Q_{PI}	Cross State Weights for Integrator and Plant States
r	Yaw Rate, rad/sec
r	Reference Input <=== (2)
R	Generic Control Weighting Matrix
R_d	Covariance of Δd
R_F	Final Control Weight Matrix for FCS Design
R_{GLOB}	Global Control Weighting Matrix for FCS Design
R_{LON}	Longitudinal Axis Control Weights
R^n	Denotes the Vector Space of n-dimensional Real Numbers
R_N	New Control Weights for Redesign
R_o	Nominal Control Weighting Matrix for Control Law Design
S	Singular Value Matrix
S_1	Non-Zero Singular Value Matrix
S_1	Weights for Control Design <=== (2)
S_d	Scaling Matrix for d
S_L	Selection Matrix for Lower Constraints
S(s)	Sensitivity Matrix
S_U	Selection Matrix for Upper Constraints
S_Z	Scaling Matrix for Z
T_1	State Weights for Control Design
u	Generic Control Vector
u	Forward Velocity, ft/sec <=== (2)
u_a	Control Vector for B737 Application

u_F Steady State Failure Response of Control

u_F^T Feed Forward Control to Reject Disturbances

u_L Lower Constraint on u

u_n Nominal (Unfailed) Trim Values of Controls

u_{new} Control Vector of Collective and Differential Controls

u_o Trim Value of u

u_p Perturbed Control Vector

u_r Feedforward Control From Pilot

u_r^F Feedforward From Pilot After Failure

u_T Trim Value of u

u_U Upper Constraint on u

U Left Singular Vector Matrix

U_1 Sub Matrix of Left Singular Vectors

U_2 Sub Matrix of Left Singular Vectors

v Side Velocity, ft/sec

V Right Singular Vector Matrix

V_1 Sub Matrix of Right Singular Vectors

V_2 Sub Matrix of Right Singular Vectors

V_s Right Singular Vectors of A_o Corresponding to Stable Eigenvalues

V_u Right Singular Vectors of A_o Corresponding to Unstable Eigenvalues

w_p Perturbed Disturbance Vector

w Disturbance Due to Failure

w Vertical Velocity, ft/sec <=== (2)

W Controlability Minus Uncertainty Grammian

W_{co} Controllability - Observability Grammian

W_o Observability Grammian

$\bar{W}_o$ Frequency Integral in Control Redesign Problem

W_s Left Singular Vectors of A_o Corresponding to Stable Eigenvalues

$W(s)$ Frequency Weighting Matrix

W_u Left Singular Vectors of A_o Corresponding to Unstable Eigenvalues

W_u Uncertainty Grammian <=== (2)

x Generic State Vector

$\dot{x}$ • Denotes Derivative With Respect to Time

x_a State Vector for B737 Application

x_{aug} Augmented State Including Integrators for FCS Design

x_F Steady State Failure Response of State

x_I State Vector of Integrator States

x_{Io} Trim Value of x_I

x_n Nominal (Unfailed) Trim Values of States

x_o Trim Value of x

x_p Perturbed State Vector

x_r States Without Integrators in Control Law

x_U Upper Constraint on x

y Generic Output Vector

y_d Desired Value of y

y_p Perturbed Output Vector

x_L Lower Constraint on x

x_T Trim Value of x

z Generic Augmented Vector

$\hat{z}$ Updated Solution Iterate

$\bar{z}$ Non-Optimal, Feasible Z

z_f Elements of Z Corresponding to Inactive Constraints

z_k k-th Iterate

z_L Lower Constraint on Z

z_s Scaled Version of Z

z_U Upper Constraint on Z

α Angle of Attack

$\beta_{ijk\ell}$ Cross Covariance Between Elements of $\overline{B}_f$

γ Flight Path Angle

δCA Collective Aileron

δ_{CE} Collector Elevator

δ_{CS} Collective Stabilator

δ_{CT} Collective Thrust

δ_{DA} Differential Aileron

δ_{DE} Differential Elevator

δ_{DS} Differential Stabilator

δ_{DT} Differential Thrust

δ_{LA} Left Aileron, deg

δ_{LE} Left Elevator, deg

δ_{LS} Left Stabilator, deg

δ_{LT} Left Engine Thrust, lbs

δ_R Rudder, deg

δ_{RA} Right Aileron, deg

δ_{RE} Right Elevator, deg

δ_{RS} Right Stabilator, deg

δ_{RT} Right Engine Thrust, lbs

ΔB Uncertainty about B_f

Δd	Uncertainty About d
ΔF	Uncertainty About F
Δz	Solution Variable for Second Subproblem in Trim
ζ	Unmeasurable Disturbance Vector
θ	Pitch Angle, rad
λ_1	Lagrange Multipliers
λ_2	Lagrange Multipliers for Second Subproblem in Trim
λ_{2L}	Lagrange Multipliers for Second Subproblem in Trim
λ_{2U}	Lagrange Multipliers for Second Subproblem in Trim
λ_F	Lagrange Multipliers for Second Subproblem in Trim
λ_L	Lagrange Multipliers for Lower Active Constraints
λ_U	Lagrange Multipliers for Upper Active Constraints
Λ_s	Diagonal Matrix of Stable Eigenvalues
Λ_u	Diagonal Matrix of Unstable Eigenvalues
ϕ	Roll Angle, rad
ω	Natural Frequency
ω_c	Natural Frequency for Evaluating Bandwidth Constraints
$*$	Denotes Optimal Value
$\|\cdot\|$	Denotes Generic Norm
$(\ )^i$	i-th Element of the Vector in Parentheses
$(\cdot)^H$	Complex Conjugate Transpose
$(\cdot)^\#$	Denotes Pseudo-Inverse

SECTION 1

INTRODUCTION

This report presents the results of a two-year effort sponsored by the NASA Langley Research Center under contract NAS1-17411 to develop automatic control design procedures for restructurable aircraft control systems. The restructurable aircraft control problem involves designing a fault tolerant control system which can accommodate a wide variety of unanticipated aircraft failures. Under NASA sponsorship, ALPHATECH has been developing and testing many of the technologies which make such a system possible. Future work under this contract will focus on developing a methodology for integrating these technologies and demonstration of a complete system.

The automatic control design procedure developed during the first year of this project [1]* assumes that failures are correctly detected and identified and makes use of feedforward and feedback controls to stabilize the aircraft and recover as much dynamic performance as is possible. The objectives of the work reported herein are to (1) thoroughly test the feedback control redesign procedure under a variety of failure conditions and (2) complete development of an automatic feedforward "trim" algorithm.

This project was divided into three tasks. Task 1 involved performing a complete linearized analysis of the feedback control redesign procedure for the Boeing 737 aircraft. This included examination of eigenvalues, singular

*References are indicated by numbers in square brackets; the list appears at the end of of this report.

values and linear simulations for a variety of failure and control redesign options. Task 2 was aimed at examining the performance of the various elements of the overall control redesign procedure on NASA Langley Research Center's nonlinear simulation. Finally, Task 3 completed development of an algorithm to automatically trim the aircraft with feedforward control and developed the integrated control system redesign procedure.

1.1 BACKGROUND

As aircraft become increasingly sophisticated, and as static stability is decreased in the interests of efficiency and maneuverability, the potential damage caused by unanticipated failure increases dramatically. Although pilots can be trained to react in the case of anticipated major failures, they cannot be expected to respond correctly, and in time, for all conceivable failures. This is particularly frustrating because modern aircraft, with complex controls, may remain controllable despite individual failures, as happened recently in two well publicized cases. In one case, (a Delta L1011 flight [2]) the pilot was able to reconfigure his available controls to save the plane. In another, (the Chicago DC10 crash [3]) the pilot could not, although hindsight revealed the plane could have been saved.

The objective of a restructurable control system is to automatically and quickly solve the control problem facing a pilot during an emergency. The class of problems of interest includes those where the failure or failures are unanticipated, but excludes those unsolvable areas (wings falling off) where the plane cannot be saved.

The general area of emergency control modification can be divided into two categories: reconfigurable and restructurable control. The first category includes failures which can be anticipated and solved in advance such as

engine or instrument failures. The most important failures in this class are analyzed and pilots are trained in emergency procedures to compensate for them. The major advances in reconfigurable controls in the near future may be expected to occur in computer storage and automatic activation of pre-solved emergency procedures. This involves computerizing "the book", and ensuring that emergency procedures do not simply rely on pilot training and memory under stress.

The second class of problems, and the one of interest here, includes those emergencies which cannot easily be anticipated and planned for. It includes those cases where "the book" must be thrown out. Ideally, the solution to this class of problems would place the experience and expertise of the best pilots and aircraft control system designers immediately at the disposal of the pilot in trouble. Such experts would analyze the problem and recommend solutions (some, perhaps, unconventional). Their actions would return the aircraft to a safe operating condition, and they would remain available to answer "what if" questions for the remainder of the flight, in particular involving changes to the aircraft to prepare for landing.

This assembly of experts would, in fact, be answering the following questions:

1. Did a failure occur?
2. What failure(s) occurred?
3. Must I restructure the controls to accommodate the failure(s), and if so, how?
4. What else will happen if I change the controls?

The first two questions constitute failure detection and identification, (FDI) and have received much research interest in the last decade [4]-[14]. Automatic techniques exist for determining whether a failure has occurred and

for isolating the failure component. Significant advances in designing robust FDI systems which can accomplish their mission with "real world" plant uncertainty and disturbances have recently been made and some early prototypes are being tested [4]-[5].

If a new aircraft model were available from an FDI system, a reliable automatic procedure would be required to answer the third and fourth question. Control restructuring must take place when a failure is beyond the accommodation capabilities of the normally configured aircraft. Thus an FDI system must provide an estimate of failure severity in order for a decision about the need for control restructuring to take place. When required, a restructuring of the control system then provides the desired forces and moments on the aircraft in spite of the failure. Techniques for accomplishing this control redesign were the topic of the first year's effort of this contract.

1.2 AN INTEGRATED APPROACH TO RFCS DESIGN

The development of an integrated Restructurable Flight Control System (RFCS) is best viewed as a problem in failure accommodation. As indicated in Fig. 1-1, failures can be accommodated either passively or actively.

Passive fault tolerance can be thought of as robustness -- the aircraft with its normal flight control system (including the pilot) can tolerate certain failures without modification. Other failures, however, may be too severe for the normal (i.e., any acceptable normal) controller to handle, and thus require active system modification. This modification involves (implicitly or explicitly) two processes: (1) failure detection and identification (including identification of the post-failure system model) and (2) control system reconfiguration in light of the identified failure.

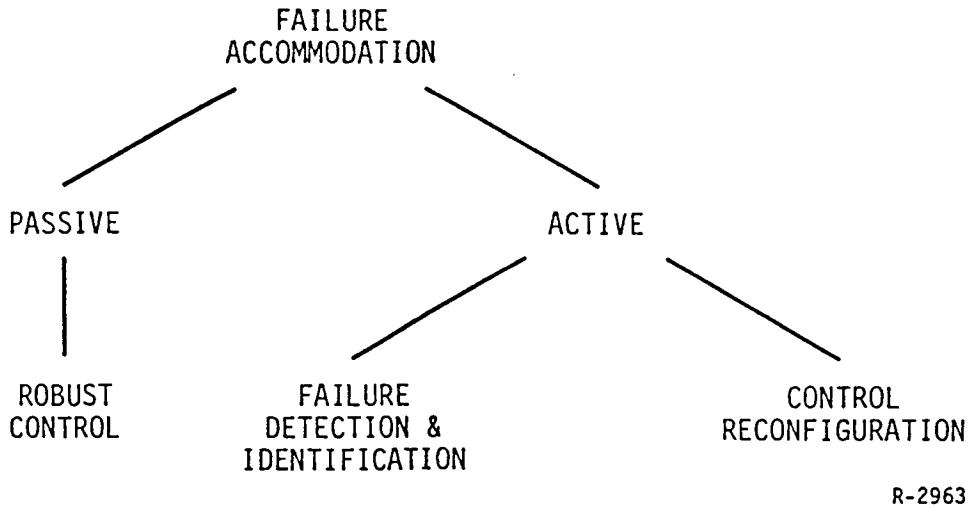

Figure 1-1. Failure Accommodation Decomposition

A successful near-term RFCS has to possess several characterisics. These include:

1. the ability to handle variations due to failures whose impact ranges from negligible to nearly debilitating,

2. the ability to perform in a highly uncertain and noisy system environment,

3. the ability to degrade gracefully with the severity of the failures, and

4. the ability to maintain the aircraft performance during and after reconfiguration. To accomplish these goals both passive and active failure accommodation methods are needed.

Figure 1-2 provides a functional component description of a RFCS which exploits both passive and active failure accommodation. This system consists of a robust multivariable flight control system, a failure detection and identification algorithm and a procedure for automatic control system redesign.

A robust multivariable flight control system is essential to any RFCS. This system must exploit the inherent control redundancy in the aircraft to minimize the effects of actuator failures and other damage. Of course, it is

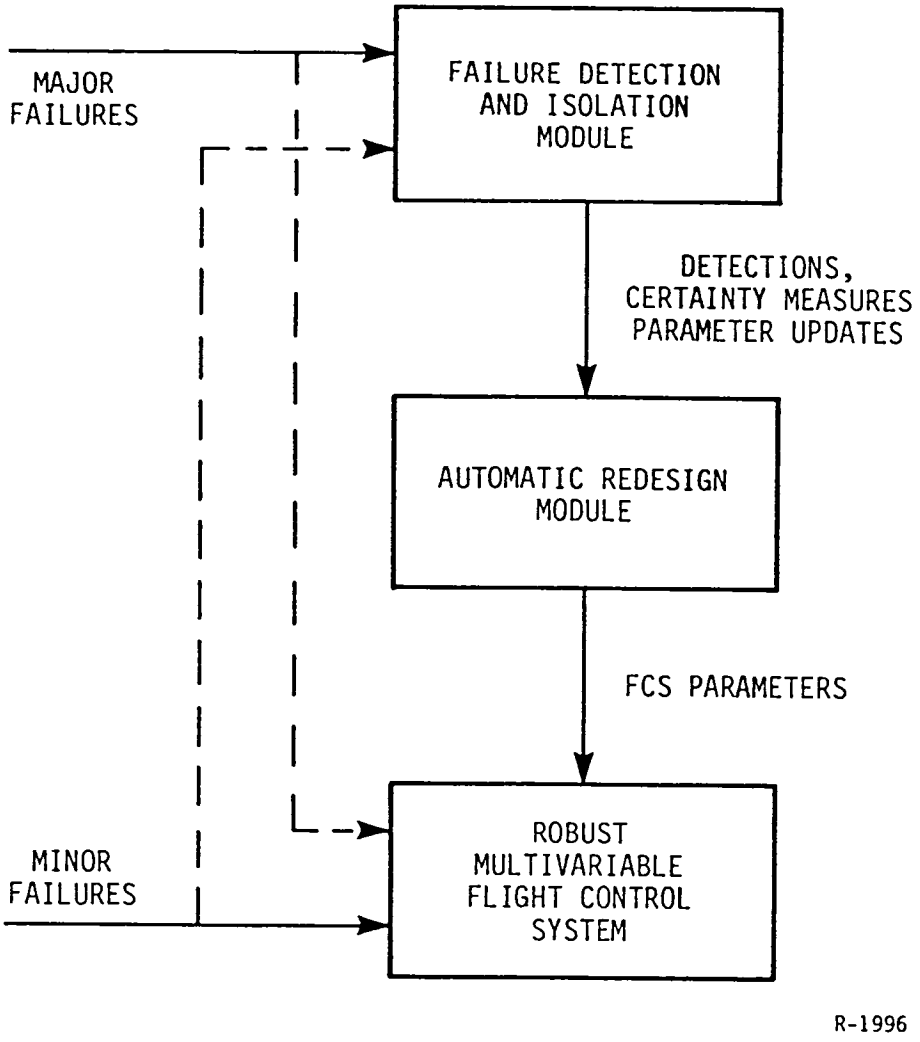

Figure 1-2. RFCS Component Decomposition

unlikely that a robust control system alone would be sufficient to handle the wide range of failure/damage modes. Such a system would require infeasibly high loop gains and bandwidth, must unacceptably compromise the performance of the unfailed aircraft, or would require unnecessarily complex FCS hardware to achieve reliability. However, a properly designed robust flight control system applied to the unfailed aircraft will be able to handle the less severe failure/damage modes, and will lengthen the time available for reconfiguring the FCS.

The more severe failure/damage modes will require a reconfiguration of the FCS. As indicated in Fig. 1-2, the reconfiguration is initiated by a FDI system. The problems of false alarms and missed detections are minimized by combining the FDI system with a nominal robust control system. As noted, the nominal control system is designed to handle as many as possible of the failure/damage conditions. The FDI system is then only required to handle failure/damages that severly impact performance. As the severity of the impact of a failure on the aircraft performance increases, the urgency of reaction increases and the time available to reconfigure decreases. However, this trend is compensated by the corresponding increase in the signature of the failure, which reduces the required time for the FDI system to respond. This phenomenon, coupled with the effects of the robust control system and robust FDI design techniques should allow a properly designed FDI system to virtually eliminate the problem of false alarms and missed detection.

The last component in Fig. 1-2 consists of an automatic control system redesign procedure and has been the primary focus of the research completed under this project [1], [15]-[17]. The automatic redesign module (ARM) uses the information about failures provided by the FDI system to modify the nominal robust FCS. To be effective, the new control system must be able to reconstruct the desired forces and moments as much as possible given the presence of large disturbances due to failures, and constraints on the control system. Since control system constraints were important in the design of the nominal robust control system, the engineering tradeoffs which went into that design should be reflected in the new control design. Furthermore, the ARM should be tolerant of FDI limitations. Incorporation of FDI uncertainty into the

redesign procedure will allow the new control system to hedge against imperfectly detected or isolated failures. Finally, graceful degradation of performance as the severity of failure increases should be a property of the ARM and can be obtained by ensuring that the nominal control system is recovered by the ARM when no failures are present.

1.3 OUTLINE OF THIS REPORT

The remainder of this report is organized as follows. Section 2 presents a precise description of the automatic control redesign problem. The problem is decomposed into finding feedforward control values which will (ideally) trim the aircraft and a modification of the nominal feedback control law which is used to remove the effects of uncertainty and provide as much dynamic response to pilot commands as is possible. Section 3 provides the details of the feedforward "automatic trim" problem and provides an algorithm for its solution. Section 4 presents a redesign procedure for determining a new feedback control law. This redesign procedure is based on the linear quadratic (LQ) regulator problem, however, it is not necessary that LQ be used to design the nominal control law which is used during unfailed operation. Section 5 puts these two subsystems (automatic trim and control law redesign) together and shows how the solutions to these problems are implemented. Section 6 applies the techniques developed in Sections 3 through 5 to a model of a modified Boeing 737 aircraft. An LQ design methodology is used to develop a robust feedback control law which forms the basis for the control law redesign procedure. Solutions to the trim problem are investigated for a variety of realistic failure modes, and a variety of linear analyses of the redesign procedure are performed for these same failure cases. The linear analyses include an

eigenvalue analysis and linear simulations. Section 7 describes an investigation of the two subsystems using the NASA Langley Research Center's nonlinear aircraft simulation. Finally, a summary and conclusions are provided in Section 8.

SECTION 2

PROBLEM FORMULATION

In this section, we provide a precise description of the restructurable control problem and discuss some of the desirable features which any solution should contain.

We assume that under normal operation, the motion of the aircraft can be described by the nonlinear, time invariant differential equation,

$$\dot{x} = f_o(x,u) \tag{2-1}$$

$$y = h_o(x,u) \tag{2-2}$$

where x is the n-dimensional state vector and u is an m-dimensional vector of controls (e.g., all control surfaces, engine controls, possible thrust vectoring, etc.) and y is a vector of "important" quantities (not necessarily measurable). The unfailed aircraft is said to be "trimmed" when

$$f_o(x_T,u_T) = 0 \tag{2-3}$$

$$h_o(x_T,u_T) = y_d \tag{2-4}$$

for some constant values of (x_T,u_T) with y_d being the desired values of the important quantities (e.g., flight path angle, forward velocity, angular rates, etc.). Furtherfore, we will assume that a nominal control system is employed (for stability augmentation, control augmentation, disturbance rejection, etc.) and takes the form,

$$u = G_o\, x + u_r \tag{2-5}$$

where in general, the feedback gain, G_o, may be a function of flight condition and u_r is a dynamic reference signal which is ultimately derived from the pilot inputs, r. Note that Eq. 2-5 assumes that any feedback compensator dynamics are embodied in Eq. 2-1.

In general, those aircraft failures which potentially result in emergency conditions can be modeled by

$$\dot{x} = f_F(x,u) + w \tag{2-6}$$

$$y = h_F(x,u) \tag{2-7}$$

Equations 2-6 and 2-7 include changes in the aerodynamics of the aircraft, changes in control effectiveness, and potentially large disturbances (e.g., due to a stuck, off-centered control surface). The nominal control gain, G_o, is typically designed without the effect of failures in mind. However, a large degree of fault tolerance may be achieved by proper choice of G_o. If G_o distributes the control authority amongst a variety of surfaces then any single surface failure becomes less critical in terms of reduction in command following performance. Furthermore, the use of integral action in the compensator (i.e., high loop gains at low frequencies) may allow the aircraft to recover automatically from a failure. That is, it may be possible to achieve

$$f_F(x_F,u_F) = 0 \tag{2-8}$$

$$h_F(x_F,u_F) = y_d \tag{2-9}$$

automatically for some failures with the proper choice of G_o.

Naturally, there will be some failures (or combination of failures) for which the nominal control system is not adequate. In these cases, we want to find a new control law of the form,

$$u = G_F\, x + u_r^F + u_F^T \qquad (2\text{-}10)$$

where G_F represents a new feedback gain, u_r^F represents a new pilot reference signal and u_F is a feedforward control that can be used to (approximately) reject the disturbances, w. The control system redesign problem becomes, therefore, one of choosing G_F,u_F, and the relationship between u_r^F and the pilot inputs, r. These choices are made so that the aircraft is stabilized, disturbances can be rejected, the aircraft will follow the pilot commands and (more importantly) so that the limitations of the aircraft are not violated. Furthermore, these choices must take into account the fact that the aircraft model in Eqs. 2-8 and 2-9 are uncertain since we may rely on some FDI algorithm to identify this model. That is, in addition to the performance goals and aircraft constraints, a degree of robustness which is typically greater than would be considered for a normal aircraft must be achieved.

The automatic redesign algorithms developed for this project were developed within this framework and address all of the issues discussed above. The nominal feedback control law is designed using an LQ design procedure which will distribute the control authority amongst all available surfaces. As a result, a large degree of fault tolerance is achievable with no reconfiguration. The feedback control redesign procedure uses the design parameters (state and control weighting matrices) of the nominal control law as a basis for any redesign. In this way, performance can be optimized while maintaining the bandwidth constraints that are embodied in the nominal design. Finally,

an automatic feedforward trim algorithm is developed so that any large disturbances due to a failure can be quickly accommodated.

In the remainder of this report, we will review the control redesign algorithm developed for this project and demonstrate the performance and robustness capabilities of a nominal LQ control design and the new control system produced by the redesign procedure for a variety of failure modes.

SECTION 3

THE AUTOMATIC TRIM PROBLEM

The solution of the automatic trim problem is one of the most time-critical components of the restructurable control system. This is because substantial deviations from the desired trim condition (following a failure) is likely to result in a situation where the remaining control authority available for recovery is insufficient. In this section, we present a formal description of the automatic trim problem and describe a decomposition of that problem which allows us to use fast and efficient algorithms in the solution procedure.

3.1 THE NONLINEAR TRIM PROBLEM

During normal flight, the motion of an aircraft with respect to some inertial reference frame can, in general, be described by the nonlinear time-invarient differential equations

$$\begin{aligned} \dot{x} &= f_o(x,u) + \zeta \\ y &= h_o(x,u) \end{aligned} \tag{3-1}$$

where x is an n-dimensional state vector, u is an m-dimensional control vector, ζ is a vector of (presumably unmeasurable) disturbances, and y is an output vector of important quantities. The aircraft is trimmed at the nominal values (x_n,u_n) when

$$\begin{aligned} f_o(x_n,u_n) &= 0 \\ h_o(x_n,u_n) &= 0 \end{aligned} \tag{3-2}$$

For example, during straight and level flight, nominal control settings, u_n, are established which maintain steady state flight ($\dot{x} = 0$) at constant altitude (flight path angle, $\gamma = \theta - \alpha = 0$) at some desired airspeed and heading and level wings.

Following a failure, the aircraft dynamics are assumed to satisfy

$$\begin{aligned} \dot{x} &= f(x,u) + \zeta + w \\ y &= h(x,u) \end{aligned} \tag{3-3}$$

where w is a constant (or slowly varying) measurable disturbance vector. For example, in the case of a stuck actuator, w represents the force and moment disturbance that results from the constant nonzero deflection. Following a failure, then, a trim condition results when

$$\begin{aligned} f(x_n,u_n) + w &= 0 \\ h(x_n,u_n) &= 0 \end{aligned} \tag{3-4}$$

The primary goal of an automatic trim function is to find a solution (x_n,u_n) which satifies Eq 3-4. We can then apply the control u_n to the aircraft directly (assuming no control system; linear combinations of x_n and u_n are applied when feedback is employed) and achieve a fast initial recovery.

This result, of course, can only be achieved if the solution (x_n,u_n) is a feasible one. That is, certain constraints on the allowable values of x_n and u_n must be imposed. For example, restrictions on u_n would include the travel limits on the control surfaces and the power limits on the engine inputs. Restrictions on x_n represent the region of validity of the aircraft model in Eq. 3-3 and would include minimum airspeeds (e.g., above stall), angle of attack limits, and altitude restrictions.

Finally, in order to create a formal well-posed problem statement we note that two cases of special interest exist. In the first case, several solutions to Eq. 3-4 exist within the feasible region. In this case, we will choose a solution which minimizes the norm (e.g., in a weighted least squares sense) of the difference between the vector (x_n,u_n) and some "desired" vector (x_n^o,u_n^o). This allows us to ensure that maximal 'residual' control authority remains available for disturbance rejection and command following. The second case arises when no solution to Eq. 3-4 exists within the feasible region. In this case we will choose the solution which minimizes the norm (again, e.g., in a weighted least squares sense) of the left hand side of Eq. 3-4.

Making the following definitions, we can now formally state the nonlinear trim problem. Let

$$z = (x_n - x_n^o,\ u_n - u_n^o)$$

$$F = \{z : x_n \text{ and } u_n \text{ are feasible solutions}\}$$

$$D = \{z : z = \arg\min(\|f(z) + w\| + \|h(z)\|)\} \quad .$$

The solution to the nonlinear trim problem, z^*, is then given by:

$$z^* = \arg\min \|z\|$$

$$\text{Subject to} \qquad z\varepsilon F,\ z\varepsilon D \qquad (3\text{-}5)$$

That is, we want to choose a feasible z which satisfies Eq. 3-4 as nearly as possible, and if more than one such solution exists, to choose the one of least norm.

As discussed in [1], while the above problem statement accurately represents the goals of an automatic trim system, solution methods may be complicated by the various nonlinear functions which are used to describe the system. Furthermore, these complexities may not be truly representative of the complexities which must be faced in establishing an adequate trim solution. For example, for small enough perturbations about some nominal value of z, Eq. 3-4 can be well approximated by a set of linear equations. As we will discuss subsequently, fast and efficient solution procedures can be utilized to solve Eq. 3-5 when Eq. 3-4 is linear.

Making use of linear approximations, we can decompose the nonlinear trim problem into two subproblems which are solved (and possibly iterated upon) in order to determine a complete solution. The first subproblem is the operating point selection problem. The primary purpose here is to determine nominal values of the states (x_n) and control variables (u_n) which results in a trimmed unfailed aircraft. A linearized version of the aircraft dynamics about this nominal can then be determined and, the constraints, objectives and/or priorities for the second subproblem, the linear trim problem, established. The linear trim problem then solves for feasible perturbations from the nominal values which adequately reject the failure induced disturbances.

The determination of a suitable operating point is a function of a number of factors and is based on the desired flight objective. For example, during a landing approach, it may be sufficient to select a single operating point which corresponds to level wings and some nominal flight path angle. If another flight path is desired, the pilot controls deviations from this nominal to achieve the desired result. A linearized model for this operating point can then be identified along with an estimate of the model's "region of

validity." This region is then translated into constraints on the state and control perturbations for the linear trim problem. After examination of the solution to the linear trim problem, the operating point selection problem may take advantage of parts of the nonlinear problem in order to find a combination of flight objective and linearized model for which an acceptable linear trim solution can be found. Included in this part of the operating point selection problem are such (nonlinear) factors as the use of "discrete" control elements which primarily influence the linear model (e.g., fuel dumping and c.g. changes), the nonlinear effect of velocity and altitude changes and possible changes to the flight objective.

3.2 THE LINEAR TRIM PROBLEM

For the linear trim problem, we assume that a linearized model of the aircraft about some nominal states and controls can be given by:

$$\dot{x}_p(t) = Ax_p(t) + Bu_p(t) + w_p \tag{3-6}$$

where $x_p(t)$ is the perturbation of the state vector ($x_p = x - x_o$, $u_p(t)$ is the vector of available control perturbations ($u_p = u - u_o$) and w_p is a vector of constant disturbances. The vector w_p can be used to represent forces and moments generated by failed surfaces.

The key quantities that are to be regulated can in general be denoted by:

$$y_p = Cx_p \tag{3-7}$$

Elements of y might represent quantities such as altitude, bank angle, flight path angle, and rotational rate perturbations. The primary objective of the linear disturbance rejection problem is to automatically select x_p and u_p such

that y achieves some desired value in steady state. More precisely, the linear trim objective can be expressed as

$$y_p = y_d \tag{3-8}$$

and

$$0 = Ax_p + Bu_p + w_p \tag{3-9}$$

As in the nonlinear trim problem, we will want to impose some constraints on the allowable perturbations (x,u) for which a solution will be sought. In the linear trim case, these restrictions must be more conservative in order to insure that the resulting trim solution remains within the region of validity of the linear model. In most cases, these constraints can be described as upper and lower limits on the allowable perturbations, viz.,

$$\begin{aligned} x_L \leq x_p \leq x_U \\ u_L \leq u_p \leq u_U \end{aligned} \tag{3-10}$$

Equations 3-8 through 3-10 describe the objectives of the linear trim problem. Like the nonlinear trim problem, in order to form a well-posed optimization problem we must examine two special cases. When several solutions to Eqs. 3-8 through 3-10 exist, we will call the problem feasible and choose (x_p,u_p) to minimize the norm of the difference between (x_p,u_p) and some desired value (x_p^o,u_p^o). In particular, we have:

Feasible Problem

$$\begin{aligned} \text{Minimize} \quad & J_1 = \|x_p - x_p^o\| + \|u_p - u_p^o\| \\ \text{Subject to} \quad & 0 = Ax_p + Bu_p + w_p \\ & y_d = Cx_p \\ & x_L \leq x_p \leq x_U \\ & u_L \leq u_p \leq u_U \end{aligned} \tag{3-11}$$

Various norms and weighting matrices can be used in Eq. 3-11 as discussed in [18]. These choices can be made off-line based on the physical characteristics of the aircraft and its control surfaces. It should also be noted that Eq. 3-11 must be solved on-line after the disturbance w has been measured or estimated. However, in the least squares case, Eq. 3-11 is a standard quadratic programming problem for which a number of fast, efficient solution algorithms have been developed.

If a solution to Eqs. 3-8 through 3-10 exists, it guarantees that the principal objectives can be satisfied. That is, the important quantities can be zeroed (Eq. 3-8), steady state flight is possible (Eq. 3-9), and no prespecified state or control constraints have been violated (Eq. 3-10). It is possible, however, that Eqs. 3-8 through 3-10 overspecify the problem. In this case, it is impossible to achieve the objectives of the linear trim problem at the chosen flight condition. However, a variation of Eq. 3-11 can be used to gain time to choose a new nominal flight condition or to achieve slowly degrading flight. The key is to try to minimize the size of both the important quantities, y_p, and the state perturbation derivatives:

Infeasible Problem

$$\begin{aligned} \text{Minimize} \quad & J_2 = \|Ax_p + Bu_p + w_p\| + \|Cx_p - y_d\| \\ \text{Subject to} \quad & x_L \leq x_p \leq x_U \\ & u_L \leq u_p \leq u_U \end{aligned} \tag{3-12}$$

The objective in Eq. 3-12 attempts to keep the size of the state derivative and key quantities small. Again, various norms and weighting matrices can be used. A solution to Eq. 3-12 will always exist. As with Eq. 3-11, a least squares formulation of Eq. 3-12 leads to a quadratic programming problem and can easily be solved on-line using fast and efficient algorithms.

As in the nonlinear trim problem, the two problems described above (feasible and infeasible) can be compactly described as follows. Let,

$$z = (x_p - x_p^o,\ u_p - u_p^o)$$

$$F = \{z : z_L < z < z_U\}$$

$$D = \{z : (x_p, u_p) = \arg\min J_2\} \quad .$$

The solution to the linear trim problem is given by,

$$\begin{aligned} & z^* = \arg\min J_1 \\ \text{Subject to} \quad & \\ & z \in F,\ z \in D \end{aligned} \tag{3-13}$$

That is, we start by solving the infeasible problem (Eq. 3-12) and determining the optimal objective function, J_2^*. If, in fact, the feasible problem has a solution, then $J_2^* = 0$, and in general, more than one solution may exist. The second stage is to minimize the objective J_1 (Eq. 3-11) subject to the constraints of Eq. 3-10 and the constraint $J_2 = J_2^*$.

This completes our discussion of the automatic trim problem and the decomposition of that problem into an operating point selection problem, and a linear trim problem. The linear trim problem provides a formulation which allows fast and efficient quadratic programming algorithms to be used when the norms are interpreted in the least squares sense. In the next section, we will describe a quadratic programming algorithm which takes special advantage of the structure of the problem (Eq. 3-13) and the constraint set, F.

3.3 A QUADRATIC PROGRAMMING ALGORITHM

In this subsection we describe a quadratic programming algorithm which takes advantage of the special structure of the problem described in the previous section. The simplicity of the constraint set and the special nature of minimum norm quadratic programming problems will allow us to use fast and efficient methods in computing the necessary quantities for the algorithm's operation.

As discussed in the previous section, the problem which we are attempting to solve is a least squares problem which can in general be represented by

$$\begin{aligned} &\text{Minimize} && (J_1 = z^T z) \\ &\text{Subject to} && z_L < z < z_U \\ & && z \varepsilon \left\{ z : z = \arg\min J_2 = \frac{1}{2} (Fz - d)^T (Fz - d) \right\} \end{aligned} \tag{3-14}$$

where the solution variables, z, are in R^n, F is an m×n matrix and d is in R^m. That is, of all the solutions, z, which minimize J_2, we want the feasible one of the least norm.

3.3.1 Solution Procedure: Overview

The most common solution procedure for any quadratic programming problem is the active set method [19]. This method is an iterative procedure in which, at each stage in the algorithm, the current iterate satisfies the inequality constraints in Eq. 3-14.

The first step in the active set solution procedure is the selection of any feasible solution to the inequality constraints in (Eq. 3-14) (e.g., z=0 when $z_L < 0$ and $z_U > 0$) and the determination of which of these constraints are active (i.e., satisfied with equality).

Next, a step direction is obtained which minimizes J_2 in the subspace of active constraints. For the problem at hand, this minimization is obtained by simply removing the elements of z which are active (constrained) from consideration, partitioning F into active and inactive columns, adding the effect of the constrained elements to the value of d in Eq. 3-14, and finally, finding the remaining elements of z by using a singular value decomposition of the inactive part of F. Details of this procedure will be provided in the next subsection. Note here, however, that the singular value decomposition of a matrix provides a basis for its' range and null spaces and as such, will be used to find the minimum norm (of the remaining elements of z) solution if the reduced problem is under-constrained.

The next step in the procedure is to check if the solution to the constrained optimum problem found above is feasible. If any of the inequality constraints are violated, then the step direction (defined by the current feasible solution and the solution to the constrained optimization problem found above) is scaled so that the next iterate is also feasible. That is,

if a step in the direction of the constrained optimum runs into a currently inactive constraint, then that constraint is added to the set of active constraints and the process above is repeated.

If, at this point in the solution procedure, the number of constraints equals the number of elements in z, then the current iterate is at a vertex of the constraint region. In this case we then check a set of stopping criteria to see if a single active constraint can be removed. If this is possible, a constraint is removed and the above process is continued. If the step direction does not need to be scaled (i.e., no inactive constraints will be violated), then the stopping criteria are also checked and the algorithm continued if an active constraint can be removed. The algorithm terminates when the stopping criteria indicate that no active constraints can be removed.

Stopping Criteria

In order to determine if the current iterate is the solution which is sought, the algorithm must check if any of the currently active constraints can be removed. If no constraints are active or if no constraints can be removed, then the current iterate solves Eq. 3-14. Furthermore, if several constraints can be removed, we must choose one of these for the algorithm to be continued. (This is to avoid so called cycling problems such as those discussed in [19]).

The method by which the above is accomplished is by the use of Lagrange multipliers [20]. In the solution to any constrained optimization problem, it is possible to compute or estimate such multipliers. The reason these quantities are useful is that they represent the price associated with the active constraints. That is, each multiplier indicates the sensitivity of the cost

function which is being optimized to a feasible perturbation of the current iterate in a subspace which corresponds to the remaining constraints. Thus, for example, if all multipliers indicate that the cost function would increase (for a minimization problem) then we may conclude that the current iterate is optimal. (Note, this is just a statement of the Kuhn/Tucker conditions given in [19],[20]).

For Eq. 3-14, there are two cost functions (J_1 and J_2) for which we desire Lagrange multipliers corresponding to the current set of active constraints. In the procedure to be detailed in the next subsection, we first compute multipliers which correspond to the sensitivity of J_2 (Eq. 3-14) to the current active constraints. If these multipliers indicate that a set of constraints can be removed, we choose the constraint which reduces the cost the most (i.e., largest multiplier, in magnitude). If these multipliers indicate that no constraint can be removed to reduce J_2, then we compute multipliers which correspond to the sensitivity of J_1 to the active constraints with the further restriction that the feasible perturbations lie in the subspace defined by $J_2 = J_2^*$ (where J_2^* = current value of J_2). As detailed in the next subsection, the latter computation is easily accomplished by computing the singular value decomposition of the matrix F (in Eq. 3-14) augmented with appropriate selection matrices corresponding to the above constraints. The constraints associated with the largest cost reduction is chosen at this point. The stopping criteria are satisfied when, at this stage, no constraint can be removed.

The algorithm described above is summarized as follows.

1. Determine an initial feasible point, $z_k(k=0)$, which satisfies the inequality constraints.

2. Compute the optimum z (say $\hat{z}$), along the current set of active constraints.

3. Compute the new step direction $P = K_s(\hat{z}-z_k)$ where α is chosen so that $z_{k+1} = z_k + P$ is feasible.

4. If $K_s = 1$ or if z_{k+1} is a vertex go to 6.

5. Else: $k = k+1$, go to 2.

6. Compute Lagrange multipliers corresponding to the active constraints for the problem of minimizing J_2.

7. If any constraints can be removed, remove the one which reduces J_2 the most. Update $k = k+1$. Go to 2.

8. If no constraint can be removed, compute the Lagrange multipliers corresponding to the active constraints for the problem of minimizing J_1 subject to $J_2 = J_2^*$.

9. If any constraint can now be removed, choose the one which reduces J_1 the most. Update $k = k+1$. Go to 2.

10. Else: Done.

3.3.2 Solution Procedure Details

In this subsection we provide some of the details of the algorithm described above. The description here follows the steps outlined in the above summary description.

Step 1: Initial Feasible Point

For most purposes, an initial value of $z = 0$ will satisfy the inequality constraints. If this is not the case, an initial feasible solution can be easily chosen as any combination of upper and lower bounds $z_L{}^i$, $z_U{}^i$ (the notation z^i will be used to denote the i'th element of z).

Step 2: Solve Constrained Minimization Problem

The upper and lower bounds on the value of any z^i cannot both be active at the same time. If we keep track of these constraints separately, somewhat

simpler computations can be achieved over those needed in the application of a standard quadratic programming algorithm to this problem. To keep track of these constraints, we define two index sets based on the current value of z;

$$I_L = \{i : z^i = z_L{}^i\}$$
$$I_U = \{i : z^i = z_U{}^i\} \tag{3-15}$$

We now define a matrix F_c,

$$F_c = [F_L \quad F_U] \tag{3-16}$$

where F_L consists of the columns of the matrix F for all $i \varepsilon I_L$ and F_U consists of the columns of the matrix F for all $i \varepsilon I_U$. Also, let

$$b^T = [b_L{}^T \ , \ b_U{}^T] \tag{3-17}$$

where b_L and b_U are elements of the bounds on z (z_L and z_U respectively) corresponding to all $i \in I_L$ and all $i \in I_U$ respectively.

In the subspace corresponding to the active constraints (indicated by Eq. 3-15) the objective function J_2 (see Eq. 3-14) can be written as

$$\bar{J}_2 = (\bar{F} z_f - \bar{d})^T (\bar{F} z_f - \bar{d}) \tag{3-18}$$

where

$\bar{F}$ = the columns of F corresponding to all inactive constraints, (i.e., the ith column of F appears in $\bar{F}$ if $i \in (I_L \cup I_U)^c \triangleq I_f$, where c denotes complement),

z_f = elements of z which are not constrained,

$\bar{d} = d - F_c \, b$.

Thus, the solution to the constrained minimization problem (i.e., minimize J_2 subject to the active constraints remaining active) can be found by solving the unconstrained problem: minimize $\bar{J}_2$. Since this is just a standard least squares problem, the solution is formally given by

$$z_f = \bar{F}^{\#} \bar{d} \tag{3-19}$$

where $\bar{F}^{\#}$ represents the Penrose pseudo inverse of $\bar{F}$. Note that in the computation of z_f by Eq. 3-19, if the problem of minimizing $\bar{J}_2$ is under-constrained, then z_f is the solution of minimum norm in the least squares sense (e.g., see [34]).

The most reliable way to compute z_f is through the singular value decomposition (SVD) of the matrix $\bar{F}$. (Many of the issues associated with this problem are also addressed in [34].) If $\bar{F}$ is an m × n matrix of numerical rank r, then its SVD takes the form

$$\bar{F} = \begin{bmatrix} U_1 & U_2 \end{bmatrix} \begin{bmatrix} S_1 & 0 \\ 0 & E \end{bmatrix} \begin{bmatrix} V_1^T \\ V_2^T \end{bmatrix} \tag{3-20}$$

$$= U \quad S \quad V^T$$

where

U_1 is an m × r matrix of left singular vectors,

U_2 is an m × m-r matrix of left singular vectors,

S_1 is an r × r diagonal matrix of singular values each of which is greater than some prespecified tolerance,

E is an m-r × n-r diagonal 'error' matrix,

V_1 is an n × r matrix of right singular vectors,

V_2 is an n × n-r matrix of right singular vectors.

Furthermore, U and V are orthonormal matrices (i.e., $U^TU = V^TV = I$). From these properties, one can show that V_2 is a basis for the null space of $\overline{F}$ and U_1 is a basis for its range space. The solution, z_f, to the unconstrained problem of minimizing $\overline{J}_2$ can then be computed by

$$z_f = (V_1)\ (S_1)^{-1}(U_1)^T\ \overline{d} \tag{3-21}$$

Step 3: Compute the New Step Direction

The new step direction, P, is defined by the equation

$$P = K_s(\hat{z} - z_k) \tag{3-22}$$

where z_k is the current iterate,

$\hat{z}^i = z_L{}^i$ for all $i \in I_L$

$\hat{z}^i = z_U{}^i$ for all $i \in I_U$

$\hat{z}^{I_f(j)} = z_f{}^j$, where $I_f(j)$ denotes the j-th element of $I_f \triangleq (I_L \cup I_U)^C$

and where K_s is computed as follows. Let

$$K_L = \min \left[1\ ,\ \frac{z_L{}^i - z_k{}^i}{\hat{z}^i - z_k{}^i} \right],\ \text{for all i:}\ \ i \in I_f\ ,\ \hat{z}^i - z_k{}^i < 0 \tag{3-23}$$

$$K_U = \min \left[1\ ,\ \frac{z_U{}^i - z_k{}^i}{\hat{z}^i - z_k{}^i} \right],\ \text{for all i:}\ \ i \in I_f\ ,\ \hat{z}^i - z_k{}^i > 0 \tag{3-24}$$

then K_s is defined by

$$K_s = \min \{K_L\ ,\ K_U\ ,\ 1\} \tag{3-25}$$

If $K_s = 1$, then no constraints need to be added. Otherwise, the index set I_L (or I_U) is updated to include the index, i, which achieves the minimum in Eq. 3-23 (or 3-24).

Step 6: Compute the First set of Lagrange Multipliers

The first set of multipliers correspond to the problem of minimizing J_2 subject to $i \in (I_L \cup I_U)$. These multipliers can be computed by forming the so-called Hamiltonian function [20],

$$H = J_2 - \sum_j \lambda_L{}^j (z_k{}^j - z_L{}^j) - \sum_i \lambda_U{}^i (z_k{}^i - z_U{}^i) \tag{3-26}$$

and setting the partial derivative of H with respect to z equal to zero (i.e., solving one of the necessary conditions of optimality as given in [20]). Since the sets I_L and I_U are mutually exclusive, it can be shown that the desired multipliers are given by

$$\begin{aligned} \lambda_1{}^T &= [\lambda_L{}^T \ , \ \lambda_U{}^T] \\ &= F^T(Fz_k - d) \end{aligned} \tag{3-27}$$

Step 7: Test Multipliers and Update Constraints

Equations 3-26 and 3-27 indicate that the current solution is globally optimal if $\lambda_L{}^i \geq 0$ for all i and if $\lambda_U{}^j \leq 0$ for all j. This can be seen as follows. At the current z_k, $z_k{}^i = z_L{}^i$ and $z_k{}^j = z_U{}^j$ for $i \in I_L$ and $j \in I_U$. Therefore, $H(z_k) = J_2(z_k)$. But, z_k was obtained by minimizing H, so for any other z_k, say $\bar{z}$, $H(z_k) \leq H(\bar{z})$. If $\bar{z}$ is feasible and if $\lambda_L{}^i \geq 0$ and $\lambda_U{}^i \leq 0$, then, referring to Eq. 3-26, $H(\bar{z}) \leq J_2(\bar{z})$. From these arguments, we have $J_2(z_k) \leq J_2(\bar{z})$ for any feasible $\bar{z}$; which is equivalent to stating that z_k is globally optimal.

If any of the Lagrange multipliers violate the conditions stated at the top of the previous paragraph, then the current iterate, z_k, is not optimal and one of the constraints can be removed. If several of the multipliers violate the above conditions, the index, i, corresponding to the largest (in absolute value) of these multipliers is chosen as the index of the constraint to be removed.

Step 8: Compute the Second Set of Multipliers

The second set of multipliers corresponds to the problem of minimizing J_1 subject to $i \in (I_L \cup I_U)$ and J_2 remaining unchanged. That is, the problem

$$\text{Min} \quad \|z_k + \Delta z\|^2$$

$$\text{Subject to} \quad (z_k + \Delta z) \in F$$

$$F\Delta z = 0$$

has the solution $\Delta z = 0$, along the currently active constraints (this is how z_k was determined in step 6) and Lagrange multipliers given by

$$\lambda_2^T = (A_2^T)^{\#} z_k \tag{3-28}$$

where

$$A^T = [F^T \quad S_L^T \quad S_U^T]$$

$$S_L(i,j) = 1 \text{ if } I_L(i) = j \; ; \text{ otherwise } S_L(i,j) = 0$$

$$S_U(i,j) = 1 \text{ if } I_U(i) = j \; ; \text{ otherwise } S_U(i,j) = 0$$

$$\lambda_2^T = [\lambda_F^T \, , \, \lambda_{2L}^T \, , \, \lambda_{2U}^T]$$

Step 9: Test Multipliers and Update Constraints

As in Step 7, the condition of global optimality is $\lambda_L{}^i > 0$, $\lambda_U{}^i < 0$. If any of these conditions are violated, we remove the constraint corresponding to the largest (in magnitude) $\lambda_2{}^i$ of those which do not satisfy the optimality conditions.

At this stage, if no constraint can be removed, (i.e., the optimality conditions are satisfied) then the algorithm terminates with the current iterate as the solution.

3.3.3 Scaling

Convergence of the quadratic programming algorithm described in subsections 3.3.1 and 3.3.2 is greatly dependent on the relative sizes of the elements in F and d in Eq. 3-14. In Section 6.3, the effect of scaling on speed of convergence is demonstrated for the B-737 application. In general, we can transform Eq. 3-14 as follows. Let,

$$\begin{aligned} z_s &= S_z{}^{-1}\, z \\ d_s &= S_d{}^{-1}\, d \end{aligned} \tag{3-29}$$

where S_z and S_d are diagonal weighting matrices. If the i-th diagonal element of S_z is large, then the i-th element of z will tend to have larger values in the feasible problem. If the i-th diagonal of S_d is large, then the error in the i-th disturbance direction will be larger. Problem (Eq. 3-14) then becomes

$$\text{Min} \quad J_1 = z_s^T z_s$$

$$\text{Subject to} \quad S_z^{-1} z_L < z_s < S_z^{-1} z_U$$

$$z \in \{z : z = \arg\min \; J_2 = |F_s \cdot z_s - S_d \cdot d_s|$$

where

$$F_s = F S_z \tag{3-30}$$

3.4 LINEAR TRIM WITH UNCERTAINTY

Until now, our discussions of the linear trim problem have focused on solutions for the case where both the disturbance w (see Eq. 3-3) and the control effectiveness matrix, B, were known exactly. As in the development of control redesign procedures ([1]), it is desirable to formulate a problem in which specific knowledge about relative uncertainty can be used. That is, for example, we would like to incorporate into the quadratic programming algorithm, the capacity for trading off the use of control surfaces which may have a large nominal, but uncertain effect for those which may have more certain but small nominal effects. Furthermore, we would like the algorithm to be able to distinguish between those disturbances which are well known and those which are uncertain so that excessive control authority is not lost in trying to compensate for a poorly modeled or estimated disturbance.

We can accomplish these goals by formulating the trim problem with uncertainty in a similar vein to the development of control system redesign procedures [1]. Suppose, in Eq. 3-14, the matrix F and disturbance d are random variables with

$$\begin{aligned} F &= F_n + \Delta F \\ E\{\Delta F\} &= 0 \\ E\{\Delta F^T \Delta F\} &= Q_F \end{aligned} \tag{3-31}$$

$$d = d_n + \Delta d$$

$$E\{\Delta d\} = 0 \tag{3-32}$$

$$E\{\Delta d^T \Delta d\} = R_d$$

where $E(\cdot)$ denotes expected value.

Using Eqs. 3-31 and 3-32, the objective function J_2 (Eq. 3-1) can then be expanded as,

$$\begin{aligned} J_2 &= (Fz - d)^T(Fz - d) \\ &= z^T F_n^T F_n z + 2 z F_n^T \Delta F z + z^T \Delta F^T \Delta F z \\ &\quad - 2 d_n^T F_n z - 2 d_n^T \Delta F z - 2 \Delta d^T F_n z - 2 \Delta d^T \Delta F z \\ &\quad + d_n^T d_n + 2 d_n^T \Delta d + \Delta d^T \Delta d \end{aligned} \tag{3-33}$$

Since ΔF and Δd are random variables, J_2 is now a random variable. In order to provide a deterministic quantity which can be optimized in the linear trim problem, we must consider some kind of statistical average of J_2. Two such averages are the average cost $E\{J_2\}$, and the mean square cost, $E\{J_2^2\}$. The average cost case is considered below.

Minimum Average Cost

Combining Eqs. 3-31 through 3-33, and assuming that Δd and ΔF are uncorrelated, the expected value of J_2 is,

$$E(J_2) = z^T(F_n^T F_n + Q_F)z - 2 d_n^T F_n z + d_n^T d_n + R_d \tag{3-34}$$

Equation 3-34 can then be put into standard form (Eq. 3-14) by completing the square resulting in,

$$E\{J_2\} = (\hat{F}z - \hat{d})^T(\hat{F}z - \hat{d}) + g \tag{3-35}$$

where

$$\hat{F}^T \hat{F} = F_n^T F_n + Q_F \tag{3-36}$$

$$\hat{F}^T \hat{d} = F_n^T d_n \tag{3-37}$$

$$\hat{d}^T \hat{d} + g = d_n^T d_n + R_d \tag{3-38}$$

The effect of including uncertainty information in the description of the linear trim problem and minimizing the average cost can be seen by examination of Eq. 3-34. The uncertainty in d results in a constant positive value (R) added to the cost, but does not change the optimal solution, z^*, which minimizes $E\{J_2\}$. The uncertainty in F results in the addition of the term $z^T Q z$ to the cost. This term amounts to an additional weighting or scaling of the solution variables, z, that reflects the relative amount of uncertainty contributed by each element of z. Elements of z with large uncertainty contribute more to the expected cost than do elements with small values so that the solution, z^*, will realize a tradeoff between the use of elements which have different nominal effectivenesses and different amounts of uncertainty associated with their disturbance rejection capabilities. Note that uncertainty in the A, B, and C matrices in Eqs. 3-6 and 3-7 can be incorporated into this formulation.

The average cost function described above provides a problem formulation that results in an automatic tradeoff between solution elements of various effectiveness and uncertainty. However, the uncertainty in the disturbance to be rejected does not affect the solution. Examining Eq. 3-33, we can see that while, on average, Δd only creates an increase in J_2 which is unrelated to

the choice of z ($\Delta d^T \Delta d$ term), the actual value of Δd does create a z-dependent effect on the actual cost function. Thus, one would expect that the z-dependent impact of Δd on the cost occurs primarily in higher order moments of the cost function (e.g., $E\{(J_2)^2\}$). Minimization of the mean square cost is then a likely candidate objective function. The resulting solution to the minimization of such an objective would provide the desired tradeoff between the use of solution elements to cancel disturbances of uncertain effect. Disturbance directions, which are not well known, result in large mean square values of J_2 when certain elements of z in the solution are large. The algorithm would then balance this uncertainty with its ability to achieve the desired nominal disturbance rejection capability. Unfortunately, the computation of $E\{J_2^2\}$ involves fourth-order moments of ΔF and Δd which would need to be specified (or derived from a Gaussian error assumption). Furthermore, the resulting objective cannot necessarily be factored in a form which results in a quadratic programming algorithm. Therefore, the minimum average cost provides the easiest method for incorporating knowledge about the uncertainty in F into the linear trim problem.

SECTION 4

AN LQ-BASED CONTROL LAW REDESIGN PROCEDURE

4.1 PRELIMINARIES

The purpose of this section is to formulate and solve an optimization problem that forms the basis for the automatic redesign procedure. The primary criteria for the automatic redesign optimization problem will be to maximize the performance of the feedback system, in a specific sense, subject to constraints on the system bandwidth. The automatic redesign system will be based on Linear Quadratic design techniques [23]-[25]. The Kalman Equality [26] is used to determine the benefits that result from a LQ design and to formulate an approximation to the bandwidth constraints of the control system. A performance measure then is formulated to approximate these benefits.

We will assume that the system is described in state variable form by:

$$\dot{x}(t) = A_o x(t) + B_o u(t) \qquad (4\text{-}1)$$

where x(t) is an n-dimensional vector consisting of both the aircraft and control system compensation states, and u(t) is an m-dimensional vector of aircraft control effectors. It will also be assumed that the aircraft control system has been designed using LQ design techniques, and hence that the control u(t) minimizes

$$J = \int_0^\infty [x^T C_o^T C_o x + u^T R_o u]dt \quad . \qquad (4\text{-}2)$$

Hence, the control u(t) is given by

$$u(t) = -R_o^{-1} B_o^T K x(t) \triangleq -G_o x(t) \tag{4-3}$$

where K solves:

$$A_o^T K + K A_o + C_o^T C_o - K B_o R_o^{-1} B_o^T K = 0 \quad . \tag{4-4}$$

For any state weighting matrix C_o and any input weighting matrix R_o, the return difference D of the LQ feedback system with the loop broken at the input to the plant satisfies the Kalman Equality [26]:

$$D(-s)^T R_o D(s) = R_o + L_o(-s)^T L_o(s) \tag{4-5}$$

where

$$D(s) = I + G_o(sI - A_o)^{-1} B_o \tag{4-6}$$

$$L_o(s) = C_o(sI - A_o)^{-1} B_o \quad . \tag{4-7}$$

Many performance issues are most readily discussed in terms of sensitivity function (i.e., the inverse of the return difference) of the closed loop system evaluated at the plant input:

$$S(s) = D(s)^{-1} \tag{4-8}$$

The relationship of S to feedback system performance has been discussed extensively in the literature (c.f. [24]-[31]). In general, one obtains benefits from feedback at those frequencies for which

$$\|S(j\omega)\| < 1 \tag{4-9}$$

The benefits include improved response due to dynamic input disturbances and a reduction of the effects of parameter variation. The frequency range over which Eq. 4-9 can be achieved is generally limited by the dynamic uncertainty of the plant, sensors, and actuators. As a result of these uncertainties, the loop transfer function

$$L(s) = G_o(sI - A_o)^{-1} B_o \qquad (4\text{-}10)$$

must be rolled off before the uncertainties become significant.

The bandwidth limitations on the loop transfer function L(s) (Eq. 4-10) can be imposed by unmodeled plant, sensor, or actuator dynamics. We will assume that these constraints can be expressed in terms of a constraint on the norm of the loop transfer function at the input of the closed loop plant of the following form:

$$\|PL(j\omega_c)\| < 1 \quad . \qquad (4\text{-}11)$$

In condition 4-11, w_c represents a frequency (typically the loop cross-over frequency) at which bandwidth constraints are to be modeled. Since the loops of a multivariable system can have different bandwidths, the weighting matrix P is used to model the relative maximum size that the control loops may have at a frequency chosen to model the constraints. In effect, the matrix P can be regarded as scaling the input matrix for redesign synthesis and analysis purposes. The ability of this constraint model to accurately represent effects of the true physical uncertainties (such as actuator rate limits and aeroelastic phenomena) relies on the ability to represent all these effects at a single frequency. In a general design setting, such a representation is usually not possible. However, by assuming that the original design

for the unfailed aircraft satisfied all such constraints and by retaining any augmented dynamics (such as notch filters or dynamics that add additional rolloff in the loop shapes), the constraint model (Eq. 4-11) becomes useful. Thus, the higher frequency loop shapes of the original design will be qualitatively retained and the constraint model (Eq. 4-11) will force the quantitative constraints. This use of the constraint model (Eq. 4-11) will be adopted by the automatic redesign procedure developed in subsection 4.2.

The constraint 4-11 uses the control loop gain G explicitly. Since the gain G is related to the LQ design parameters C and R in a complex, nonlinear manner, it is desirable to approximate Eq. 4-11 with a constraint that employs C and R explicitly. Fortunately, a simple approximation to Eq. 4-11 can be obtained from the Kalman Equality (Eq. 4-5).

The attempt to ensure that the loop transfer function is small (i.e., condition 4-11 can be roughly approximated by trying to keep the return difference small (i.e., near unity). The latter can be accomplished by controlling the size of the right-hand side of Eq. 4-5. Let N denote the square root of R_o^{-1}:

$$R_o^{-1} = N_o N_o^T$$

or (4-12)

$$R_o = N_o^{-T} N_o^{-1}$$

After premultiplying Eq. 4-5 by N_o^T and postmultiplying by N_o, Eq. 4-5 becomes:

$$[N_o^{-1} D(-s) N_o]^T[N_o^{-1} D(s) N_o] = I + L_c(-s)^T L_c(s) \qquad (4\text{-}13)$$

where

$$L_c(s) = C_o(sI - A_o)^{-1} B_o N_o \quad . \qquad (4\text{-}14)$$

Thus, we can approximately impose Eq. 4-11 by using the transfer function $L_c(s)$ in Eq. 4-11 rather the true transfer function L(s). That is, we can replace Eq. 4-11 by:

$$\| PC_o(j\omega_c I - A_o)^{-1} B_o N_o \| < 1 \quad . \tag{4-15}$$

Thus, Eq. 4-15 approximately represents the bandwidth limiations and is expressed only in terms of open loop and design quanities.

4.2 DEVELOPMENT OF THE AUTOMATIC DESIGN PROCEDURE

Given a failure of one or more aircraft control surfaces, the objective of the linear restructurable control system is to redesign the linear control law in a manner that preserves as much of the aircraft safety and performance as possible. Clearly, the primary objective is to stabilize the aircraft. Assuming that this is possible for the given flight condition and available actuator power and bandwidth, the secondary but still important objective of maintaining aircraft performance can then be considered. This objective can be translated into the control system objective of maximizing the amount of beneficial feedback in order to both maximize robustness due to uncertain system parameters and to minimize disturbance effects.

The preceding considerations form the basis for the linear restructuring algorithm developed in this section. The automatic redesign procedure will use LQ regulator designs for the restructured FCS. Thus the design parameters to be chosen by the automatic redesign procedure are the quadratic penalty matrices C and R.

We will assume that a nominal LQ design for the unfailed aircraft is available. The design can be characterized by the quadratic weights C_o and R_o that were used to develop the nominal design. The automatic redesign

procedure exploits the engineering trade-offs that were made in the choice of C_o and R_o for the unfailed aircraft by fixing the new state weights,

$$C_N = C_o \tag{4-16}$$

and choosing new control weights, R_N. The choice of C_N, as in Eq. 4-16, ensures that the relative importance of each state (or combination of states) is maintained in the Linear Quadratic regulator problem for the failed aircraft design, thereby incorporating the physical engineering trade-offs from the unfailed FCS design in the restructured design.

The remaining design parameter that must be specified by the automatic redesign procedure is the input penalty matrix R. The formal objective of the automatic design procedures will be to choose R to maximize performance in an appropriate sense while satisfying the bandwidth constraints (Eq. 4-15).

Following a failure, we will assume that the automatic redesign module is supplied with estimates of the state and control matrices, A_f and B_f of the failed aircraft. To simplify the presentation, we will assume that $A_f = A_o$. The estimated control effectiveness matrix B_f will differ from the true control effectiveness matrix $\overline{B}_f$ of the failed aircraft by an amount ΔB:

$$\overline{B}_f = B_f + \Delta B \tag{4-17}$$

where ΔB represents the uncertainty in the effectiveness. We will assume that the uncertainty has zero mean:

$$E\{\Delta B\} = 0 \tag{4-18}$$

and that the covariance between the (i,j)th element and the (k,ℓ)th element is:

$$E\{\Delta B_{ij}\ \Delta B_{k\ell}\} = \beta_{ijk\ell} \quad . \tag{4-19}$$

It should be emphasized that this error model for the uncertainty of the control effectiveness coefficient is for the estimates of the failed aircraft coefficients. Since it is assumed that the nominal values are supplied by the FDI algorithm, it is reasonable to assume that these estimates are unbiased.

The post-failure control system performance is a function of the new gain G (which we wish to select) and is determined by the "size" of the return difference:

$$\bar{D}(s) = I + G(sI - A_o)^{-1} \bar{B}_f \tag{4-20}$$

Since $\bar{B}_f$ is random, so is $\bar{D}(s)$. In order to ensure that $\bar{D}$ is large when control effectiveness uncertainty exists, we wish to choose G so that both the expected size of $\bar{D}$ is large and the expected size of the uncertainty about $\bar{D}$ is small. This can be done as follows. Define $\hat{D}(s) = N^{-1} \bar{D}(s) N$, where N is the square root of the new control weighting matrix R_N. The cost functional, which we wish to minimize, is:

$$J = \left\| E\{\hat{D}(-s)^T \hat{D}(s)\} - E\left\{[\hat{D}(-s) - E\{\hat{D}(-s)\}]^T [\hat{D}(s) - E\{\hat{D}(s)\}]\right\}\right\|$$

The cost J will be large when the expected size of $\bar{D}$ is large and the expected size of the uncertainty is small. Using the Kalman Equality we can rewrite J as,

$$\begin{aligned} J = \| I + N^T B_f(-sI - A_o)^{-T} C_o^T C_o (sI - A_o)^{-1} B_f N \\ - N^T E\{\Delta B^T (-sI - A_o)^{-T} G^T R_N G(sI - A_o)^{-1} \Delta B\} N \| \end{aligned} \tag{4-21}$$

Equation 4-21 will be used as the measure of performance that is to be maximized by the choice of R_N (i.e., N) and, hence, G. We now define the norm in Eq. 4-21 as the trace of the integral of the frequency terms,

$$J = \mathrm{Tr}\{N^T[W_{co} - W_u]N\} \tag{4-22}$$

where

$$W_{co} = B_f^T W_o B_f \tag{4-23}$$

$$W_u = E\{\Delta B^T \bar{W_o} \Delta B\} \tag{4-24}$$

$$W_o = \int_0^\infty (-j\omega I - A_o)^{-T} C_o^T C_o (j\omega I - A_o)^{-1} d\omega \tag{4-25}$$

$$\bar{W_o} = \int_0^\infty (-j\omega I - A_o)^{-T} G^T R_N G (j\omega I - A_o)^{-1} d\omega \quad . \tag{4-26}$$

Formulas 4-23 and 4-26 can be simplified. First, by using the approximation

$$G^T R G \approx C_o^T C_o \tag{4-27}$$

Eqs. 4-25 and 4-26 become identical. By Parseval's theorem, if A_o has all its eigenvalues in the left half plane, W_o is the solution to the Lyapunov equation:

$$A_o^T W_o + W_o^T A_o + C_o^T C_o = 0 \quad . \tag{4-28}$$

If A_o has one or more eigenvalues in the right half plane, a stable factorization of Eq. 4-25 can be used to compute W_o from an analogous Lypunov equation. Assume that the system matrix has the spectral decomposition:

$$A_o = [W_s \; W_u] \begin{bmatrix} \Lambda_s & 0 \\ 0 & \Lambda_u \end{bmatrix} \begin{bmatrix} V_s^H \\ V_u^H \end{bmatrix} \tag{4-29}$$

where Λ_s is a diagonal matrix with its diagonal elements being the left half plane eigenvalues of A_o, and Λ_u is a diagonal matrix with its diagonal elements being the right half plane eigenvalues of A_o. Define

$$\bar{A} = [W_s \; W_u] \begin{bmatrix} \Lambda_s & 0 \\ 0 & -\Lambda_u \end{bmatrix} \begin{bmatrix} V_s H \\ V_u H \end{bmatrix} \tag{4-30}$$

Then W_o is the solution of the Lyapunov equation (Eq. 4-28) with $\bar{A}$ replacing A_o. For computational purposes, W and V in Eqs. 4-29 and 4-30 can be replaced by any matrices that effect a decomposition of A_o into its stable and unstable invariant subspaces. Assuming that the system matrix is not significantly affected by the failure, these matrices can be computed off-line. If the failure effects on the system must be incorporated, the matrices can be computed efficiently and accurately.

Finally, Eq. 4-24 can be rewritten as:

$$W_{u_{ij}} = \sum_{k=1}^{n} \sum_{\ell=1}^{n} W_{o_{k\ell}} \beta_{ki\ell j} \quad . \tag{4-31}$$

where $\beta_{ki\ell j} = E\{\Delta B_{ki} \; \Delta B_{\ell j}\}$.

The objective is to maximize J in Eq. 4-22. This is to be achieved subject to the bandwidth limitations as expressed by Eq. 4-15. That is, we must satisfy,

$$\| PC_o(j\omega_c - A_o)^{-1} \; B_f N \| \leq 1 \quad . \tag{4-32}$$

Using the Schwarz inequality,

$$\| PC_o(j\omega_c - A_o)^{-1} \; B_f N \| \leq \| PC_o(j\omega_c - A_o)^{-1} \; B_f N_o \| \cdot \| N_o^{-1} \; N \| \quad .$$

If we are dealing only with failures that result in decreased effectiveness and/or decreased bandwidth, then

$$\| PC_o(j\omega_c - A_o)^{-1} \; B_f N_o \| \leq \| PC_o(j\omega_c - A_o)^{-1} \; B_o N_o \| \leq 1$$

where the last inequality comes from the assumption that the nominal LQ design satisfies the bandwidth constraints as modeled by Eq. 4-15. Thus, Eq. 4-32 is achieved when N satisfies,

$$\|N_o^{-1} N\| < 1 \quad . \tag{4-32b}$$

Hence the objective of maximizing performance in the presence of control effectiveness uncertainty is formulated as solving Eq. 4-22 subject to Eq. 4-32b.

4.3 SOLUTION OF THE OPTIMIZATION PROBLEM

Define

$$Y = N_o^{-1} N \quad . \tag{4-33}$$

Then Eqs. 4-22 and 4-32b become:

$$\max \mathrm{Tr}\{Y^T W Y\} \tag{4-34}$$

subject to

$$\|Y\| < 1 \tag{4-35}$$

where

$$W = N_o^T [W_{co} - W_u] N_o \quad . \tag{4-36}$$

The solution can be obtained in terms of the eigenvectors of W. Let the columns of Y be an orthonormal basis for the invariant subspace (eigenspace) of W corresponding to the nonnegative eigenvalues of W. Then Y solves Eqs. 4-34 through 4-36. The matrix N is given by

$$N = N_o Y \tag{4-37}$$

and the design matrix R and is specified by

$$R_N^{-1} = N N^T \quad . \tag{4-38}$$

4.4 DISCUSSION

Objective 4-22 has a nice interpretation in terms of the effectiveness of control on the important state variables. Recall that it was assumed that C_o has been chosen to reflect the relative importance of the various state variables to the performance of the aircraft. The matrix $B_f^T W_o B_f$ then reflects the amount of energy that can be transmitted to those variables, weighted by their perceived importance, from each of the available control surfaces. Hence, Eq. 4-22 captures the issue of quantifying control effectiveness via the matrix W_{co}. Objective 4-22 also captures the issue of quantifying control surface uncertainty through the matrix W_u. Hence, the objective is to maximize the beneficial feedback (W_{co}) minus the uncertainty (W_u).

The solution (Eqs. 4-37 and 4-38) reflects these issues. A negative eigenvalue of W results only if uncertainty exceeds benefit in some direction. This direction is represented by the corresponding eigenvector of W and is eliminated from consideratin in the control law design. Hence, the solution eliminates those combinations of controls for which the control uncertainty exceeds the control effectiveness within the feedback design.

The automatic design algorithm can be summarized as follows. It assumes that a nominal LQ design has been chosen with nominal weights C_o and R_o. It also assumes that an FDI algorithm has indicated a control surface failure:

Step 1: Form the matrices B_f and N_o.

Step 2: Compute W from Eqs. 4-23, 4-28 through 4-31 and 4-36.

Step 3: Find the eigenvectors $v_1,\ldots,v_\ell$ corresponding to the nonnegative eigenvalues of W. Define

$$N = N_o[v_1,\ldots,v_\ell] \quad .$$

Step 4: Compute

$$R_N^{-1} = N\,N^T \quad .$$

Step 5: Solve the LQ regulator problem

$$A_o^T K + K A_o + C_o^T C_o - K B_f R_N^{-1} B_f^T K = 0$$

$$G = R_N^{-1} B_f^T K \quad .$$

If $W_u = 0$, the solution of the automatic redesign optimization problem (Eqs. 4-22 and 4-32) is almost trivial. Since

$$W_o > 0 \tag{4-39}$$

the objective functional, J, (Eq. 4-22) is also positive for any choice of N, and is monotonely nondecreasing as N increases in size. Thus, N should be chosen as large as possible. The only constraint on N is the bandwidth constraint 4-32b. Hence the choice

$$N = N_o \tag{4-40}$$

solves the automatic redesign problem.

Thus, in the case when information about control effector uncertainty is not used by the automatic redesign procedure, the procedure simply solves a LQ regulator problem with the new system description supplied by the FDI algorithm and the nominal design quadratic weights C_o and R_o. This has the advantage of not requiring any computation to choose the design parameters. Yet, since it is the solution to the automatic redesign optimization, this simple procedure effectively maximizes the achievable performance within the bandwidth constraints of the system.

4.5 EXTENSION OF THE REDESIGN PROCEDURE FOR PLANTS WITH INTEGRATOR STATES

In this subsection, we modify the redesign procedure so that plants with integrator states (poles at the origin) may be handled. Recall that when we had unstable poles, a unique positive definite solution to the Lyapunov equation was obtained by evaluating the observability Grammian for the same system with the unstable poles reflected about the $j\omega$ axis. This procedure is necessitated by the fact that the procedure for computing the grammian guarantees a unique positive definite solution only when the system is stable. The grammian obtained by this method solves the desired frequency integral for the unstable system.

When the system has poles at the origin, the desired frequency integral is infinite so we must modify the procedure to obtain meaningful answers. To begin our discussion, recall that the redesign procedure is based on maximizing some matrix norms of the frequency integral,

$$W_{co} = \int_{j\omega = -\infty}^{\infty} L(s)\, L(-s)^H\, ds \tag{4-41}$$

where

$$L(s) = C(sI - A)^{-1} B \tag{4-42}$$

and

$$Q = C^T C \tag{4-43}$$

Furthermore, when the system has integator states, we can write,

$$A = \begin{bmatrix} A_p & 0 \\ C_I & 0 \end{bmatrix} \tag{4-44}$$

$$B = \begin{bmatrix} B_p \\ 0 \end{bmatrix} \tag{4-45}$$

$$C = \left[\begin{array}{c|c} M_p & M_I \end{array}\right] \tag{4-46}$$

$$Q = \begin{bmatrix} Q_p & Q_{pI} \\ Q_{pI}^T & Q_I \end{bmatrix} \quad . \tag{4-47}$$

where

$$Q_p = M_p^T M_p$$

$$Q_I = M_I^T M_I$$

$$Q_{pI} = M_p^T M_I \quad .$$

Using Eqs. 4-44 through 4-47 in Eq. 4-22, we have

$$L(s) = M_p(sI - A_p)^{-1} B_p + \frac{1}{s} M_I C_I (sI - A_p)^{-1} B_p \quad . \tag{4-48}$$

At low frequencies, the second term in Eq. 4-48 dominates while at high frequencies, the first term is dominant. In the frequency region of interest, both terms may be important.

The notion that a particular range of frequencies is of primary importance can now be exploited for our purposes. Suppose we define a new loop transfer function,

$$L_w(s) = L(s) \cdot W(s) \quad . \tag{4-49}$$

Then the integral (Eq. 4-41) using $L_w(s)$ instead of $L(s)$ is just a frequency weighted integral,

$$\int L(s)\ H(s)\ L(-s)^H \tag{4-50}$$

where

$$H(s) = W(s)\ W(-s)^H \quad . \tag{4-51}$$

The weighting W(s) can now be used to cancel the integrator poles and thereby make W_{co} finite.

To see how this is implemented, consider a simple example with,

$$W(s) = I \cdot \left(\frac{s}{s+a} \right) \tag{4-52}$$

Note that in general, one may want to use different frequency weightings for each loop (e.g., $[W(s)]_{ii} = \frac{s}{s + a_i}$). Now although one could simply argue that the state matrix, A, with the additional dynamics for W(s), define a new Q matrix, and solve the Lyapunov equation, this procedure will result in numerical problems because of the implicit pole-zero cancellations. In order to avoid these numerical problems, we perform the pole-zero cancellations explicitly and develop a new A and Q matrix which results in the desired W_{co} when the Lyapunov equation is solved.

Using Eqs. 4-52, 4-49,and 4-48, we have

$$L_w(s) = M_p(sI - A_p)^{-1} B_p \frac{s}{s+a} + M_I C_I (sI - A_p)^{-1} Bp \frac{1}{s+a} \quad . \tag{4-53}$$

Let W(s) be obtained from the minimal realization,

$$W(s) = C_w(sI - A_w)^{-1} B_w + D_w \tag{4-54}$$

with

$$A_w = -aI$$

$$B_w = I$$

$$C_w = -aI$$

$$D_w = I \quad .$$

If we define,

$$A_a = \begin{bmatrix} A_p & 0 \\ B_w & A_w \end{bmatrix} \tag{4-55}$$

$$B_a = \begin{bmatrix} B_p \\ 0 \end{bmatrix} \tag{4-56}$$

$$C_a = \left[\begin{array}{c|c} M_p & M_I C_I - a\, M_p \end{array}\right]$$

then it can be verified that

$$L_w(s) = C_a(sI - A_a)^{-1}\, B_a \tag{4-57}$$

with

$$Q_a = C_a{}^T C_a = \left[\begin{array}{c|c} Q_p & -aQ_p + Q_{PI}C_I \\ \hline -aQ_p{}^T + C_I{}^T Q_{PI}{}^T & C_I{}^T Q_I C_I + a^2 Q_p - aC_I{}^T Q_{PI}{}^T - aQ_{PI}C_I \end{array}\right] . \tag{4-58}$$

Finally,

$$W_{co} = \int L_w(s)\; L_w(-s)^H\, ds \tag{4-59}$$

is solved by the Lyapunov equation

$$A_a{}^T W_o + W_o{}^T A_a + Q_a = 0 \tag{4-60}$$

and

$$W_{co} = B_a{}^T\, W_o\, B_a \quad . \tag{4-61}$$

SECTION 5

A PROTOTYPE RESTRUCTURABLE CONTROL SYSTEM

This subsection will give an explicit description of the entire restructurable control system, so that the operation of the system can be seen.

5.1 PRELIMINARIES

We assume that we have our linearized aircraft model in state-space form

$$\begin{aligned} \dot{x} &= Ax + Bu \qquad u \in R^m \ , \ x \in R^n \\ y &= Cx \qquad\qquad y \in R^p \\ x_r &= C_r x \qquad\quad x_r \in R^{n-p} \end{aligned} \tag{5-1}$$

$$C = \underset{p\times p \quad p\times n-p}{\left[\begin{array}{c:c} I & 0 \end{array}\right]} \qquad C_r = \underset{n-p\times p \quad n-p\times n-p}{\left[\begin{array}{c:c} 0 & I \end{array}\right]}$$

$$x = \begin{bmatrix} y \\ x_r \end{bmatrix}$$

where y are the important states that we would like to control very closely. Note that we must have (A,B) a controllable pair and (A,C) an observable pair, with rank (C) = p, rank (B) $\geq$ p in order to independently control the output y.

While the automatic trim system will attempt to reduce the effect of disturbances (e.g., stuck surfaces), there will always be some residual constant

disturbance that we didn't predict. In order to reject this disturbance completely from those important states we need to add integrators. Thus, we form the new augmented system

$$\begin{bmatrix} \dot{x} \\ \dot{x}_I \end{bmatrix} = \begin{bmatrix} A & 0 \\ C & 0 \end{bmatrix} \begin{bmatrix} x \\ x_I \end{bmatrix} + \begin{bmatrix} B \\ 0 \end{bmatrix} u \tag{5-2}$$

or

$$\dot{z} = \tilde{A}z + \tilde{B}u \quad . \tag{5-3}$$

We now pose the LQ problem for this augmented system:

Find u(t) to minimize

$$J = \int_0^\infty [z^T Q z + u^T R u]dt \tag{5-4}$$

where $Q = Q^T \geq 0$ is $n+p \times n+p$ and $R = R^T > 0$ is $m \times m$.

The solution is given by

$$u = -Gz = -\left[\begin{array}{c:c:c} G_y & G_r & G_I \end{array}\right] \begin{bmatrix} y \\ x_r \\ x_I \end{bmatrix} \tag{5-5}$$

where

$$G = R^{-1}B^T K \tag{5-6}$$

and $K = K^T \geq 0$ solves

$$0 = \tilde{A}^T K + K\tilde{A} + Q - K\tilde{B}\tilde{R}^{-1}\tilde{B}^T K \quad . \tag{5-7}$$

A command-following control system using this state-feedback gain G is shown in Fig. 5-1. Here, r is the desired deviation from the setpoint y_o and is controlled by the pilot through some input shaping filter.

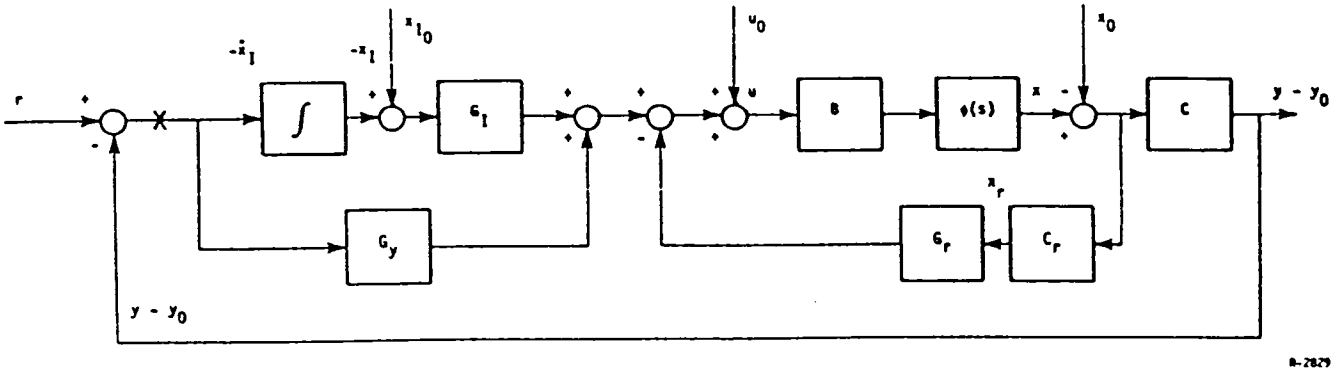

Figure 5-1. Command Following With LQ

Due to the integrators, we will achieve $y = r + y_o$ exactly in steady state (i.e., $r \equiv$ constant). The closed-loop system of Fig. 2-10 with $r \equiv 0$ is

$$\dot{z} = \tilde{A}z + \tilde{B}[-Gz + u_o + Gz_o] \tag{5-8}$$

where u_o and z_o are the setpoints desired by the automatic trim system. They must satisfy

$$0 = \tilde{A}z_o + \tilde{B}u_o \quad . \tag{5-9}$$

Note that we are selecting $z_o = \begin{bmatrix} x_o \\ x_{IO} \end{bmatrix}$ so that we can pick a setpoint for the integrator states x_I. Suppose we pick x_{IO} to be zero. That means that the integrated value of $y = Cx$ must be zero (since x_I approaches x_{IO} in steady state) and in general, we will obtain an overshoot in our initial condition response, even if all eigenvalues of A-BG are real. To see this, consider the simple example in Fig. 5-2, with the initial conditions

$$x_1(0) = 0 \tag{5-10}$$

$$x_2(0) = -1 \tag{5-11}$$

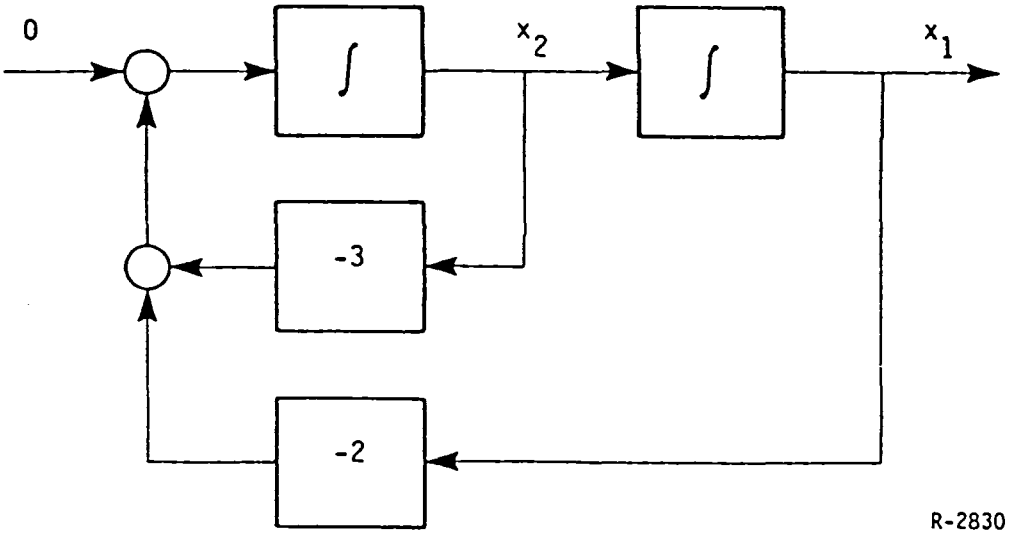

Figure 5-2. Simple Example Demonstrating Overshoot

Since the system is stable, x_1, x_2 both decay to zero, but

$$x_1(t) = \int_0^t x_2(\tau)d\tau \qquad (5\text{-}11)$$

so that the area under $x_2(t)$ must go to zero - so we have overshoot. Note that the eigenvalues of this system are -1 and -2 and are both real. To see what the freedom in picking the initial condition of the integrator state (x_1 here) can do for us, consider the eigenvectors of the A matrix associated with the above system:

$$A = \begin{bmatrix} 0 & 1 \\ -2 & -3 \end{bmatrix}$$

$$\lambda_1 = -1 \; ; \; v_1 = \begin{bmatrix} .707 \\ -.707 \end{bmatrix}$$

$$\lambda_2 = -2 \; ; \; v_2 = \begin{bmatrix} -1 \\ 2 \end{bmatrix}$$

Thus, if we pick $x_o = \begin{bmatrix} 1 \\ -1 \end{bmatrix}$, we have $x(t) = x_o e^{\lambda_1 t}$ and there is no overshoot. Another possibiliby would be to pick $x_o = \begin{bmatrix} .5 \\ -1 \end{bmatrix}$ and we would see only the eigenvalue at -2, and thus a much faster response.

From this simple example, it seems very likely that the freedom of choosing the integrator setpoint can have an impact on the resulting initial condition response. This subject will remain a topic for future research and will not be addressed any more in this report. It should be emphasized, however, that this type of overshoot with well-damped poles does not occur in the command response and is only important for determining the dynamic transient-response to changes in setpoint.

5.2 A RESTRUCTURABLE FLIGHT CONTROL SYSTEM

Now we are ready to put the whole system together. We link all the subsystems together as shown in Fig. 5-3. The Failure Detection and Isolation (FDI) block determines when a failure has occurred and computes the new A and B matrices for the aircraft. Since here we are only concerned with actuator failures, only the B matrix will change. The automatic trim system block then determines the best operating point for the aircraft, based on the solution of the trim problem described in Section 3. This operating point is used by the dynamic compensator (as in Fig. 5-1). The control redesign block also uses the A,B matrices from the FDI block in order to compute the new gain matrix G which is used by the dynamic compensator. The Q and R matrices are parameters for the control redesign block and are computed from the redesign procedures described in Section 4. Under no uncertainty, Q and R remain the same and G is computed by solving the regulator problem with the new A and B matrices.

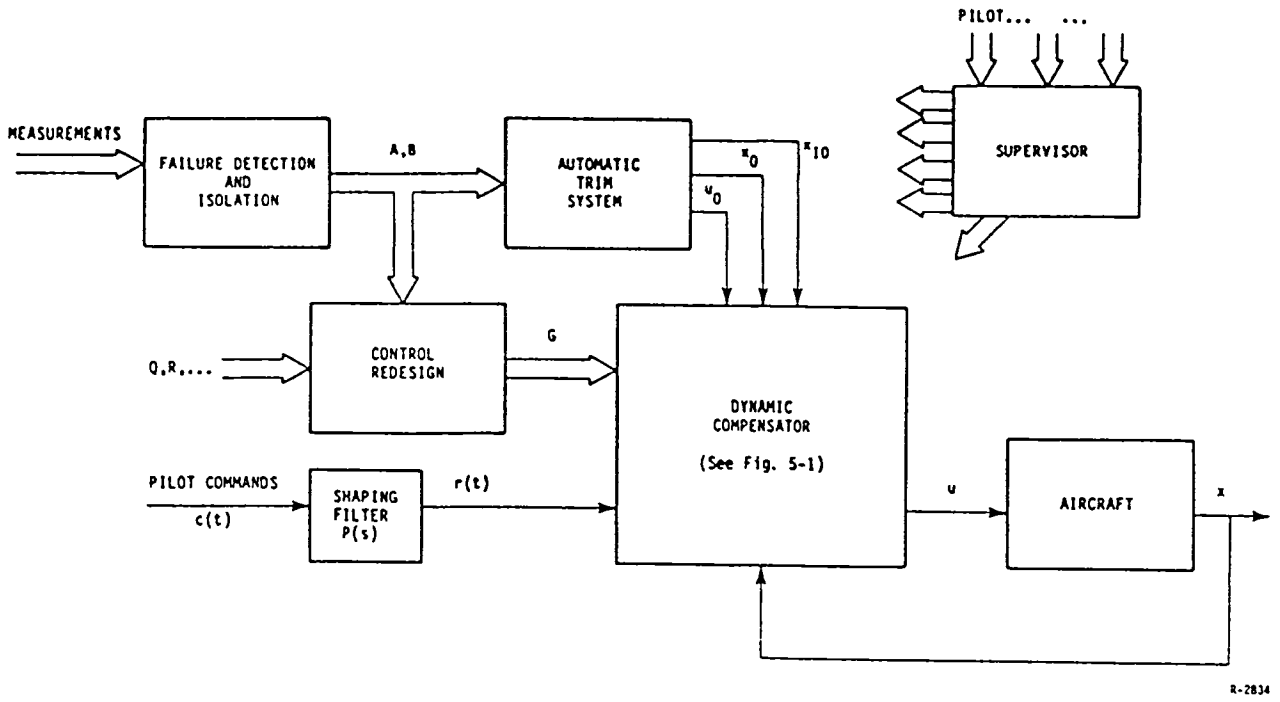

Figure 5-3. Complete Restructurable Control System

The pilots commands go through a shaping filter before being introduced into the control loop. This is to both mix the pilot commands (if necessary) and to slow them down if necessary. They are mixed so that the pilot stick commands are interpreted correctly by the control system. They are filtered so that steps are not introduced into the control loops, thus reducing overshoots and control saturation. A possible form for a preshaping filter is given in Fig. 5-4. Note that what the pilot controls is a deviation from the operating point which is determined by the trim problem. Thus, if undesirable attitude coupling appears in the trim solution (e.g., side slip during a rudder failure which necessitates a de-crab maneuver before touchdown) it can be removed by the pilot through application of non-zero, constant r(t).

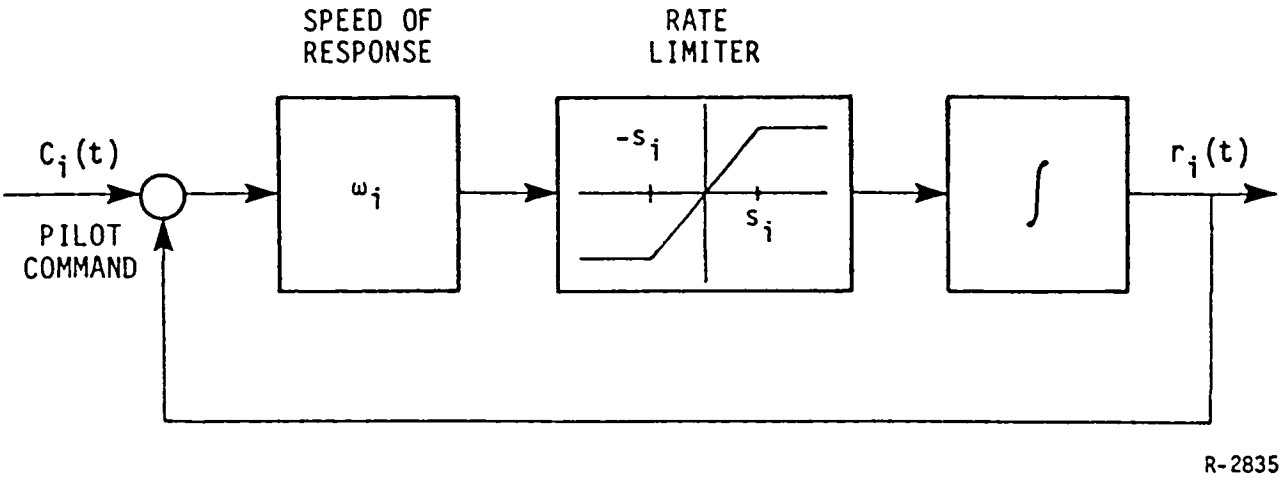

Figure 5-4. Example of a Shaping Filter for the i-th Control Channel

Finally, the supervising block determines the flow and order of reconfiguration actions. This block must decide on a variety of issues which include:

1. Sequencing and fading of trim and redesign solution application,
2. Adequacy of trim solution and need to select a new operating point,
3. Immediacy versus accuracy of trim solutions which require large numbers of iterations for convergence,
4. Weightings and scalings of variables in the trim problem,
5. The need for refinement of redesign and trim solutions based on more accurate FDI information, and
6. Logical interfacing with the pilot through a flight-director.

SECTION 6

APPLICATION TO A TRANSPORT CLASS AIRCRAFT (BOEING 737 MODEL)

The automatic redesign procedure (presented in Section 4) and the automatic trim solution (presented in Section 3) will be demonstrated in this section on a linearized model of a modified Boeing 737 aircraft. The model is described in subsection 6.1. Subsection 6.2 develops the nominal state-feedback design for the unfailed aircraft, and subsections 6.3 and 6.4 present some linear analyses of the trim and redesign procedures.

6.1 AIRCRAFT MODEL

A linearized model of the modified NASA Boeing 737 aircraft operating at different flight conditions was supplied by NASA to ALPHATECH to demonstrate the automatic design procedure. Since the aircraft potentially has nine independent control surfaces, it is an ideal candidate for control restructuring. For this demonstration, an operating point with a flight angle (γ) of -3 degrees, pitch angle (θ) of -.7 degrees, forward velocity (u) of 215 feet/sec, downward velocity (w) of 8.7 feet/sec, and altitude of 1500 ft was chosen. The flaps are set at 40 degrees.

The linear aircraft model is in the form

$$\dot{x}_a(t) = A_a\, x_a(t) + B_a\, u_a(t) \qquad (6\text{-}1)$$

where $x_a(t)$ is a state vector of the linear aircraft dynamics and $u_a(t)$ is the vector of available control surfaces. The state vector is given by

$$x_a = \begin{bmatrix} u \\ w \\ q \\ \theta \\ v \\ p \\ r \\ \phi \end{bmatrix} = \begin{bmatrix} \text{forward velocity, ft/sec} \\ \text{vertical velocity, ft/sec} \\ \text{pitch rate, rad/sec} \\ \text{pitch angle, rad} \\ \text{side velocity, ft/sec} \\ \text{roll rate, rad/sec} \\ \text{yaw rate, rad/sec} \\ \text{roll angle, rad} \end{bmatrix} \tag{6-2}$$

The NASA model included a ninth state for yaw angle which was eliminated since it will not be controlled by the regulation system. The longitudinal dynamics are decoupled from the lateral dynamics in the unfailed aircraft. The first four states represent the longitudinal dynamics and the second four represent the lateral dynamics.

The input vector is given by

$$u_a = \begin{bmatrix} \delta_{LT} \\ \delta_{RT} \\ \delta_{LS} \\ \delta_{RS} \\ \delta_R \\ \delta_{LE} \\ \delta_{RE} \\ \delta_{LA} \\ \delta_{RA} \end{bmatrix} = \begin{bmatrix} \text{left engine thrust, lbs} \\ \text{right engine thrust, lbs} \\ \text{left stabilator, deg} \\ \text{right stabilator, deg} \\ \text{rudder, deg} \\ \text{left elevator, deg} \\ \text{right elevator, deg} \\ \text{left aileron, deg} \\ \text{right aileron, deg} \end{bmatrix} \tag{6-3}$$

The system matrix for this operating condition is given by

$$A_a = \left[\begin{array}{cccccccc}
-0.03735 & 0.1055 & -8.692 & -32.17 & 0.0 & 0.0 & 0.0 & 0.0 \\
-0.2763 & -0.7054 & 215.41 & 0.4196 & 0.0 & 0.0 & 0.0 & 0.0 \\
-0.0002007 & -0.006228 & -0.5193 & -0.0003222 & 0.0 & 0.0 & 0.0 & 0.0 \\
0.0 & 0.0 & 0.0 & 1.0 & 0.0 & 0.0 & 0.0 & 0.0 \\
\hline
0.0 & 0.0 & 0.0 & 0.0 & -0.1451 & 10.35 & -214.5 & 32.17 \\
0.0 & 0.0 & 0.0 & 0.0 & -0.01685 & -1.529 & 0.8053 & 0.000003381 \\
0.0 & 0.0 & 0.0 & 0.0 & 0.003239 & -0.1212 & -0.1458 & -0.004113 \\
0.0 & 0.0 & 0.0 & 0.0 & 0.0 & 1.0 & -0.0120 & 0.0
\end{array}\right] \qquad (6\text{-}4)$$

The input matrix is given by

$$B_a = \left[\begin{array}{ccccccccc}
0.0003785 & 0.0003785 & 0.006813 & 0.006813 & 0.0 & 0.003266 & 0.0032660 & 0.003647 & 0.003647 \\
-0.0000002952 & -0.0000002952 & -0.1688 & -0.1688 & 0.0 & -0.08093 & -0.08093 & -0.09037 & -0.09037 \\
0.000006263 & 0.000006263 & -0.0221 & -0.0221 & 0.0 & -0.01059 & -0.01059 & -0.002849 & -0.002849 \\
0.0 & 0.0 & 0.0 & 0.0 & 0.0 & 0.0 & 0.0 & 0.0 & 0.0 \\
\hline
0.0 & 0.0 & 0.0 & 0.0 & 0.1389 & 0.0 & 0.0 & 0.0004774 & -0.0004774 \\
0.000002128 & -0.000002128 & 0.007411 & -0.007411 & 0.009317 & 0.003552 & -0.003552 & 0.008208 & -0.008208 \\
0.00001245 & -0.00001245 & 0.0004336 & -0.0004336 & -0.0109 & 0.0002637 & -0.0002637 & 0.0007019 & -0.0007019 \\
0.0 & 0.0 & 0.0 & 0.0 & 0.0 & 0.0 & 0.0 & 0.0 & 0.0
\end{array}\right] \qquad (6\text{-}5)$$

The open-loop eigenvalues of the aircraft are:

Longitudinal	Short Period:	$-0.614 \pm 1.5j$
	Phugoid:	$-0.0167 \pm 0.17j$
Lateral	Dutch Roll:	$-.058 \pm 1.106j$
	Spiral:	$-.0063$
	Roll Subsidence:	-1.699

6.2 CONTROLLER DESIGN

This subsection describes the design process followed to arrive at the final state-feedback controller. Since the longitudinal and lateral dynamics are decoupled for the unfailed aircraft, we can design them separately. To decouple the inputs, we need to mix them to obtain differential and collective inputs. We do this as follows. Let

$$B_{MIX} \triangleq \left[\begin{array}{cccc|c|cccc} 0 & 0 & 1 & 1 & 0 & 0 & 0 & 0 & 0 \\ 0 & 0 & 0 & 0 & 0 & 1 & 1 & 0 & 0 \\ 1 & 1 & 0 & 0 & 0 & 0 & 0 & 0 & 0 \\ 0 & 0 & 0 & 0 & 0 & 0 & 0 & 1 & 1 \\ 0 & 0 & 0 & 0 & 1 & 0 & 0 & 0 & 0 \\ 0 & 0 & 0 & 0 & 0 & 0 & 0 & 1 & -1 \\ 0 & 0 & 1 & -1 & 0 & 0 & 0 & 0 & 0 \\ 0 & 0 & 0 & 0 & 0 & 1 & -1 & 0 & 0 \\ 1 & -1 & 0 & 0 & 0 & 0 & 0 & 0 & 0 \end{array}\right]_{9\times 9} \qquad (6\text{-}6)$$

so

$$u_{NEW} = B_{MIX} \cdot u_a$$

where

$$u_{new} = \left[\begin{array}{c} \delta_{CS} \\ \delta_{CE} \\ \delta_{CT} \\ \delta_{CA} \\ \hline \delta_R \\ \delta_{DA} \\ \delta_{DS} \\ \delta_{DE} \\ \delta_{DT} \end{array}\right] = \left[\begin{array}{ll} \text{collective stabilator} & \left.\begin{array}{l} \\ \\ \\ \end{array}\right\} \text{Longitudinal} \\ \text{collector elevator} & \\ \text{collective thrust} & \\ \text{collective aileron} & \\ \hline \text{rudder} & \left.\begin{array}{l} \\ \\ \\ \\ \\ \end{array}\right\} \text{Lateral} \\ \text{differential aileron} & \\ \text{differential stabilator} & \\ \text{differential elevator} & \\ \text{differential thrust} & \end{array}\right] \qquad (6\text{-}7)$$

We now need to scale the inputs according to their maximum values. Note that we cannot define absolute maximum limits for differential and collective inputs independently. However, as we are just using this to scale the inputs so things are weighted correctly, it is not as important. We pick the scaling for the new inputs as follows

$$u_p = S_1^{-1} u_{new}$$

where

$$S_1 \triangleq \text{diag}(10,20,1000,20,20,20,10,20,1000) \quad . \tag{6-8}$$

We then let

$$B_1 = B_a(B_{MIX})^{-1} S_1 \tag{6-9}$$

be our new B matrix, which is mixed and scaled.

In order to make the state variables easier to work with, we would like to scale them so that 1 unit in each of the state variables is approximately equivalent in terms of importance. If we choose

$$x_p = T_1 \cdot x_a \tag{6-10}$$

where

$$T_1 = \text{diag}(0.01,0.01,1,1,0.01,1,1,1) \tag{6-11}$$

then our new system matrices are

$$A_p = T_1 \cdot A_a \cdot T_1^{-1} \tag{6-12}$$

$$B_p = T_1 \cdot B_1 \tag{6-13}$$

and the linear aircraft model becomes

$$\dot{x}_p = A_p x_p + B_p u_p \quad .$$

We can now split the aircraft model into a longitudinal model and a lateral model, and devise an LQ design for each of these.

6.2.1 Lateral Design

The lateral model is given by

$$A_{LAT} = \begin{bmatrix} -0.1451 & 0.1035 & -2.1450 & 0.3216 \\ -1.6853 & -1.5292 & 0.8053 & 0.0000 \\ 0.3239 & -0.1212 & -0.1458 & -0.0041 \\ 0.0000 & 1.0000 & -0.0120 & 0.0000 \end{bmatrix} \qquad (6\text{-}14)$$

$$B_{LAT} = \begin{bmatrix} 0.0278 & 0.0001 & 0.0000 & 0.0000 & 0.0000 \\ 0.1863 & 0.1642 & 0.0741 & 0.0710 & 0.0021 \\ -0.2180 & 0.0140 & 0.0043 & 0.0053 & 0.0124 \\ 0.0000 & 0.0000 & 0.0000 & 0.0000 & 0.0000 \end{bmatrix} \qquad (6\text{-}15)$$

The states are the scaled versions of the lateral states, viz.,

$$x = \begin{bmatrix} v/100 \\ p \\ r \\ \phi \end{bmatrix} = \begin{bmatrix} \text{side velocity, ft/sec} \\ \text{roll rate, rad/sec} \\ \text{yaw rate, rad/sec} \\ \text{roll angle, rad} \end{bmatrix} \qquad (6\text{-}16)$$

and the scaled inputs are

$$u = \begin{bmatrix} \delta_R/20 \\ \delta_{DA}/20 \\ \delta_{DS}/10 \\ \delta_{DE}/20 \\ \delta_{DT}/1000 \end{bmatrix} \qquad (6\text{-}17)$$

One of the goals we would like to achieve in the lateral axis is automatically coordinated flight. One way to achieve this approximately is to control side-velocity and bank angle. Thus, a nonzero commanded bank angle with a zero-commanded side velocity would produce a steady turn, with only a small residual side acceleration that the pilot can eliminate with the side velocity controls (rudder pedals). This also allows for coordinated turns with failures, without the pilot having to worry about the coordination of the turn.

Thus, we decide to control side velocity, v, and bank angle, ϕ. To eliminate steady-state errors, we put integrators on those states. Let

$$C_{LAT} = \begin{bmatrix} 1 & 0 & 0 & 0 \\ 0 & 0 & 0 & 1 \end{bmatrix} \tag{6-18}$$

so that

$$y = \begin{bmatrix} v \\ \phi \end{bmatrix} = C_{LAT}\, x \tag{6-19}$$

Our new augmented plant is given by

$$\dot{z} = \begin{bmatrix} \dot{x} \\ \dot{x}_I \end{bmatrix} = \begin{bmatrix} A_{LAT} & 0 \\ C_{LAT} & 0 \end{bmatrix} \begin{bmatrix} x \\ x_I \end{bmatrix} + \begin{bmatrix} B_{LAT} \\ 0 \end{bmatrix} u \tag{6-20}$$

or

$$\dot{z} = \tilde{A}z + \tilde{B}u \quad . \tag{6-21}$$

Our first trial was

$$R = I$$

$$Q = I \quad .$$

The resulting closed-loop eigenvalues are

$$-0.377 \pm 1.200j$$

$$-1.7058$$

$$-0.435 \pm 0.269j$$

$$-0.139$$

These closed-loop eigenvalues are too lightly damped. So, in order to increase the damping, we increased the weighting on the roll rate. In addition, in order to raise the integrator action somewhat, we increased the weights on the two integrator states. We finally settled on

$$R = I \tag{6-22}$$

$$Q_{LAT} = \begin{bmatrix} 3 & 0 & 0 & 0 & 0 & 0 \\ 0 & 20 & 0 & 0 & 0 & 0 \\ 0 & 0 & 1 & 0 & 0 & 0 \\ 0 & 0 & 0 & 1 & 0 & 0 \\ 0 & 0 & 0 & 0 & 40 & 0 \\ 0 & 0 & 0 & 0 & 0 & 40 \end{bmatrix} \tag{6-23}$$

which produced closed-loop eigenvalues of

$$-0.855 \pm 1.50j$$

$$-.616 \pm 0.504j$$

$$-1.877$$

$$-1.104$$

and a state-feedback gain matrix of

$$G_{LT} = \begin{bmatrix} 8.0152 & -0.8558 & -12.6637 & -2.8876 & 5.9409 & -2.1514 \\ -2.6946 & 5.1579 & 5.5219 & 10.3317 & 1.8254 & 5.0554 \\ -1.1336 & 2.2747 & 2.3427 & 4.5473 & 0.8477 & 2.2211 \\ -1.1340 & 2.2109 & 2.3305 & 4.4249 & 0.7986 & 2.1638 \\ -0.5543 & 0.4002 & 1.0030 & 0.8584 & -0.1300 & 0.4463 \end{bmatrix} \quad (6\text{-}24)$$

By examining the individual elements of G_{LT}, we can determine that the control gains are not too large and are quite acceptable. Remember that the inputs and states have been scaled.

The singular values of the scaled loop transfer function for this final design are given in Fig. 6-1. The dominant contributing inputs to each loop are shown on the plot, as determined by examining the left singular vectors. The loop transfer function crossover frequency of about 3 rad/sec provides sufficient bandwidth for command following and adequate stability margins. Figure 6-2 shows the singular values of the loop broken at the error signal for command following (x in Fig. 5-1). They look quite good and we expect the lateral subsystem to follow v and ϕ commands very well. Figure 6-3 shows the singular values of the closed-loop map from reference inputs to actual outputs. We expect it to follow commands well out to about 1 rad/sec, and do extremely well out to 0.1 rad/sec.

6.2.2 Longitudinal Design

The longitudinal model we have is given by

$$A_{LON} = \begin{bmatrix} -0.0374 & 0.1055 & -0.0869 & -0.3217 \\ -0.2763 & -0.7054 & 2.1541 & 0.0042 \\ -0.0201 & -0.6228 & -0.5193 & -0.0003 \\ 0.0000 & 0.0000 & 1.0000 & 0.0000 \end{bmatrix} \quad (6\text{-}25)$$

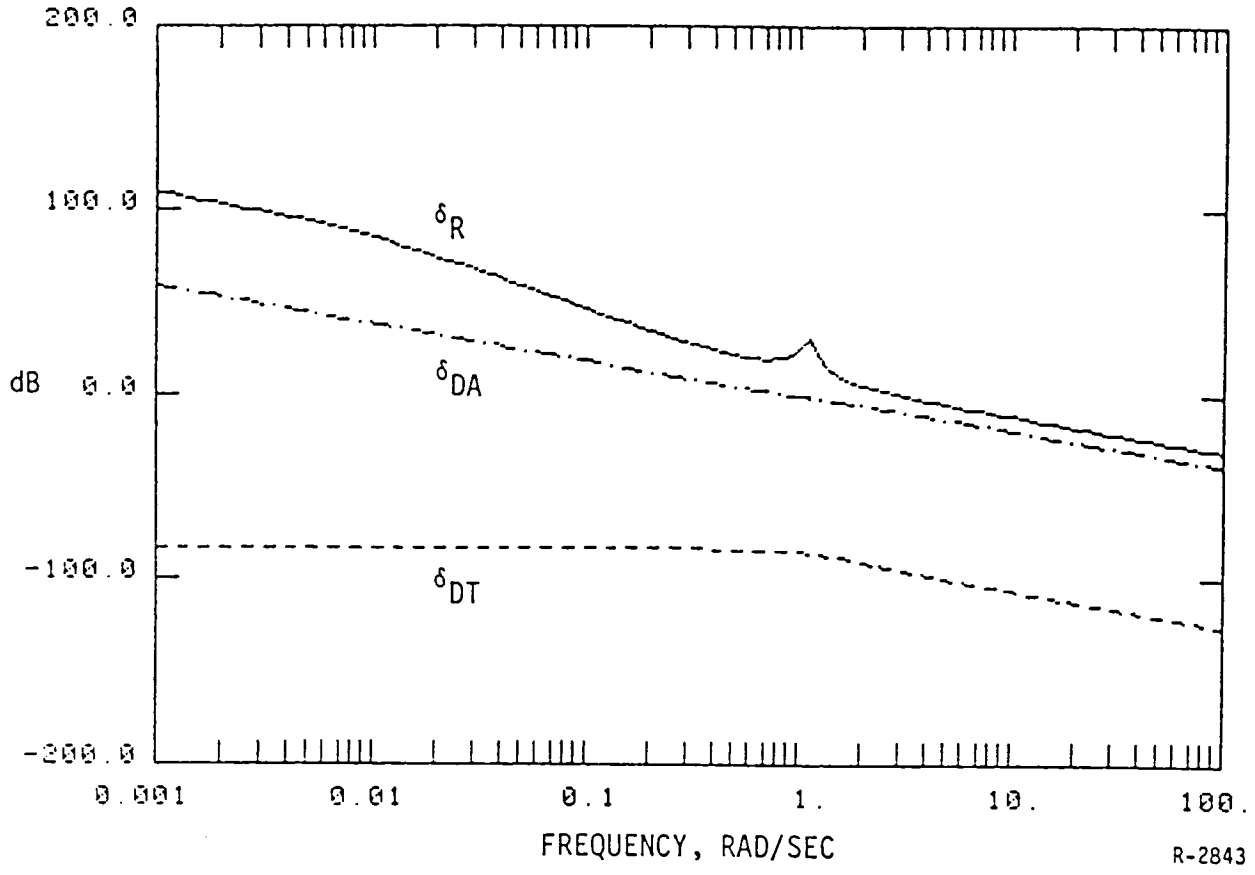

Figure 6-1. Singular Values of Lateral Loop at Plant Input

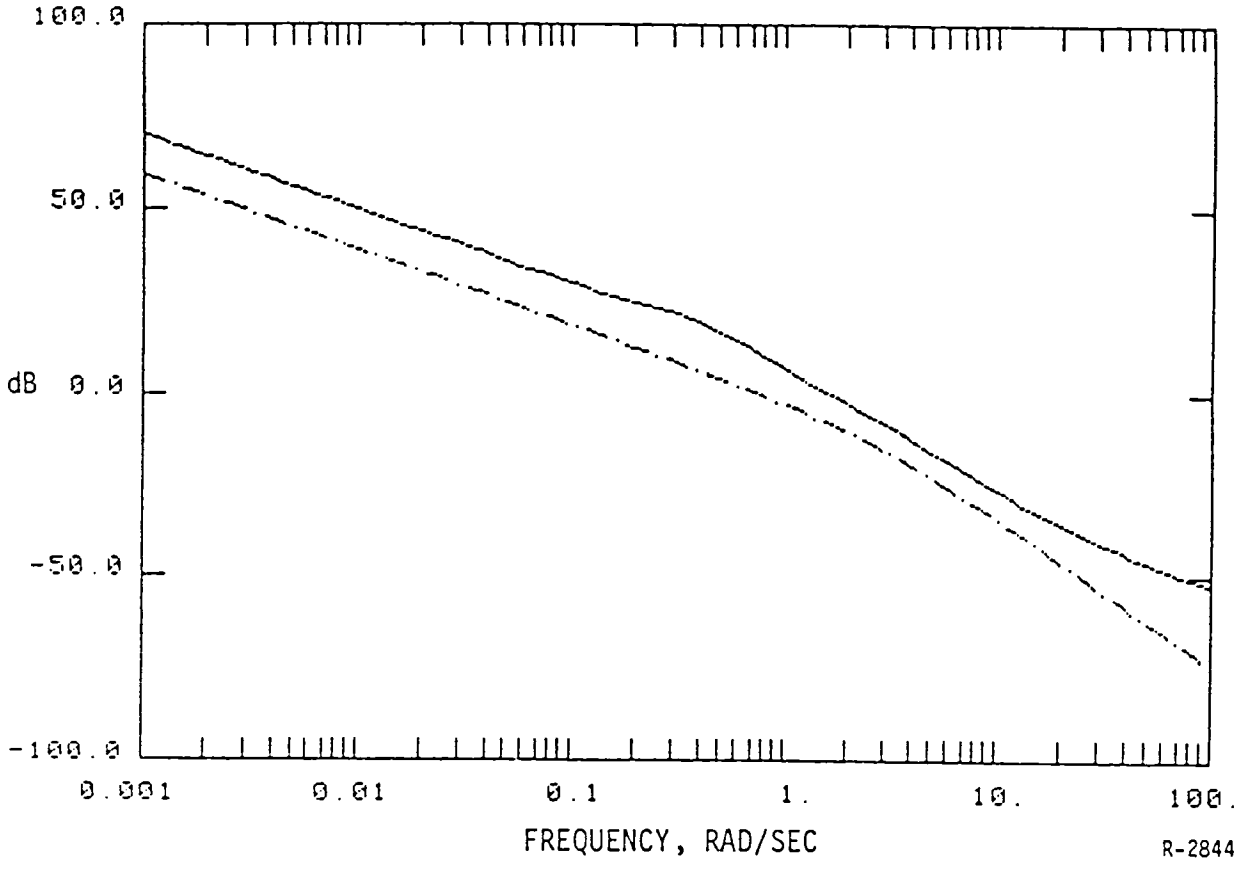

Figure 6-2. Singular Values of Lateral Loop at Error Signal

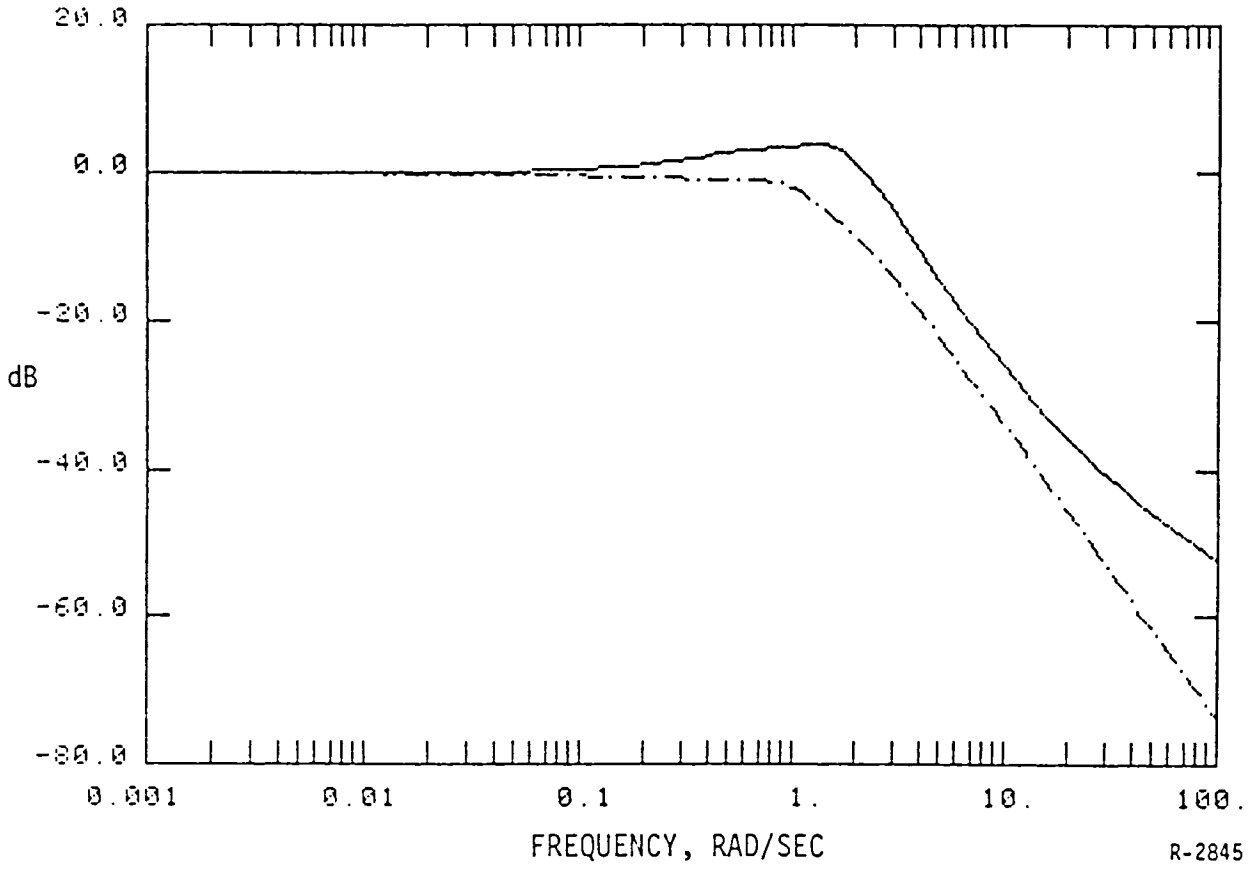

Figure 6-3. Singular Values of Closed-Loop Command to Outputs

$$B_{LON} = \begin{bmatrix} 0.0007 & 0.0007 & 0.0038 & 0.0007 \\ -0.0169 & -0.0162 & 0.0000 & -0.0181 \\ -0.2210 & -0.2118 & 0.0063 & -0.0570 \\ 0.0000 & 0.0000 & 0.0000 & 0.0000 \end{bmatrix} \tag{6-26}$$

with states

$$x = \begin{bmatrix} u/100 \\ w/100 \\ q \\ \theta \end{bmatrix} = \begin{bmatrix} \text{forward velocity,} & \text{ft/sec} \\ \text{downward velocity,} & \text{ft/sec} \\ \text{pitch rate,} & \text{rad/sec} \\ \text{pitch angle,} & \text{rad} \end{bmatrix} \tag{6-27}$$

and inputs

$$u = \begin{bmatrix} \delta_{CS}/10 \\ \delta_{CE}/20 \\ \delta_{CT}/1000 \\ \delta_{CA}/20 \end{bmatrix} \tag{6-28}$$

At first, it was decided to control just pitch angle in the longitudinal axis. The pilot's thrust control would then be used as a setpoint for the control system, with the feedback system making adjustments to that setpoint.

In order to control pitch angle with zero error in steady state, we augment the system with an integrator on pitch angle. Let

$$C_{LON} = \begin{bmatrix} 0 & 0 & 0 & 1 \end{bmatrix} \tag{6-29}$$

so that

$$\theta = C_{LON}\, x \tag{6-30}$$

Then our new (augmented) system model becomes

$$\begin{bmatrix} \dot{x} \\ \dot{x}_I \end{bmatrix} = \dot{z} = \begin{bmatrix} A_{LON} & 0 \\ C_{LON} & 0 \end{bmatrix} \begin{bmatrix} x \\ x_I \end{bmatrix} + \begin{bmatrix} B_{LON} \\ 0 \end{bmatrix} u \qquad (6\text{-}31)$$

or

$$\dot{z} = \tilde{A}z + \tilde{B}u$$

We then proceed to design an LQ regulator for this augmented model. We used

$$R_{LON} = I \qquad (6\text{-}32)$$

and tried several diagonal Q matrices. However, we could not get the eigenvalues sufficiently far into the left-half plane to obtain satisfactory speeds of response, so we used the following trick. We let

$$A_T = \tilde{A} + \alpha I \qquad (6\text{-}33)$$

for $\alpha = 0.1$. We then solve the LQ problem for some Q_o and R_o matrices using A_T and $\tilde{B}$. This corresponds to solving the problem of minimizing

$$J = \int_0^\infty e^{2\alpha t}\left[x^T Q x + u^T R u \right] dt \quad . \qquad (6\text{-}34)$$

When the resulting state-feedback matrix G is used with the matrix $\tilde{A}$, we are guaranteed that

$$\mathrm{Re}\{\lambda_i(\tilde{A}-\tilde{B}G)\} < -\alpha \quad , \quad i = 1,2,\ldots,n+p \quad . \qquad (6\text{-}35)$$

In order to be able to recalculate this G with the normal Riccati equation, we note that the Riccati equation for this problem is

$$0 = K[\tilde{A}+\alpha I] + [\tilde{A}+\alpha I]^T K + Q_o - K\tilde{B}R_o^{-1}\tilde{B}^T K \qquad (6\text{-}36)$$

or

$$0 = K\tilde{A} + \tilde{A}^T K + [Q_o+2\alpha K] - K\tilde{B}R_o^{-1}\tilde{B}^T K \quad . \qquad (6\text{-}37)$$

Therefore, if we solve Eq. 6-36 for K, then Eq. 6-37 shows that the solution is identical to the standard solution with

$$Q_{LON} = Q_o + 2\alpha K \quad . \qquad (6\text{-}38)$$

We have, as usual, $G = -R_o^{-1}\tilde{B}K$. The computation of Q_{LON} in Eq. 6-38 is necessary for redesign purposes. We selected

$$Q_o = \begin{bmatrix} 2 & 0 & 0 & 0 & 0 \\ 0 & 2 & 0 & 0 & 0 \\ 0 & 0 & 40 & 0 & 0 \\ 0 & 0 & 0 & 6 & 0 \\ 0 & 0 & 0 & 0 & 60 \end{bmatrix} \quad . \qquad (6\text{-}39)$$

The heavy weighting on the pitch rate state tends to help damp those modes associated with it and the weighting on the integrator state brings the integrator action (as seen in the singular values) up to a suitable level.

The singular values of the loop transfer function for this design are shown in Fig. 6-4. Note that the loop corresponding to thrust is quite low. This implies that those states which are regulated using collective thrust will not be regulated very well. By projecting the left singular vector corresponding to this loop onto the space spanned by the columns of the G matrix

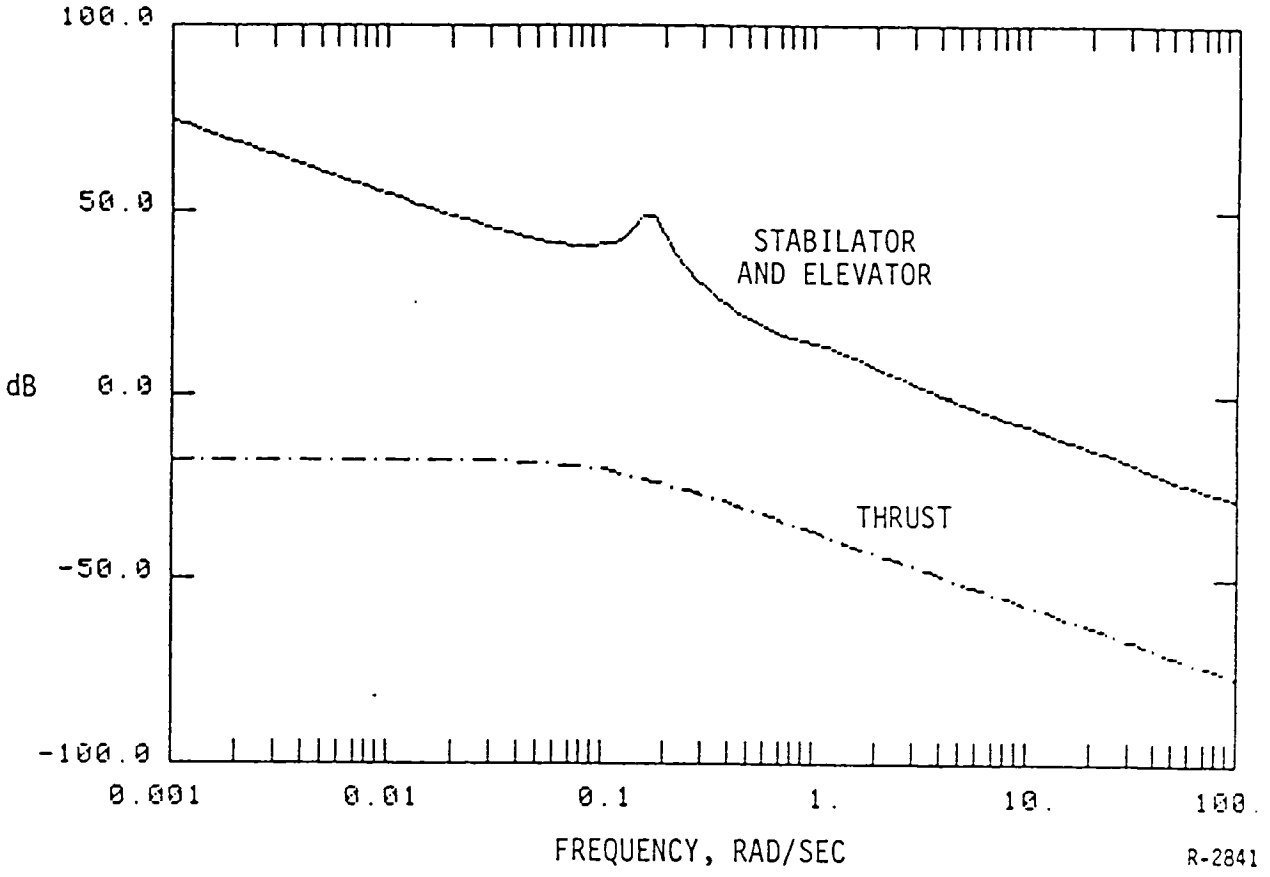

Figure 6-4. Singular Values of Longitudinal Loop at Input

for this design, we see that forward velocity is the dominant state being controlled at low frequencies for this loop. Thus, we would expect inadequate regulation of u from this design. This is shown in Fig. 6-5 which gives the scaled closed-loop response to a step in commanded pitch angle.

While this design may be adequate for a pilot in the loop control systems, our present goal is to develop a control law which can be demonstrated autonomously on the NASA-Langley Research Center nonlinear simulation. Therefore, better regulation of forward velocity (u) is desired. Several designs which brought the thrust loop up to a higher level at low frequencies were examined. However, none were able to achieve good steady state regulation without severely reducing the robustness of the design to the highly significant throttle dynamics. For this reason, we added an integrator state corresponding to the integral of forward velocity.

With this additional integrator, the augmented system model is given by Eq. 6-31 with

$$C_{LON} = \begin{bmatrix} 0 & 0 & 0 & 1 \\ 1 & 0 & 0 & 0 \end{bmatrix} . \qquad (6\text{-}40)$$

Initially, we tried using the trick described by Eqs. 6-33 through 6-38 with,

$$Q_o = \text{diag}[2,\ 2,\ 40,\ 6,\ 60,\ 2] \qquad (6\text{-}41)$$

(which is the same as Eq. 6-39 with an additional weight for the integral of u state). This design produced good steady state regulation of u and good robustness to engine dynamics, but resulted in too much control action in δ_{CA}. In order to keep the singular values of the scaled loop transfer function the same and shift the control action from δ_{CA} to δ_{CT}, the diagonal element of the

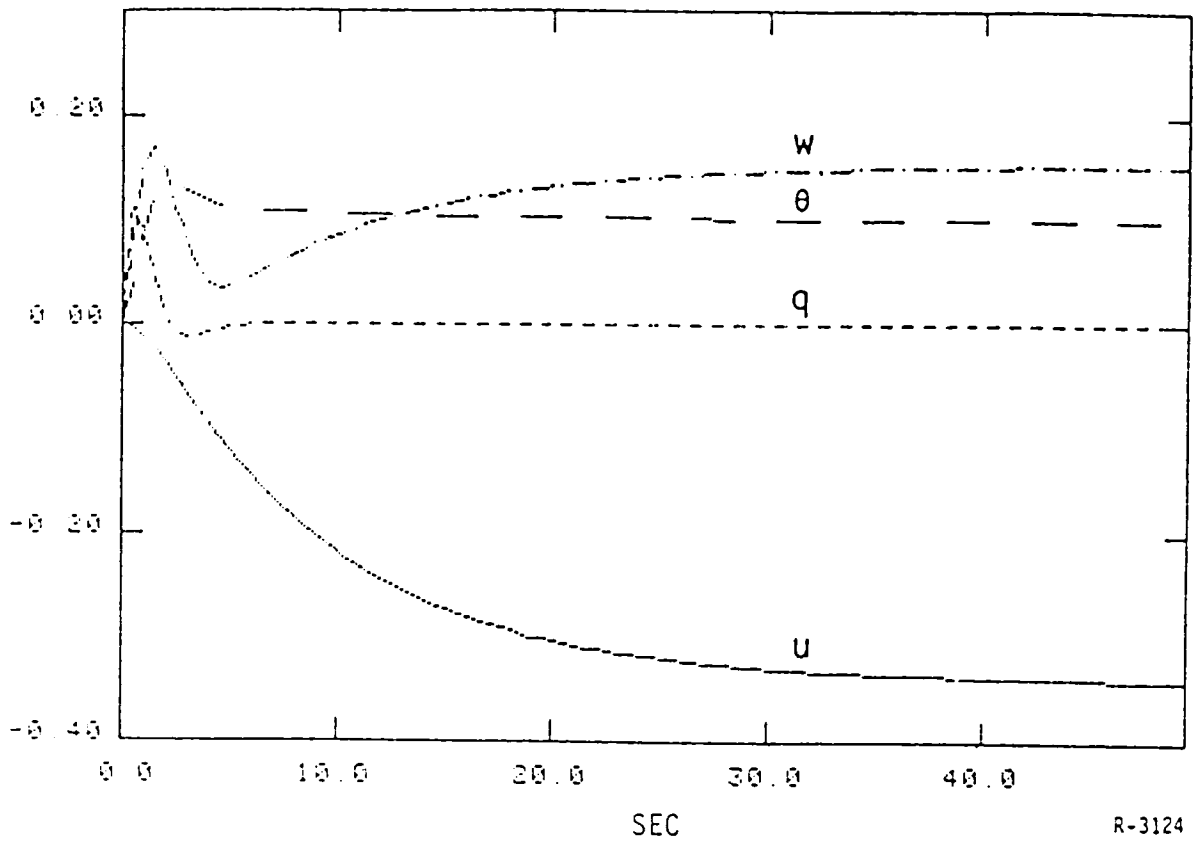

Figure 6-5. Scaled Closed Loop Response to Pitch Angle Step Command

R_{LON} corresponding to thrust was decreased by a factor of ten and the rows and columns of the Q matrix computed from Eq. 6-41 and Eqs. 6-33 through 6-38 which correspond to weightings on u and $\int u$ were also reduced by a factor of ten. The result is,

$$R_{LON} = \text{diag}[1,\ 1,\ .1,\ 1] \tag{6-42}$$

$$Q_{LON} = \begin{bmatrix} 69.7531 & 9.5838 & -3.1061 & -19.7252 & 13.6632 & 1.3749 \\ 9.5838 & 4.5549 & -1.6185 & -6.0149 & 1.5320 & 0.1662 \\ -3.1061 & -1.6185 & 46.2520 & 11.1358 & 5.3199 & -0.0729 \\ -19.7252 & -6.0149 & 11.1358 & 46.2064 & 16.8045 & -0.3857 \\ 13.6632 & 1.5320 & 5.3199 & 16.8045 & 88.8258 & 0.1769 \\ 1.3749 & 0.1662 & -0.0729 & -0.3857 & 0.1769 & 0.6618 \end{bmatrix} \tag{6-43}$$

and

$$G_{LON} = \begin{bmatrix} 1.3978 & 1.4598 & -6.8311 & -11.6557 & -6.2575 & 0.1939 \\ 1.3388 & 1.3988 & -6.5467 & -11.1701 & -5.9972 & 0.1858 \\ 27.9237 & 3.8726 & 1.4870 & -4.0887 & 10.0066 & 2.4249 \\ -0.8064 & 0.1156 & -1.6578 & -2.4716 & -1.9209 & -0.0407 \end{bmatrix} \tag{6-44}$$

The singular values of the scaled loop transfer function for this design are shown in Fig. 6-6. The design has adequate robustness to engine dynamics and improves the regulation of u during a pitch step as shown in Fig. 6-7. Of course, increased use of thrust is made during the pitch step of .1 radian. In fact, it requires about 8000 lbs. of collective thrust in the steady state to regulate forward velocity during this maneuver. This is deemed reasonable.

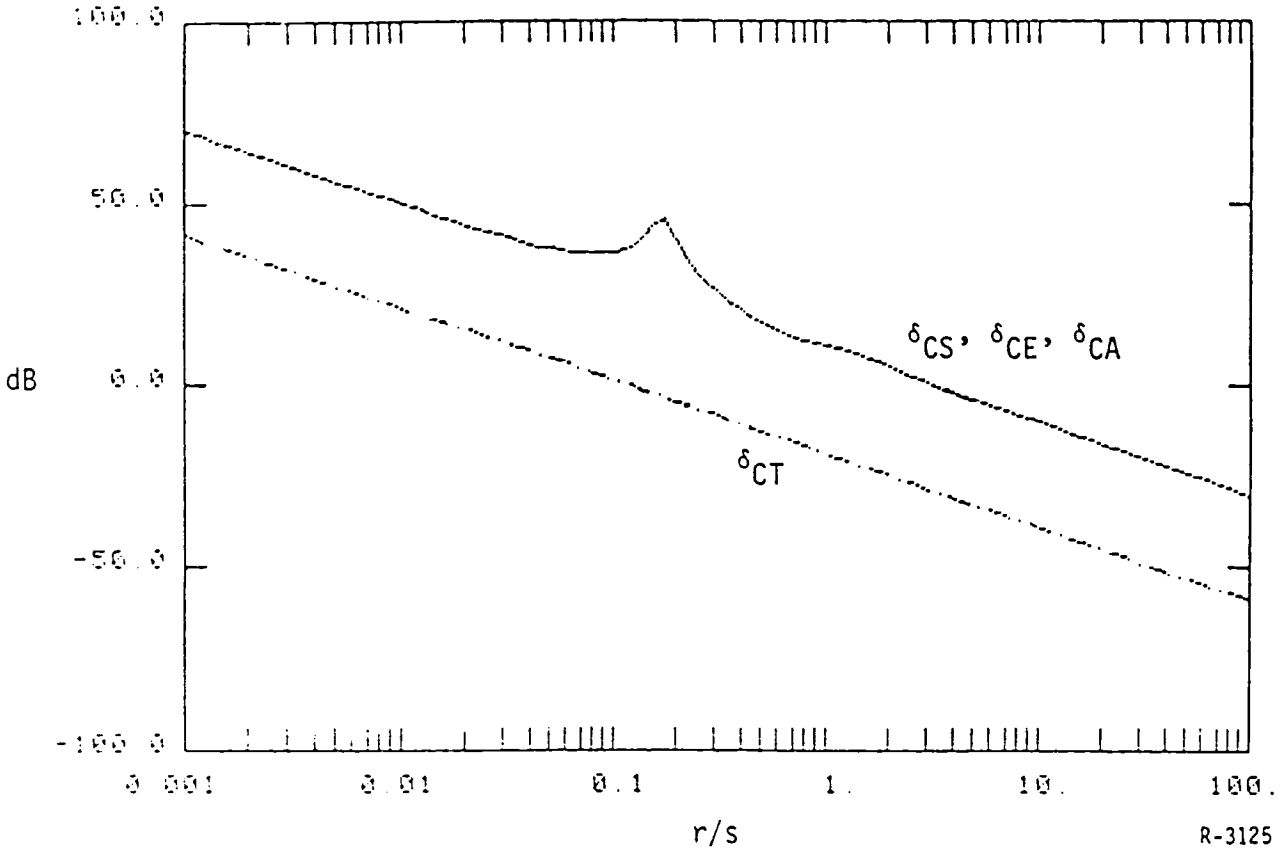

Figure 6-6. Singular Values of Scaled Longitudinal Loop at Plant Input

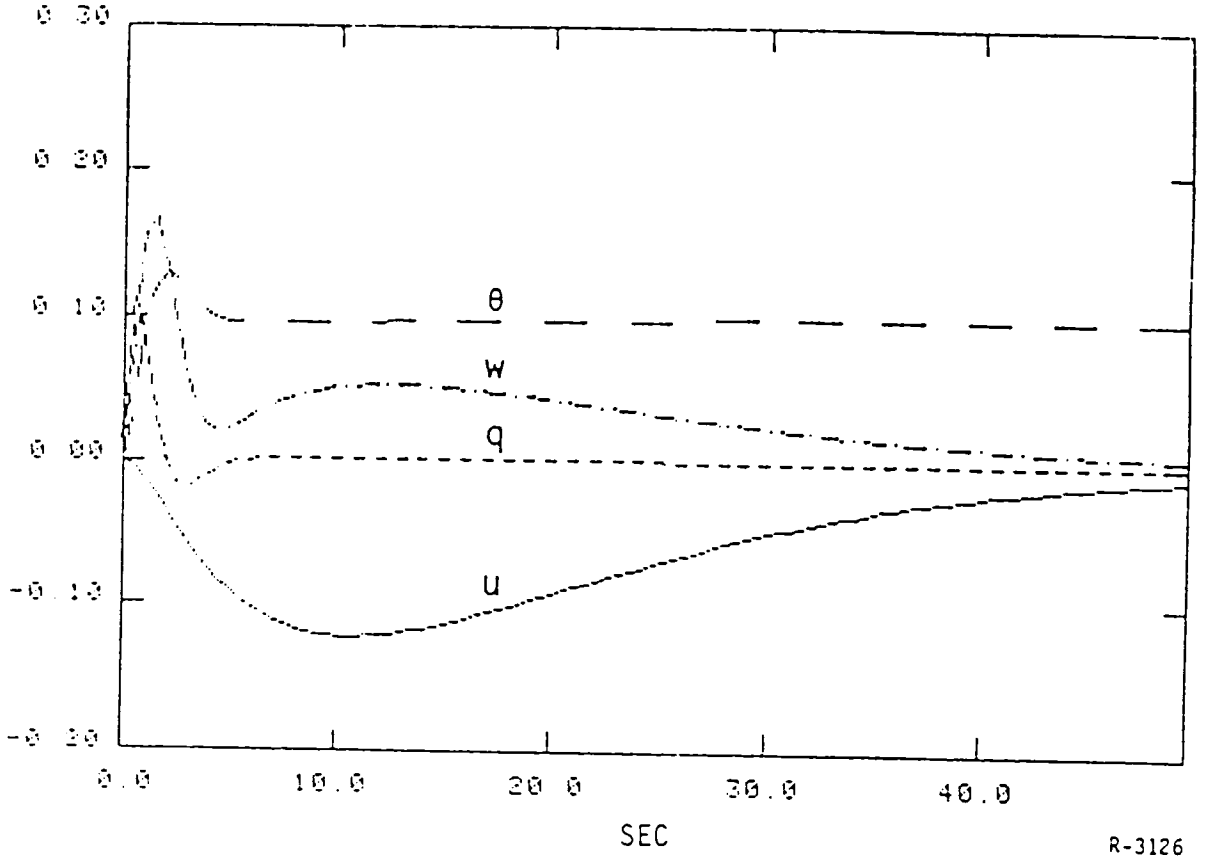

Figure 6-7. Closed Loop Response to Pitch Step (Scaled Quantities)

The closed loop eigenvalues are

$$\begin{matrix} -1.17 \pm .97j \\ -1.07 \\ -.71 \\ -.10 \pm .02j \end{matrix} \quad . \tag{6-45}$$

Figure 6-8 shows the closed loop command following singular values. Based on this figure, velocity following is good to about .05 r/s and pitch angle following is good to about 2 r/s.

6.2.3 Global Design

We can now assemble the two subsystem designs into one global design. To do this, we simply set

$$A_{GLOB} = \begin{bmatrix} A_{LON} & 0 \\ 0 & A_{LAT} \end{bmatrix} \quad 12\times12 \tag{6-46}$$

$$B_{GLOB} = \begin{bmatrix} B_{LON} & 0 \\ 0 & B_{LAT} \end{bmatrix} \quad 12\times9 \tag{6-47}$$

where (A_{LON},B_{LON}) is the augmented longitudinal subsystem and (A_{LAT},B_{LAT}) is the augmented lateral subsystem. We continue

$$Q_{GLOB} = \begin{bmatrix} Q_{LON} & 0 \\ 0 & Q_{LAT} \end{bmatrix} \quad 12\times12 \tag{6-48}$$

$$R_{GLOB} = \begin{bmatrix} R_{LON} & 0 \\ 0 & R_{LAT} \end{bmatrix} \quad 9\times9 \tag{6-49}$$

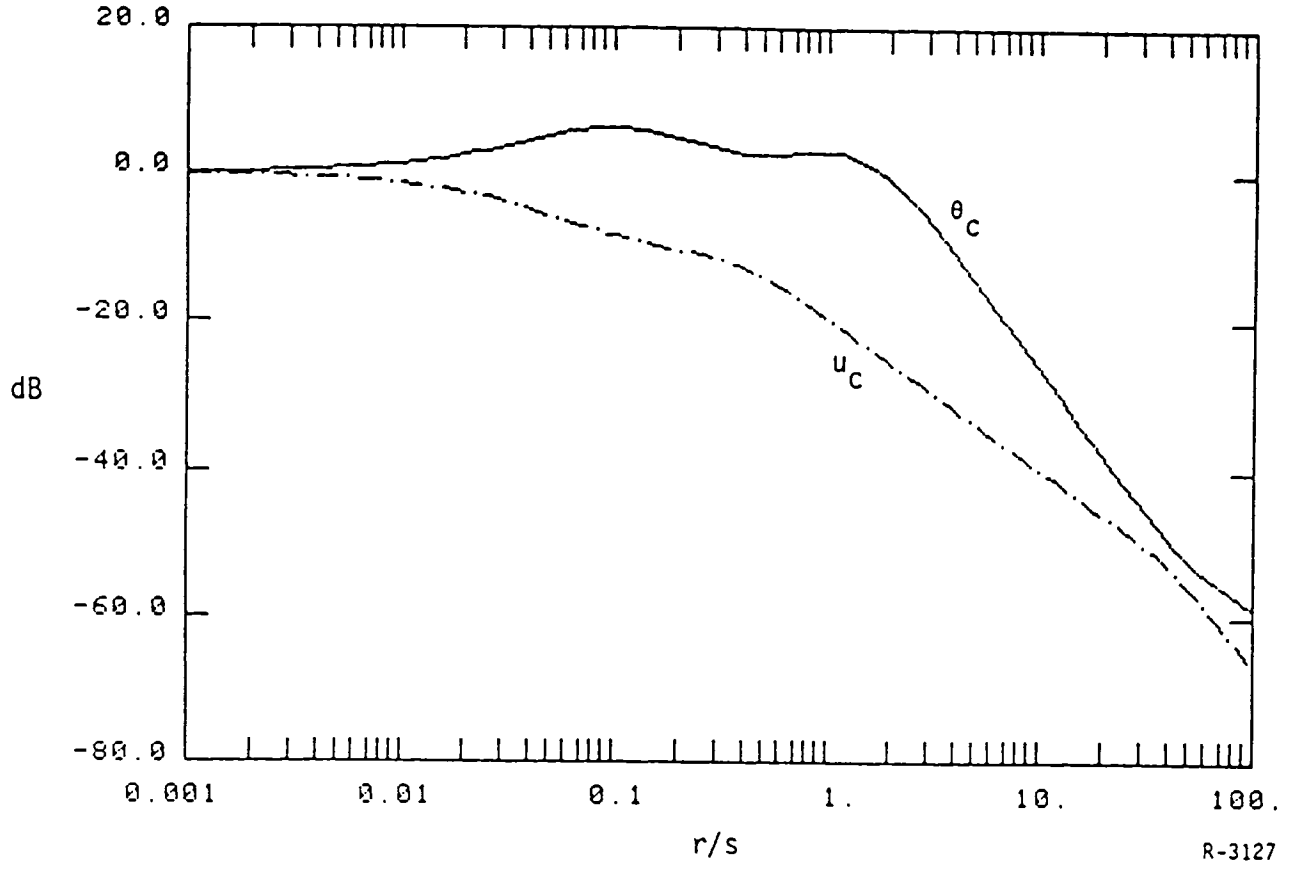

Figure 6-8. Closed Loop Singular Values for Command Following

and we can solve one large Riccati equation to get the feedback gain

$$G_{GLOB} = \begin{bmatrix} G_{LON} & 0 \\ 0 & G_{LAT} \end{bmatrix} \quad 9\times12 \tag{6-50}$$

where G_{LON} and G_{LAT} should equal the gains we calculated in the previous two subsections (6.2.1 and 6.2.2).

We would like to convert our feedback gain back to the original inputs and states, so that it can be used on the full nonlinear simulation. Since

$$x_p = T_1 \cdot x_a \tag{6-51}$$

$$u_p = S_1^{-1} \cdot B_{MIX} \cdot u_a \tag{6-52}$$

and our regulator design minimizes

$$J = \int_0^\infty [x_p{}^T \, Q_{GLOB} \, x_p + u_p{}^T \, R_{GLOB} \, u_p]dt \tag{6-53}$$

for x_p and u_p scaled. We could use

$$J = \int_0^\infty [x_{aug}{}^T \, Q_F x_{aug} + u_a \, R_F u_a]dt \tag{6-54}$$

where $x_{aug}{}^T = (x_a{}^T, \, Cx_a{}^T)$

and

$$A_F = \begin{bmatrix} A_a & 0 \\ C & 0 \end{bmatrix} \quad 12\times12 \tag{6-55}$$

$$B_F = \begin{bmatrix} B_a \\ 0 \end{bmatrix} \quad 12\times9 \tag{6-56}$$

$$C = \begin{bmatrix} 0 & 0 & 0 & 1 & 0 & 0 & 0 & 0 \\ 0 & 0 & 0 & 0 & 1 & 0 & 0 & 0 \\ 0 & 0 & 0 & 0 & 0 & 0 & 0 & 1 \\ 1 & 0 & 0 & 0 & 0 & 0 & 0 & 0 \end{bmatrix} \tag{6-57}$$

so that

$$\dot{x}_{aug} = A_F\, x_{aug} + B_F\, u_a \tag{6-58}$$

and

$$\begin{bmatrix} \theta \\ v \\ \phi \\ u \end{bmatrix} = Cx_a \quad . \tag{6-59}$$

We then define a larger scaling matrix

$$T_2 = \text{diag}\left(.01,\ .01,\ 1,\ 1,\ 1,\ .01,\ \vdots\ .01,\ 1,\ 1,\ 1,\ .01,\ 1 \right) \tag{6-60}$$

where we must scale the integrator states too, and a permutation matrix P

$$P = \begin{bmatrix} 1 & 0 & 0 & 0 & 0 & 0 & 0 & 0 & 0 & 0 & 0 & 0 \\ 0 & 1 & 0 & 0 & 0 & 0 & 0 & 0 & 0 & 0 & 0 & 0 \\ 0 & 0 & 1 & 0 & 0 & 0 & 0 & 0 & 0 & 0 & 0 & 0 \\ 0 & 0 & 0 & 1 & 0 & 0 & 0 & 0 & 0 & 0 & 0 & 0 \\ 0 & 0 & 0 & 0 & 0 & 0 & 0 & 0 & 1 & 0 & 0 & 0 \\ 0 & 0 & 0 & 0 & 0 & 0 & 0 & 0 & 0 & 0 & 0 & 1 \\ 0 & 0 & 0 & 0 & 1 & 0 & 0 & 0 & 0 & 0 & 0 & 0 \\ 0 & 0 & 0 & 0 & 0 & 1 & 0 & 0 & 0 & 0 & 0 & 0 \\ 0 & 0 & 0 & 0 & 0 & 0 & 1 & 0 & 0 & 0 & 0 & 0 \\ 0 & 0 & 0 & 0 & 0 & 0 & 0 & 1 & 0 & 0 & 0 & 0 \\ 0 & 0 & 0 & 0 & 0 & 0 & 0 & 0 & 0 & 1 & 0 & 0 \\ 0 & 0 & 0 & 0 & 0 & 0 & 0 & 0 & 0 & 0 & 1 & 0 \end{bmatrix} \quad 12 \times 12 \tag{6-61}$$

in order to mix the integrator states back into the order we used for A_{GLOB}. Then we use

$$Q_F = P^T \cdot T_2{}^T \cdot Q_{GLOB} \cdot T_2 \cdot P \tag{6-62}$$

and

$$R_F = \left(S_1^{-1} B_{MIX}\right)^T \cdot R_{GLOB} \cdot \left(S_1^{-1} \cdot B_{MIX}\right) \qquad (6\text{-}63)$$

with the model (Eqs. 6-55 and 6-56) to obtain a state feedback matrix which corresponds to the scaled design versions (i.e., same physical feedback). The matrices are

$R_F =$

1.1000D-06	-9.0000D-07	0.0000D+00	0.0000D+00	0.0000D+00	0.0000D+00	0.0000D+00	0.0000D+00	0.0000D+00
-9.0000D-07	1.1000D-06	0.0000D+00	0.0000D+00	0.0000D+00	0.0000D+00	0.0000D+00	0.0000D+00	0.0000D+00
0.0000D+00	0.0000D+00	2.0000D-02	0.0000D+00	0.0000D+00	0.0000D+00	0.0000D+00	0.0000D+00	0.0000D+00
0.0000D+00	0.0000D+00	0.0000D+00	2.0000D-02	0.0000D+00	0.0000D+00	0.0000D+00	0.0000D+00	0.0000D+00
0.0000D+00	0.0000D+00	0.0000D+00	0.0000D+00	2.5000D-03	0.0000D+00	0.0000D+00	0.0000D+00	0.0000D+00
0.0000D+00	0.0000D+00	0.0000D+00	0.0000D+00	0.0000D+00	5.0000D-03	0.0000D+00	0.0000D+00	0.0000D+00
0.0000D+00	0.0000D+00	0.0000D+00	0.0000D+00	0.0000D+00	0.0000D+00	5.0000D-03	0.0000D+00	0.0000D+00
0.0000D+00	0.0000D+00	0.0000D+00	0.0000D+00	0.0000D+00	0.0000D+00	0.0000D+00	5.0000D-03	0.0000D+00
0.0000D+00	0.0000D+00	0.0000D+00	0.0000D+00	0.0000D+00	0.0000D+00	0.0000D+00	0.0000D+00	5.0000D-03

(6-64)

$Q_F =$

6.9753D-03	9.5838D-04	-3.1061D-02	-1.9725D-01	0.0000D+00	0.0000D+00	0.0000D+00	0.0000D+00	1.3663D-01	0.0000D+00	0.0000D+00	1.3749D-04
9.5838D-04	4.5549D-04	-1.6185D-02	-6.0149D-02	0.0000D+00	0.0000D+00	0.0000D+00	0.0000D+00	1.5320D-02	0.0000D+00	0.0000D+00	1.6616D-05
-3.1061D-02	-1.6185D-02	4.6256D+01	1.1136D+01	0.0000D+00	0.0000D+00	0.0000D+00	0.0000D+00	5.3199D+00	0.0000D+00	0.0000D+00	-7.2934D-04
-1.9725D-01	-6.0149D-02	1.1136D+01	4.6206D+01	0.0000D+00	0.0000D+00	0.0000D+00	0.0000D+00	1.6804D+01	0.0000D+00	0.0000D+00	-3.8571D-03
0.0000D+00	0.0000D+00	0.0000D+00	0.0000D+00	3.0000D+04	0.0000D+00	0.0000D+00	0.0000D+00	0.0000D+00	0.0000D+00	0.0000D+00	0.0000D+00
0.0000D+00	0.0000D+00	0.0000D+00	0.0000D+00	0.0000D+00	2.0000D+01	0.0000D+00	0.0000D+00	0.0000D+00	0.0000D+00	0.0000D+00	0.0000D+00
0.0000D+00	0.0000D+00	0.0000D+00	0.0000D+00	0.0000D+00	0.0000D+00	1.0000D+00	0.0000D+00	0.0000D+00	0.0000D+00	0.0000D+00	0.0000D+00
0.0000D+00	0.0000D+00	0.0000D+00	0.0000D+00	0.0000D+00	0.0000D+00	0.0000D+00	1.0000D+00	0.0000D+00	0.0000D+00	0.0000D+00	0.0000D+00
1.3663D-01	1.5320D-02	5.3199D+00	1.6804D+01	0.0000D+00	0.0000D+00	0.0000D+00	0.0000D+00	8.8826D+01	0.0000D+00	0.0000D+00	1.7688D-03
0.0000D+00	0.0000D+00	0.0000D+00	0.0000D+00	0.0000D+00	0.0000D+00	0.0000D+00	0.0000D+00	0.0000D+00	4.0000D-03	0.0000D+00	0.0000D+00
0.0000D+00	0.0000D+00	0.0000D+00	0.0000D+00	0.0000D+00	0.0000D+00	0.0000D+00	0.0000D+00	0.0000D+00	0.0000D+00	4.0000D+01	0.0000D+00
1.3749D-04	1.6616D-05	-7.2934D-04	-3.8571D-03	0.0000D+00	0.0000D+00	0.0000D+00	0.0000D+00	1.7688D-03	0.0000D+00	0.0000D+00	6.6181D-05

(6-65)

$G_F =$

1.3961F+02	1.9358D+01	7.4412D+02	-2.0427D+03	-2.7713D+00	2.0010D+02	5.0151D+02	4.2919D+02	5.0039D+03	-6.5007D-01	2.2317D+02	1.2124D+01
1.3961D+02	1.9358D+01	7.4412D+02	-2.0427D+03	2.7713D+00	-2.0010D+02	-5.0151D+02	-4.2919D+02	5.0039D+03	6.5007D-01	-2.2317D+02	1.2124D+01
7.0062D-02	7.3015D-02	-3.4156D+01	-5.8283D+01	-5.6680D-02	1.1374D+01	1.1714D+01	2.2737D+01	-3.1282D+01	4.2385D-02	1.1106D+01	9.7114D-03
7.0062D-02	7.3015D-02	-3.4156D+01	-5.8283D+01	5.6680D-02	-1.1374D+01	-1.1714D+01	-2.2737D+01	-3.1282D+01	-4.2385D-02	-1.1106D+01	9.7114D-03
1.2901D-15	2.9076D-16	-3.5417D-14	-5.2611D-14	1.6030D+00	-1.7116D+01	-2.5327D+02	-5.7752D+01	1.0922D-14	1.1882D+00	-4.3027D+01	2.0720D-16
1.3360D-01	1.3984D-01	-6.5466D+01	-1.1169D+02	-1.1340D-01	2.2109D+01	2.3305D+01	4.4249D+01	-5.9980D+01	7.9658D-02	2.1638D+01	1.8555D-02
1.3360D-01	1.3984D-01	-6.5466D+01	-1.1169D+02	1.1340D-01	-2.2109D+01	-2.3305D+01	-4.4249D+01	-5.9980D+01	-7.965D-02	-2.1638D+01	1.8555D-02
-8.0708D-02	1.1551D-02	-1.6578D+01	-2.4714D+01	-2.6946D-01	5.1579D+01	5.5219D+01	1.0332D+02	-1.9211D+01	1.8254D-01	5.0554D+01	-4.0715D-03
-8.0708D-02	1.1551D-02	-1.6578D+01	-2.4714D+01	2.6946D-01	-5.1579D+01	-5.5219D+01	-1.0332D+02	-1.9211D+01	-1.8254D-01	-5.0554D+01	-4.0751D-03

(6-66)

These matrices can now be used with the original scaling and organization of inputs.

Let

$$G_y = [G_4\ G_5\ G_8\ G_1] \tag{6-67}$$

$$G_r = [G_2\ G_3\ G_6\ G_7] \tag{6-68}$$

$$G_I = [G_9\ G_{10}\ G_{11}\ G_{12}] \tag{6-69}$$

where G_i is the ith column of G_F in Eq. 6-66 .

Then the equations of the compensator are:

$$\dot{x}_I = -r + Cx_a - Cx_o \tag{6-70}$$

$$u = u_o - G_r x_r - G_y C x_a + G_y C x_o + G_y r - G_I x_I \tag{6-71}$$

where

$$C = \begin{bmatrix} 0 & 0 & 0 & 1 & 0 & 0 & 0 & 0 \\ 0 & 0 & 0 & 0 & 1 & 0 & 0 & 0 \\ 0 & 0 & 0 & 0 & 0 & 0 & 0 & 1 \\ 1 & 0 & 0 & 0 & 0 & 0 & 0 & 0 \end{bmatrix} \tag{6-72}$$

$$x_r = C_r x_a$$

$$C_r = \begin{bmatrix} 0 & 1 & 0 & 0 & 0 & 0 & 0 & 0 \\ 0 & 0 & 1 & 0 & 0 & 0 & 0 & 0 \\ 0 & 0 & 0 & 0 & 0 & 1 & 0 & 0 \\ 0 & 0 & 0 & 0 & 0 & 0 & 1 & 0 \end{bmatrix} \tag{6-73}$$

and u_o and x_o are the desired setpoints.

6.2.4 Summary of Nominal Control Design

A variety of linear simulations of the unfailed aircraft were performed. These included responses to command steps with and without wind gusts. For the gust simulations, the Dryden wind model [32] was used with a 1000 ft. turbulence scale length in the vertical and horizontal directions and a low rms velocity (σ = 2 ft/s).

Since these linear simulations resemble the nonlinear simulation results described in Section 7, we forego discussion of these results at this point.

6.3 INVESTIGATION OF TRIM SOLUTIONS FOR STUCK FAILURES

In this subsection, we provide some results of applying the quadratic programming algorithm described in Section 3 to the linear trim problem for a landing approach scenario. We assume, as usual, that sufficient information about the failure is made available from the FDI algorithm (see Fig. 5-3).

Scenario Definition

The normal (unfailed) operating point for a B-737 aircraft flying at 127 knots, 1000 feet, and a -3 degree flight path angle is given by the nominal state vector, x_n,

$$x_n = \begin{pmatrix} u \\ w \\ q \\ \theta \\ v \\ p \\ r \\ \phi \end{pmatrix} \begin{matrix} = 215 \text{ ft/s} \\ = 8.7 \text{ ft/s} \\ = 0 \text{ r/s} \\ = -.68 \text{ deg.} \\ = 0 \text{ f/s} \\ = 0 \text{ r/s} \\ = 0 \text{ r/s} \\ = 0 \text{ deg.} \end{matrix} \begin{matrix} = \text{velocity along the x-body axis} \\ = \text{velocity along the z-body axis} \\ = \text{angular velocity about y-body axis} \\ = \text{pitch angle} \\ = \text{velocity along the y-body axis} \\ = \text{angular velocity about x-body axis} \\ = \text{angular velocity about z-body axis} \\ = \text{roll angle} \end{matrix} \qquad (6\text{-}74)$$

and the nominal input vector, u_n,

$$u_n = \begin{pmatrix} \delta_{LT} \\ \delta_{RT} \\ \delta_{LS} \\ \delta_{RS} \\ \delta_{R} \\ \delta_{LE} \\ \delta_{RE} \\ \delta_{LA} \\ \delta_{RA} \end{pmatrix} \begin{matrix} = 4251 \text{ lbs} = \text{left engine thrust} \\ = 4251 \text{ lbs} = \text{right engine thrust} \\ = -5.45 \text{ deg.} = \text{left stabilator deflection} \\ = -5.45 \text{ deg.} = \text{right stabilator deflection} \\ = 0 \text{ deg.} = \text{rudder deflection} \\ = 0 \text{ deg.} = \text{left elevator servo deflection} \\ = 0 \text{ deg.} = \text{right elevator servo deflection} \\ = 0 \text{ deg.} = \text{left aileron deflection} \\ = 0 \text{ deg.} = \text{right right aileron deflection} \end{matrix} \qquad (6\text{-}75)$$

The above flight condition includes a 40 degree flap extension, no spoiler deflection and extended landing gear at a gross weight of 85,000 pounds.

A linear model for the aircraft about this operating point is given by Eqs. 6-1 through 6-5. For this investigation, we will assume that the measurable disturbance (w_p in Eq. 3-6) which we wish to reject is caused by a stuck failure of a control element. That is, the disturbance w_p, in each of the cases we will examine takes the form

$$w_p = \Delta d_i \; b_i \qquad (6\text{-}76)$$

where Δd_i is the difference between the stuck value of the i'th control element and its nominal value, and b_i is the i'th column of the B matrix in Eq. 6-1.

Regulated Variables

As demonstrated in [18], the choice of important quantities, y, for trim regulation greatly impacts the resulting solution. When y = x, for example,

the linear trim problem results in a balancing of the force and moment disturbances by forces and moments applied by the control elements alone. While this result may satisfactorily reject the disturbances, the amount of remaining control authority available for use in controlling the airplane is substantially smaller than when other choices of y are made.

For the current demonstration, our choice of y is motivated by two factors. First a landing approach scenario, the primary objective should be to maintain the desired approach flight path angle (in this case -3 degrees). If this objective is met, and the aircraft can achieve it in a steady state condition (i.e., $\dot{x}=0$) then runway intercept can be achieved as long as the pilot/control-system has sufficient remaining control authority to establish/re-establish the desired altitude and heading. Note that, while one might specify heading angle as a desired regulated variable, the trim solution will not achieve the desired heading on its own. This is due to the fact that, while the trim problem guarantees that its solution is an equilibrium point for the system (Eq. 6-1), it does not guarantee that application of the resulting nominal control values will achieve the solution unless the system is strictly stable. Since heading angle appears as an integrator state in the open loop aircraft, it can only be chosen as a regulated quantity if a heading loop is present in the control system. Also, the solution to the trim problem (if feasible) guarantees that the linear system used to approximate the aircraft is in steady state. To insure that the true aircraft is in steady state, the nonlinear equations of motion must be examined. The kinematic equations relating angular rates to Euler angles (e.g., see [33]), suggest that we can achieve constant Euler angles (e.g., $\dot{\theta} = \dot{\phi} = 0$) by requiring that all angular rates equal zero (i.e., $P = Q = R = 0$). If the linear model used

in solving the trim problem corresponds to zero nominal angular rates, then we will achieve steady state flight by requiring the angular rate perturbations to be zero.

For the results that follow, $y^T = (\gamma,q,p,r)$, where γ represents perturbations to the desired (nominal) flight path angle, and p,q,r represent perturbations to the desired (nominal) angular rates. As in [18], the flight path angle, γ, is nonlinearly related to the states in Eq. 6-74. The C matrix needed in Eq. 3-7 is, therefore, composed of the linear coefficients of the Taylor expansion for this relationship. As shown in [18], we have

$$C = \begin{bmatrix} .00019 & -.00465 & 0 & 1 & 0 & 0 & 0 & 0 \\ 0 & 0 & 1 & 0 & 0 & 0 & 0 & 0 \\ 0 & 0 & 0 & 0 & 0 & 1 & 0 & 0 \\ 0 & 0 & 0 & 0 & 0 & 0 & 1 & 0 \end{bmatrix} \qquad (6\text{-}77)$$

Note that in the above, the constraint q = 0 is redundant for this linear trim problem since at this operating point (Eqs. 6-74 and 6-75) $\dot{\theta} = q$. Thus q = 0 is already specified by the linear trim problem by the requirement $\dot{x} = 0$.

Constraints

In order to make the solution to the linear trim problem reasonable, we must constrain the states and controls to the linear and realizable region of the model in Eq. 6-1. First, we assume that the absolute limits on each control are given by

$$\begin{aligned} \delta_{LT},\ \delta_{RT} &\in [1600,\ 17{,}000]\ \text{lbs} \\ \delta_{LS},\ \delta_{RS} &\in [-14,\ 3]\ \text{degrees} \\ \delta_{R} &\in [-10,\ 10]\ \text{degrees} \\ \delta_{LE},\ \delta_{RE} &\in [-10,\ 10]\ \text{degrees} \\ \delta_{LA},\ \delta_{RA} &\in [-10,\ 10]\ \text{degrees} \end{aligned} \qquad (6\text{-}78)$$

Furthermore, we would like to leave about 5 degreees of control authority for each control surface so that these controls do not saturate when used dynamically.

The linear region in state space is determined by a number of factors.

1. For nonviscous flows such as those encountered in most aircraft, the lift and drag forces caused by control surface deflection is approximately proportional to dynamic pressure or, equivalently, to total velocity squared. Thus, each B matrix element can be written

$$B_{ij} = \beta_{ij}V^2 = \beta_{ij}(V_n+v)^2 \tag{6-79}$$

where V_n is the nominal total velocity and v is the perturbation to V_n. For an allowable error of 20 percent in the B matrix we must require that

$$\beta_{ij}(V_n+v)^2 - \beta_{ij}V_n^2 < .2\beta_{ij}V_n^2 \tag{6-80}$$

For $v << 2V_n$, Eq. 6-80 is true for $|v| < .1V_n$ or about 20 ft/sec.

2. For the flight path angle linearization (represented by C in Eq. 6-77) to be valid, perturbations to V_x and V_z must be limited. If we plot values of true γ versus linear predicted γ for various combinations of V_z and V_x, we see that the error in γ can be limited to.5 degrees by requiring perturbations to V_x to be smaller than 20 ft/sec., and perturbations to V_z to lie about within the range [-30, 20] ft/sec. Of course, if we limit the angle of attack to a presumably linear range of 0 to 10 degrees, the constraint on perturbations to V_z becomes roughly [-8.7, 20] ft/sec.

3. Assuming a linear envelope of plus and minus 5 degrees sideslip angle, the side velocity perturbation limits are roughly plus and minus 19 ft/sec. (based on a maximum velocity magnitude of $V_n + v = 215 + 20 = 225$ ft/sec.).

4. For a landing approach, the attitude of the aircraft must be such that the pilot can see the runway, and a safe landing achieved. This implies that θ be within the range of about plus and minus 10 degrees and ϕ be within about ±5 degrees.

5. Since we will be minimizing perturbations to P, Q, and R, limits on these values are arbitrary. In the algorithm definition, we will use limits of $[-\pi, \pi]$ radians/sec. which will never be active. However, in cases where P, Q, and R are not regulated, we might require $|P| < 3$ deg/s and $|Q|, |R| < 15$ deg/s.

Results

One of the most important factors in obtaining a fast and meaningful solution to the linear trim problem is the scaling of the solution variables. As mentioned in [18], we can reflect the relative importance of the various elements in x and u by choosing a diagonal weighting or scaling matrix S such that

$$\bar{z} = S^{-1}z$$

where z is the vector of states and controls given by $z^T = (x^T, u^T)$. Referring to the quadratic programming problem (Eq. 3-14), the new (scaled) cost J_2 becomes

$$\bar{J}_2 = (FS\,\bar{z} - d)^T(FS\,\bar{z} - d) \qquad (6\text{-}81)$$

and the solution, z is given by $z = S\bar{z}$. The objective J_1 will be the Euclidean norm of $\bar{z}$, and the constraints on $\bar{z}$ are $S^{-1}z_L \leq \bar{z} \leq S^{-1}z_U$.

The use of the scaling matrix S as detailed above implies that variables which have large scale factors tend to be used more in the final solution. For the purposes of this investigation, a reasonable choice of scale factors result when the remaining "authority" of each variable is used as its scaling. That is, if the limit on z_i is symmetric about zero and equal to $z_L{}^i$, then S_{ii} is set equal to $z_L{}^i$. This will mean that variables whose nominal values are far from their limits will be used more in achieving the minimum norm solution. Also, this scaling implies that the scaled limits on z_i are $-1 \leq \bar{z}_i \leq 1$.

Summarizing, the parameters of the quadratic programming algorithm (Eq. 3-14) for this investigation, we have,

$$z_L{}^T = (-20,-8.7,-3,-0.20,-19,-3,-3,-.09,-2650,\ -2650,-3.5,-3.5,-5,-8,-8,-5,-5) \qquad (6\text{-}82)$$

$$z_U{}^T = (20,20,3,.20,19,3,3,.09,7750,7750,3.5,\ 3.5,5,2,2,5,5) \qquad (6\text{-}83)$$

$$S = \text{diag}\left[z_U \right] \tag{6-84}$$

(i.e., S is a diagonal matrix with the values of z_U given in Eq. 6-83 along its diagonal)

$$F = \begin{bmatrix} A & B \\ C & 0 \end{bmatrix} \tag{6-85}$$

$$d = \begin{pmatrix} -w \\ 0 \end{pmatrix} \tag{6-86}$$

Table 6-1 presents the linear trim solutions for disturbances, w, corresponding to single stuck or frozen control elements at non-zero positions (as in Eq. 6-76).

The engine failure (first column in the table) corresponds to a total loss of thrust. In this case, the failure is compensated by applying a large thrust to the remaining engine and then compensating for the remaining imbalances by a combination of surface deflections and state perturbations. The resulting flight-path angle can be computed by applying the perturbations of V_x, V_z and θ to the nominal values in Eq. 6-74 and 6-75 and computing the resulting value of $\gamma = \theta - \arctan(V_z/V_x) = -3.5$ degrees. Note that the total V_y and ϕ values are nonzero indicating that the aircraft is using a sideslip configuration to reject some of the lateral disturbances. This effect, and the use of nonzero perturbations of V_x, V_z, and θ, we will call "attitude coupling." The use of attitude coupling in the trim solution allows the aircraft to achieve the desired condition ($\dot{x}=0$, $y=y_d$) with smaller values of surface deflection as compared to the case where forces and moments are balanced

TABLE 6-1. QP SOLUTIONS FOR VARIOUS FAILURES

FAILURE / SOLUTION	LEFT ENGINE -4251 LBS	LEFT STABILATOR -8 DEG	RUDDER 10 DEG	LEFT ELEVATOR -12 DEG	LEFT AILERON 10 DEG
STATE PERTURBATIONS:					
V_x (f/s)	-20	-20	2.9	-4.9	.08
V_z (f/s)	8.0	7.9	-1.2	2.0	-1.0
Q (r/s)	0	0	0	0	0
θ (r/s)	.036	.041	-.006	.01	-.005
V_y (f/s)	6.3	-5.4	11	-2.7	5.4
P (r/s)	0	0	0	0	0
R (r/s)	0	0	0	0	0
ϕ (r)	.049	-.018	.006	-.009	.017
CONTROL PERTURBATIONS:					
LT (lbs)	0	-150	2750	24	-336
RT (lbs)	3113	-580	-2650	-200	130
LS (deg)	3.5	0	1.6	2.5	-.69
RS (deg)	-3.0	3.5	-1.2	2.3	-.32
R (deg)	-5.0	-1.5	0	-.81	1.7
LE (deg)	2.0	1.7	.26	0	-.11
RE (deg)	-8.0	1.6	-.20	.36	-.05
LA (deg)	5.0	2.95	3.3	.80	0
RA (deg)	-5.0	2.1	-3.8	.37	.28
NUMBER OF ITERATIONS FOR CONVERGENCE:	10	3	2	1	1

by the control surfaces alone (i.e., forcing all states to remain unperturbed and solving for a minimum $J_2 = \|Bu + w\|$). The use of attitude coupling is particularly pronounced in the rudder failure case where a sideslip angle of about 3 degrees results, and in the engine failure case where a bank angle of 2.8 degrees is maintained.

The effect of scaling is demonstrated by comparing Table 6-1 with Table 6-2. In Table 6-2 the same failure cases are used, but the scaling matrix S is set equal to the identity (i.e., no scaling). For the rudder and engine failures, two effects are clearly discernible. First, with no scaling (Table 6-2), the tendency is to use considerably more control-surface and attitude-coupling perturbations with less thrust perturbations. This might be expected since the scaled results (Table 6-1) put a smaller price on the use of thrust perturbations. Also, in these two cases, several variables are at their limits, and as a result, the number of iterations needed to find these solutions is substantially greater than those in Table 6-1. In the other failure cases, substantially smaller thrust perturbations appear as compared to Table 6-1, but the control surface and attitude coupling perturbations are not affected as greatly as in the case of rudder and engine failures.

The above solutions provide some idea of the capabilities of the linear trim algorithm for some fairly severe failure situations. In all cases defined above, the feasible solution provided perfect disturbance rejection capabilities (in the sense that $Fz - d = 0$ in Eq. 3-14). One of the issues raised in early assessments of the restructurable control problem (e.g., see [34]), was how the use of various nonstandard control surfaces would impact the ability to recover a stable flight condition following a major failure. The above results suggest that sufficient control authority among the normal

TABLE 6-2. QP SOLUTIONS FOR VARIOUS FAILURES - NO SCALING

FAILURE / SOLUTION	LEFT ENGINE -4251 LBS	LEFT STABILATOR -8 DEG	RUDDER 10 DEG	LEFT ELEVATOR -12 DEG	LEFT AILERON 10 DEG
STATE PERTURBATIONS:					
V_x (f/s)	-20	-12.9	-20	.07	5.3
V_z (f/s)	5.5	4.4	8.4	-.03	-3.1
Q (r/s)	-.006	0	0	0	0
θ (r)	.017	.02	.04	-.0002	-.01
V_y (f/s)	1.9	-6.3	15.8	-1.3	3.9
P (r/s)	-.002	0	0	0	0
R (r/s)	-.0002	0	0	0	0
ϕ (r)	.03	-.018	.03	-.004	.01
CONTROL PERTURBATIONS:					
LT (lbs)	0	-30	1510	-.01	-.21
RT (lbs)	2030	-30	-2140	-.01	-.2
LS (deg)	3.5	0	3.5	3.5	-2.6
RS (deg)	-3.5	3.5	-3.0	1.8	2.4
R (deg)	-5.0	-2.3	0	-.5	1.6
LE (deg)	1.6	2.0	2.0	0	-1.2
RE (deg)	-8.0	2.0	-8.0	.87	1.2
LA (deg)	5.0	5.0	5.0	.99	0
RA (deg)	5.0	5.0	-5.0	-.93	-1.6
NUMBER OF ITERATIONS FOR CONVERGENCE:	>30	6	9	2	1

control elements seems to be available for rejecting the disturbances caused by any single stuck or frozen control element failure. Therefore, the only impact of using nonstandard control elements in the failure cases we have examined would be in increasing the amount of remaining control authority of the primary surfaces while maintaining the desired disturbance rejection capabilities. We now demonstrate this effect by including the use of spoilers in conjunction with the other surfaces in solving the trim problem.

Three issues which must be addressed before adding spoilers as a control element in the trim problem are: (1) the nominal deflection value (about which minimum perturbations will be sought), (2) the scale factor or weight which will be used, and (3) the linear range of spoiler deflection.

While some advantage to using nonzero nominal spoiler deflections in the trim problem exist (e.g., the ease with which these surfaces might be included in a redesigned control system), such use is likely to result in spoiler deployment upon a false failure alarm. While this may not be a major drawback, it would increase the burden on any executive control logic system for determining when spoiler deployment is desirable. Therefore, in the results that follow, we will assume a nominal value of zero spoiler angle in which, if there are no disturbances to reject, all of the unfailed nominal deflections will be maintained.

In order to insure that the spoilers are used when a failure does exist, their use must be made cheap by proper choice of their corresponding scale factors. For example, we can guarantee that a full spoiler deflection (of say 10 degrees) is used before, say, 0.5 degrees of another surface (if they would produce the same disturbance rejection capabilities) by making the ratio of

their scale factors 200:1. For example, a scale factor of 5 on other surfaces gives a desired spoiler scale factor 1000 degrees. Finally, to maintain model accuracy, we must limit spoiler deflection to the range [0,8] degrees.

The augmented B matrix for the results that follow is

$$B = \begin{bmatrix} 0.38E\text{-}03 & 0.38E\text{-}03 & 0.0068 & 0.0068 & 0.0000 & 0.0032 & 0.0032 & 0.0036 & 0.0036 & -0.0164 & -0.0164 \\ -0.29E\text{-}06 & -0.29E\text{-}06 & -0.1688 & -0.1688 & 0.0000 & -0.0809 & -0.0809 & -0.0904 & -0.0904 & 0.1733 & 0.1733 \\ 0.63E\text{-}05 & 0.63E\text{-}05 & -0.0221 & -0.0221 & 0.0000 & -0.0106 & -0.0106 & -0.0028 & -0.0028 & 0.0021 & 0.0021 \\ 0.0000 & 0.0000 & 0.0000 & 0.0000 & 0.0000 & 0.0000 & 0.0000 & 0.0000 & 0.0000 & 0.0000 & 0.0000 \\ 0.0000 & 0.0000 & 0.0000 & 0.0000 & 0.1389 & 0.0000 & 0.0000 & 0.0005 & -0.0005 & 0.0262 & -0.0262 \\ 0.21E\text{-}05 & -0.21E\text{-}05 & 0.0074 & -0.0074 & 0.0093 & 0.0036 & -0.0036 & 0.0082 & -0.0082 & -0.0197 & 0.0197 \\ 0.12E\text{-}04 & -0.12E\text{-}04 & 0.0004 & -0.0004 & -0.0109 & 0.0003 & -0.0003 & 0.0007 & -0.0007 & -0.0026 & 0.0026 \\ 0.0000 & 0.0000 & 0.0000 & 0.0000 & 0.0000 & 0.0000 & 0.0000 & 0.0000 & 0.0000 & 0.0000 & 0.0000 \end{bmatrix} \quad (6\text{-}87)$$

where the last two columns correspond to the estimated spoiler effectiveness.

Table 6-3 summarizes the result of applying the quadratic programming algorithm with the spoiler-augmented B matrix to the linear trim problem for the failure cases used in the previous discussion. Comparing Tables 6-1 and 6-3, we see that in the case of engine, rudder and aileron failures, the use of spoilers, as expected, reduces the amount that the primary control surfaces must contribute to the trim solution.

Summary

The results presented in this section demonstrate the operation of a quadratic programming algorithm in the solution of the linear trim problem for several failure cases of interest. The importance of scaling the solution variables was demonstrated and it was seen that: (1) the amount of control usage of one element relative to other elements (and the relative amount of attitude coupling) could be modified by proper choice of scale factors, and

TABLE 6-3. QP SOLUTIONS FOR VARIOUS FAILURES - WITH SPOILER DEFLECTIONS

FAILURE / SOLUTION	LEFT ENGINE -4251 LBS	LEFT STABILATOR -8 DEG	RUDDER 10 DEG	LEFT ELEVATOR -12 DEG	LEFT AILERON 10 DEG
STATE PERTURBATIONS:					
V_x (f/s)	-6.9	-20	1.33	-4.8	.92
V_z (f/s)	4.6	7.9	1.29	2.07	-.01
Q (deg/s)	0	0	0	0	0
θ (deg)	1.3	2.3	.32	.60	-.01
V_y (f/s)	9.25	-5.4	15.6	-1.9	.36
P (deg/s)	0	0	0	0	0
R (deg/s)	0	0	0	0	0
ϕ (deg)	3.93	-1.02	1.9	-.34	-.06
CONTROL PERTURBATIONS:					
LT (lbs)	0	-148	1815	9.6	129
RT (lbs)	4558	-577	-1222	-140	119
LS (deg)	.80	0	.31	2.51	-.30
RS (deg)	-1.3	3.50	.18	2.39	-.30
R (deg)	-5.0	-1.51	0	-.52	-.13
LE (deg)	.14	1.69	.05	0	-.05
RE (deg)	-.23	1.63	.02	.37	-.05
LA (deg)	3.6	2.95	.35	.74	0
RA (deg)	-2.0	2.10	-.12	.44	-.05
LSP (deg	0	0	0	0	4.90
RSP (deg)	8.0	0	8.0	.65	1.08
NUMBER OF ITERATIONS FOR CONVERGENCE:	20	3	5	2	3

(2) the number of iterations needed to obtain a solution is greatly influenced by the particular choice of scale factors. In addition, the use of nonstandard control elements was demonstrated by considering the addition of spoiler control elements. In most cases, the addition of spoilers caused the resulting solution to achieve the desired flight condition with smaller values of nominal primary control surface perturbations.

6.4 LINEAR ANALYSIS OF CONTROL LAWS FOR STUCK FAILURES

In this subsection we present a brief summary of the results of an extensive linear analysis of the control redesign procedure. The matrix of test cases is shown in Table 6-4. For each test case, the closed-loop eigenvalues were determined, the singular values of the loop transfer function (LTF) were plotted versus frequency, a linear simulation of the aircraft response to wind gusts was performed, step responses to stabilator and engine failures were examined, and, in the correct redesign cases (4xx), the initial condition response to a particular trim solution was found. In addition, wind gust responses for the no-failure case were found. Note that in these trials using the redesigned control law when there is no failure, is identical to the case when there is a failure and it is correctly identified. The simulations are all based on a linear rigid body approximation to the aircraft dynamics. No actuator dynamics and no travel limits are imposed, however, in most cases, the control surfaces remain within their saturation limits. Some characteristic results are presented below.

TABLE 6-4. MATRIX OF TEST CASES WITH MNEMONICS

	NO REDESIGN	CORRECT REDESIGN	INCORRECT REDESIGN	INCORRECT REDESIGN	
LT	3LT	4LT			
LS	3LS	4LS	5LS/LE		
R	3R	4R	5R/LA		
LE	3LE	4LE	5LE/RE	5LE/LS	
LA	3LA	4LA	5LA/R		
LA & RA	3LARA	4LARA			
LS & RS	3LSRS	4LSRS			
LS & LE	3LSLE	4LSLE			

Key: R/LT = Right/Left Engine

R/LS = Right/Left Stabilizer

R = Rudder

R/LE = Right/Left Elevator

R/LA = Right/Left Aileron

3XX = No Redesign Cases

4xx = Correct Redesign Cases

5xx = In Correct Redesign Cases

Table 6-5 provides the eigenvalues (listed in order of decreasing real part) for some of the no redesign and correct redesign cases (3xx and 4xx). Note that no distinction between lateral and longitudinal modes is made in the table since the aircraft does not, in general, decouple when a failure occurs. For comparison, the open loop eigenvalues (including the 4 integrator states) are:

Longitudinal Modes		Lateral Modes		
-.61 ± 1.5j	(short period)	-1.7	(roll subsidence)	
-.017 ± .17	(phugoid)	-.058 ± 1.1j	(dutch roll)	
0.0	(integrator)	-.0063	(spiral)	(6-88)
0.0	(integrator)	0.0	(integrator)	
		0.0	(integrator)	

and the closed loop eigenvalues for the baseline design are

Longitudinal Modes	Lateral Modes	
-1.2 ± .97j	-1.9	
-1.1	-1.1	(6-89)
-.71	-.86 ± 1.5j	
-.10 ± .023j	-.62 ± .50j	

In Table 6-5, a * denotes eigenvalues which are significantly different with the redesigned control law as compared to the nominal control law when the corresponding failure is present.

The most striking result is for the rudder failure (test cases 3R and 4R). With no redesign, one eigenvalue appears at -.007 r/s. Although this is close to the open loop spiral mode, the eigenvector associated with this mode is actually comprised mostly of the side velocity integrator state. The redesigned control law moves this mode to -.16 r/s which is presumably superior.

TABLE 6-5. CLOSED LOOP EIGENVALUES FOR TEST CASES (3XX) AND (4XX)

3LT	4LT	3LS	4LS	3R	4R
-1.9	-1.9	-1.9	-1.9	-1.9	-1.9
-1.2 ± .97j	-1.2 ± .97j	-1.1	-1.1	-1.2 ± .97j	-1.2 ± .97j
-1.1	-1.1	-1.1 ± 1.2j	-1.1 ± 1.1j	-1.1	-1.1
-1.1	-1.1	-.85 ± 1.5j	-.86 ± 1.5j	-.71	-.71
-.86 ± 1.5j	-.86 ± 1.5j	-.65 ± .36j	-.78 ± .14j*	-.47 ± .54j	-.50 ± .55j
-.72	-.71	-.56 ± .46j	-.62 ± .48j*	-.13 ± 1.1j	-.18 ± 1.1j
-.62 ± .5j	-.62 ± 0.5j	-.1 ± .02j	-.1 ± .02j	-.10 ± .02j	-.16*
-.082	-.085			-.007	-.10 ± .02j
-.065	-.066				

3LE	4LE	3LA	4LA
-1.9	-1.9	-1.8	-1.8
-1.1	-1.1 ± 1.1j	-1.2 ± .99j	-1.2 ± .98j
-1.1 ± 1.2j	-1.1	-1.1	-1.1
-.85 ± 1.5j	-.86 ± 1.5j	-1.0	-1.0
-.66 ± .34j	-.79 ± .12j*	-.82 ± 1.5j	-.86 ± 1.5j
-.56 ± .47j	-.61 ± .49j	-.74	-.73
-.10 ± .02j	-.10 ± .02j	-.44 ± .46j	-.60 ± .42j*
		-.10 ± .02j	-.10 ± .02j

The wind gust response for these (rudder failure) cases shows slightly better regulation of bank angle with the redesigned control law, although in both designs, the oscillations are not desirable and much larger than the gust response of the unfailed aircraft with the nominal control law. This is shown in Figs. 6-9 through 6-11. Although the bank angle appears divergent in Figs. 6-10 and 6-11, it is actually reasonably regulated when the simulation is run for longer time periods. With the redesigned control law, any improvement in regulation is accomplished through the increased use of differential elevators, stabilators and throttle. It appears that differential aileron is used in the same manner for both cases 3R and 4R.

Table 6-6 shows the closed loop eigenvalues for several combinations of stuck failures. For the failure of both ailerons (test cases 3LARA and 4LARA), the eigenvalue at $-.84 \pm .05j$ with no redesign becomes overdamped at -1.0 and -.98 when the redesigned control law is implemented. In the other cases, underdamped modes with no redesign become better damped when the redesigned control law is used. In addition, it is interesting to note that in many cases, the redesigned eivenvalues revert back closer to the original baseline eigenvalues than do the non-redesigned eivenvalues. The wind gust responses for cases 3LSLE and 4LSLE show that better regulation of forward velocity (u) is achieved with the redesigned control law and that this is accomplished through the increased use of collective ailerons and throttle. Figures 6-12 and 6-13 compare the velocity regulation performance of the nominal and redesigned control law with stuck left stabilator and left elevator.

The step response of the closed loop system to a hard-over failure is given by

$$\dot{x} = (A-BG)x + w \qquad (6-90)$$

where x is the perturbation of the state variables from their unfailed trim values, w is the step disturbance caused by a hard-over failure (see Eq. 6-76), B is the effectiveness matrix for the failed aircraft, and G is the feedback gain. Figures 6-14 and 6-15 compare the response to a failed throttle using the nominal feedback gain (no restructuring) and the feedback gain determined by the control resdesign procedure. Surprisingly, the aircraft seems to recover from the failure without saturation of any control element even with no control law redesign. The maximum angle of attack during this recovery is 3.5 degrees and the maximum bank angle is about 1 degree. Forward velocity is reduced by about 8 fps before it begins to increase. With the redesigned control law, the most noticable effect is the slightly decreased use of rudder and aileron controls during recovery.

The step response to a stabilator runaway (both stabilators hard-over to their negative limit) was also examined. In both the cases (redesign and no redesign) recovery is accomplished only by exceeding the saturation limits of the elevators. When the feedforward trim solution is applied for this case, recovery is accomplished without saturation of the elevators, however, the remaining throttle is initially retarded to zero thrust which, presumably, violates allowable operation. Further examination of these cases appears in Section 7, where they are simulated on a nonlinear aircraft model which includes the various surface travel and rate limits as well as actuator dynamics.

Finally, Table 6-7 shows the closed loop eigenvalues for several misclassification cases. That is, the actual control effectiveness (B matrix) corresponds to one failure, but the control law redesign is implemented for another. The net effect of a misclassification is to remove both the surface which is failed and the surface which is identified as failed from use in the redesigned

control system. As a result, the eigenvalues in Table 6-6 tend to resemble the cases corresponding to a failure with no redesign. This is particularly evident for case 5R/LA where we see the integrator mode at -.008 r/s which is very close to the mode at -.007 for case 3R.

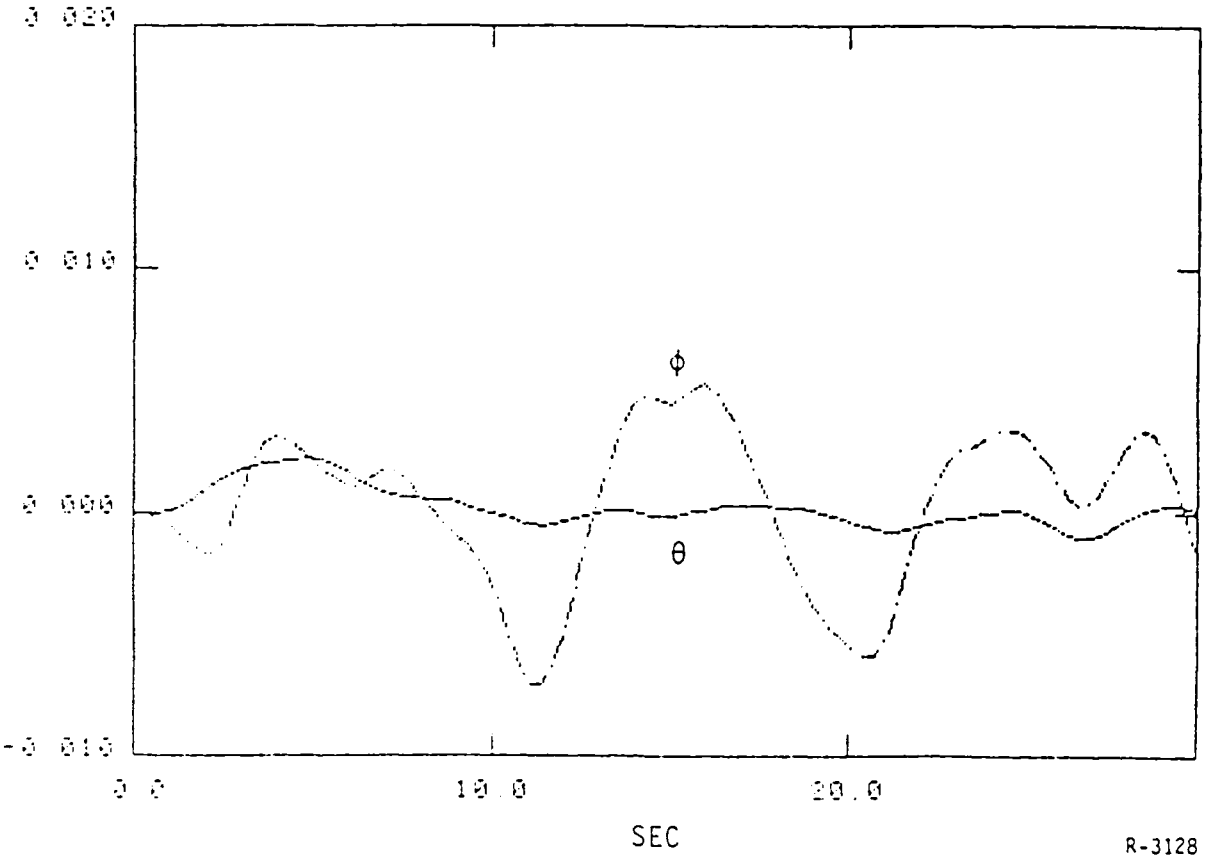

Figure 6-9. Gust Response for No Failure and Nominal Control Law

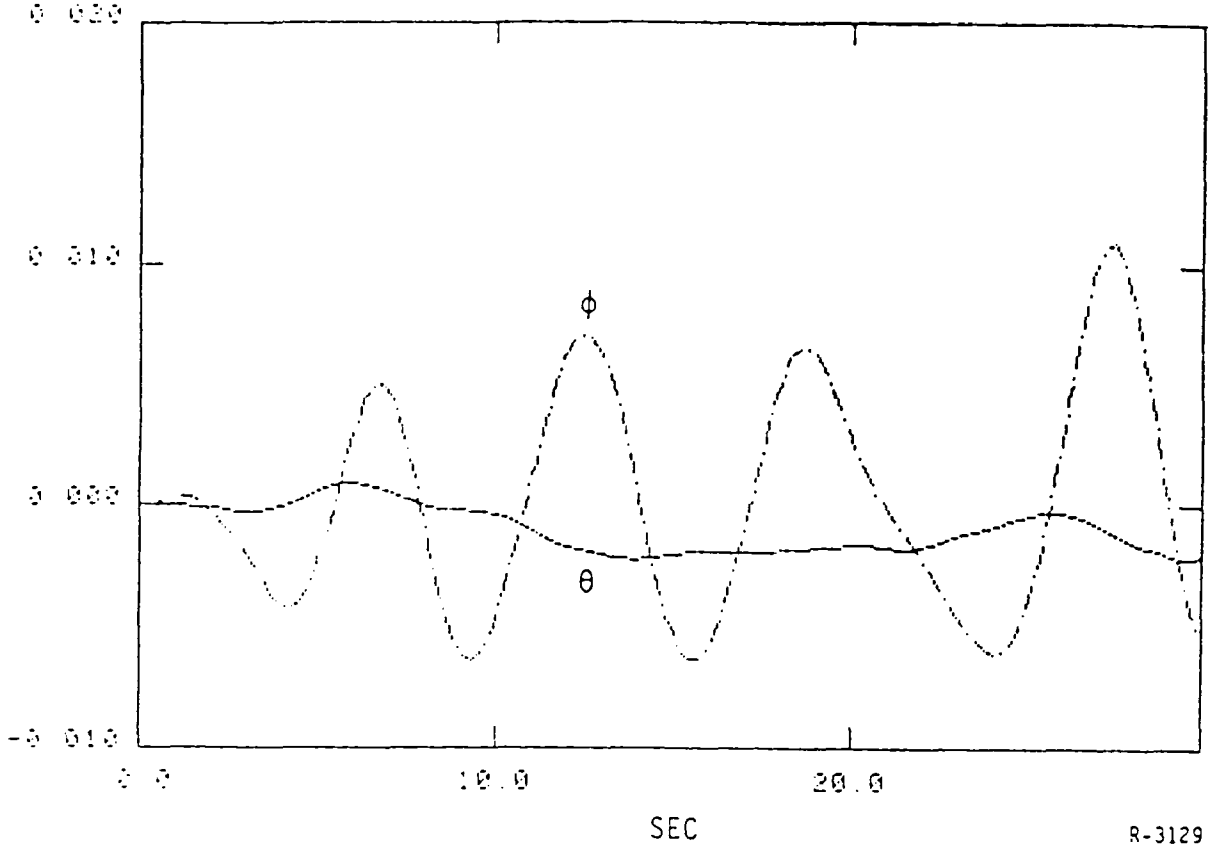

Figure 6-10. Gust Response for Rudder Failure with No Redesign

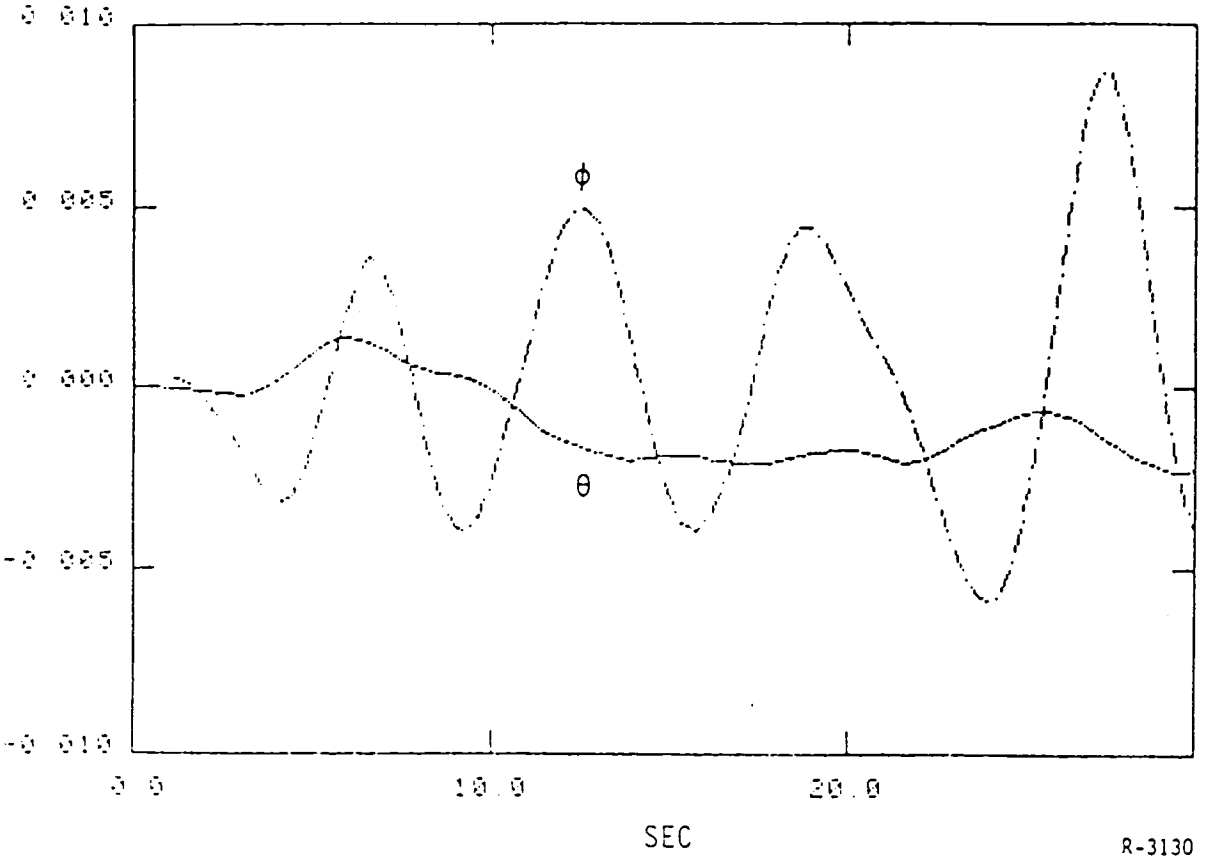

Figure 6-11. Gust Response for Rudder Failure with Redesigned Control Law

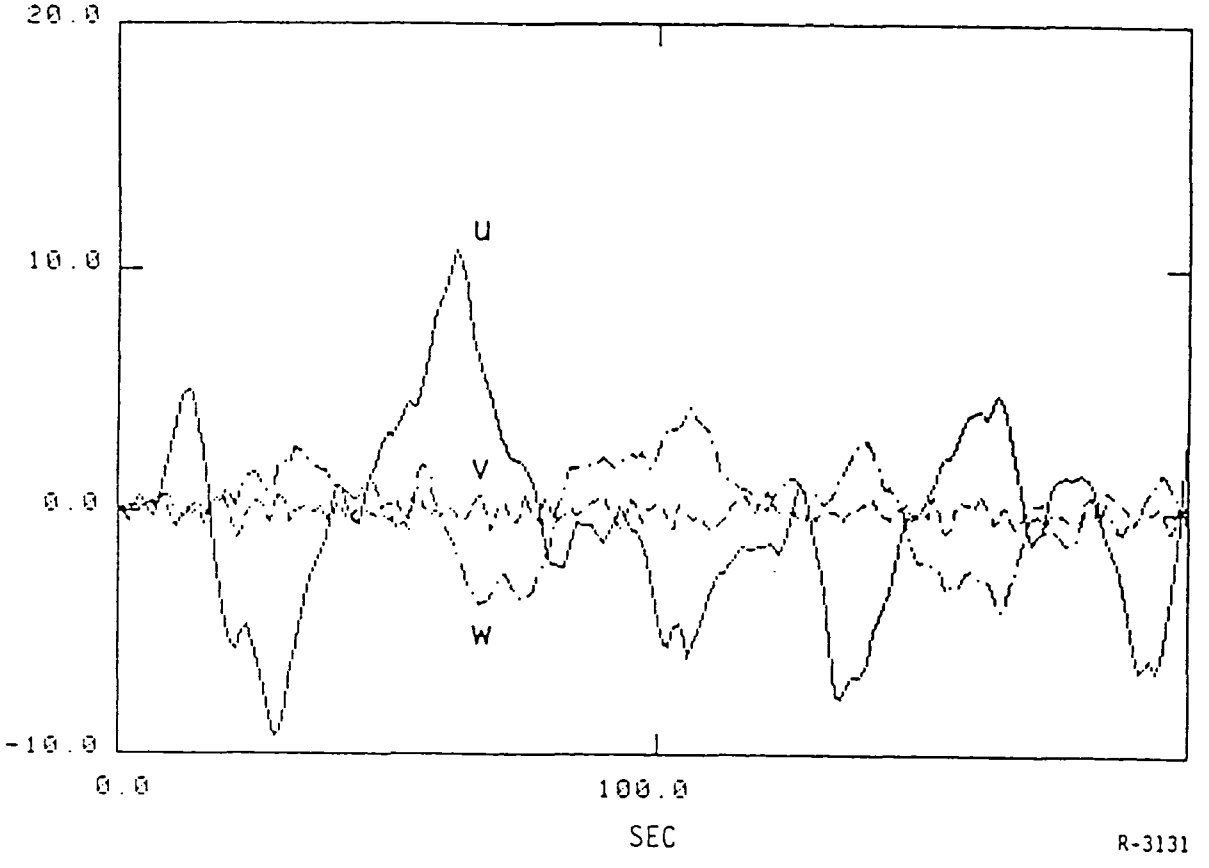

Figure 6-12. Closed Loop Gust Response for Case 3LSLE

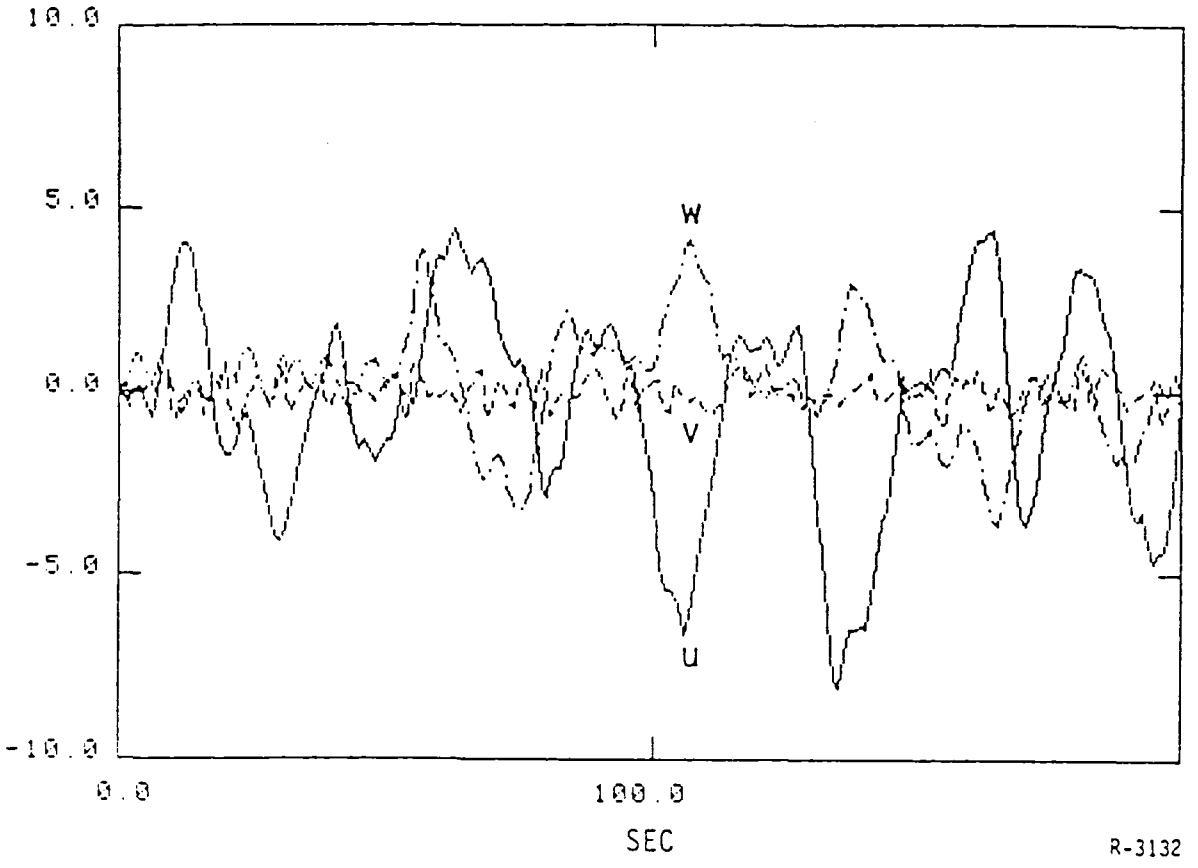

Figure 6-13. Closed Loop Gust Response for Case 4LSLE

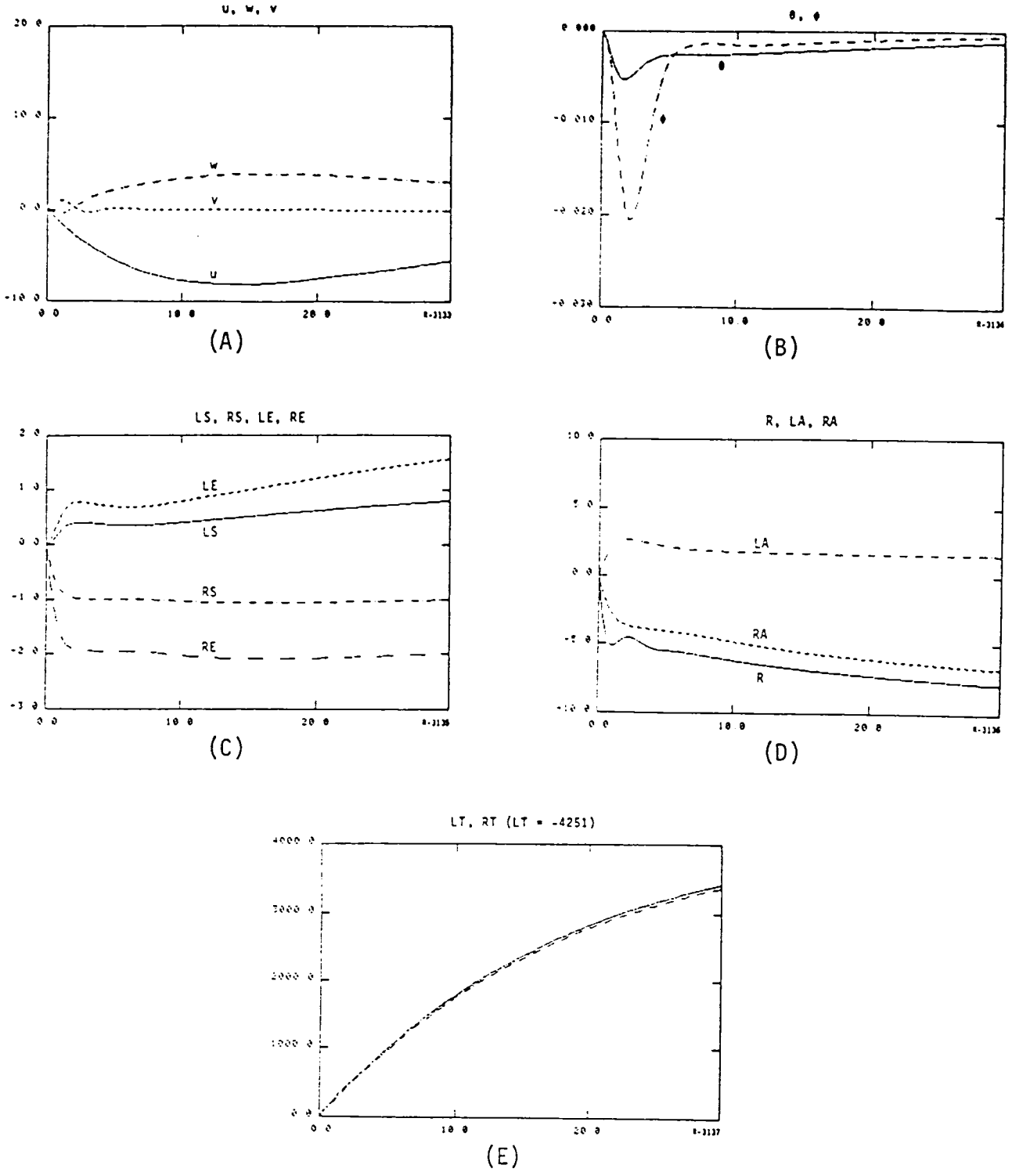

Figure 6-14. Recovery Response to a Left Engine Failure with No Redesign (Case 3LT - No Trim Perturbation from Eqs. 6-74 and 6-75)

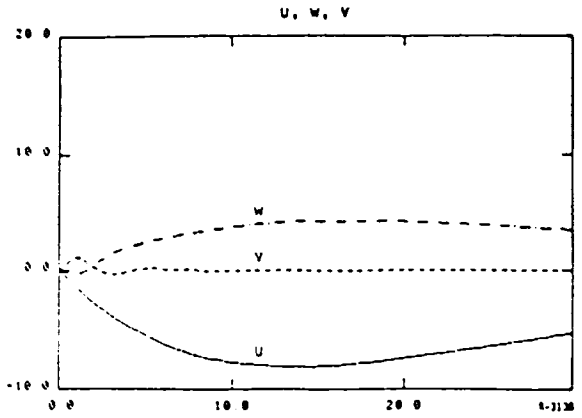

(A)

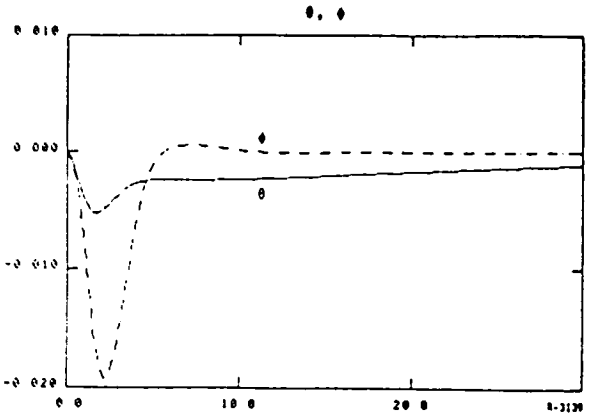

(B)

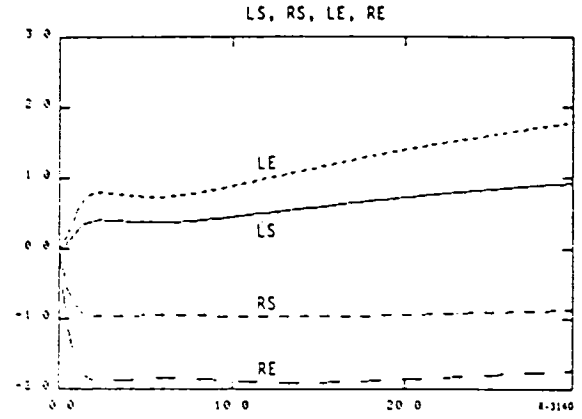

(C)

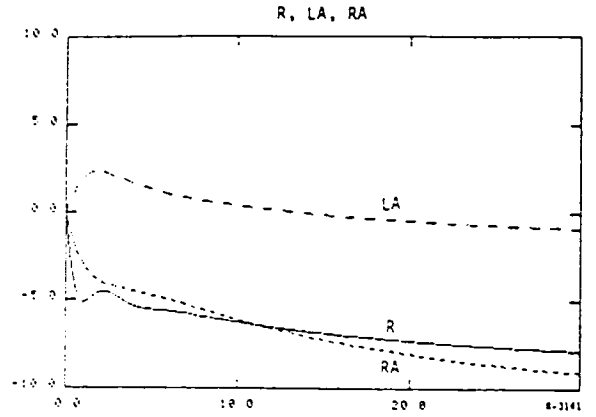

(D)

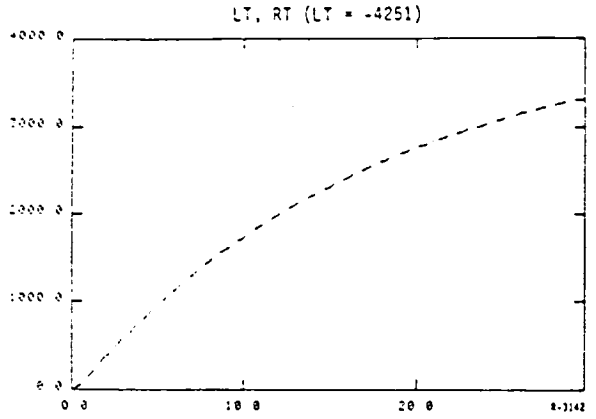

(E)

Figure 6-15. Recovery Response to a Left Engine Failure with Redesign (Case 4LT - No Trim Perturbations from Eq. 6-74 and 6-75)

TABLE 6-6. CLOSED LOOP EIGENVALUES FOR COMBINED FAILURE TEST CASES

3LARA	4LARA	3LSRS	4LSRS	3LSLE	4LSLE
-1.7	-1.7	-1.8	-1.8	-1.9	-1.9
-1.2	-1.2 ± .98j	-1.1	-1.1	-1.1	-1.1
-1.2 ± 1.0j	-1.0*	-.87 ± 1.3j	-1.0 ± 1.2j	-.90 ± 1.3j	-1.0 ± 1.1j
-.84 ± .05j	-.98* -.73	-.85 ± 1.5j	-.86 ± 1.5j	-.83 ± 1.5j	-.86 ± 1.5j
-.80 ± 1.5j	-.87 ± 1.5j	-.55 ± .49j	-.69 ± .22j*	-.65 ± .44j	-.66 ± .24j
-.26 ± .35j	-.59 ± .24j*	-.45 ± .39j	-.61 ± .47j*	-.36 ± .41j	-.63 ± .45j*
-.10 ± .02j	-.10 ± .02j	-.10 ± .02j	-.10 ± .02j	-.10 ± .02j	-.10 ± .02j

TABLE 6-7. CLOSED LOOP EIGENVALUES FOR MISCLASSIFICATION CASES (5XX)

5LE/RE	5LE/LS	5LS/LE	5R/LA	5LA/R
-1.8	-1.9	-1.9	-1.8	-1.8
-1.1	-1.1	-1.1	-1.2 ± .98j	-1.2 ± .99j
-.96 ± 1.3j	-.95 ± 1.3j	-.95 ± 1.3j	-1.0	-1.0
-.85 ± 1.5j	-.84 ± 1.5j	-.84 ± 1.5j	-.72	-.74
-.58 ± .46j	-.65 ± .43j	-.65 ± .43j	-.41 ± .48j	-.33 ± .50j
-.57 ± .37j	-.14 ± .40j	-.43 ± .40j	-.11 ± 1.1j	-.15 ± 1.1j
-.10 ± .02j	-.10 ± .02j	.10 ± .02j	-.10 ± .02j	-.16
			-.008	-.10 ± .02j

SECTION 7

SIMULATION RESULTS

The performance of the restructurable flight control system (RFCS) described in Section 5 was tested at the NASA Langley Research Center using that facility's modified B-737 aircraft (batch) simulation. This simulation was chosen because of its extensive capabilities for simulating realistic responses (during normal and failed flight) of the B-737 aircraft. Models of this aircraft were used during this project for design and evaluation of the RFCS concept and it is anticipated that some limited flight tests on NASA's Advanced Transport Operations (ATOPS) B-737 aircraft may be possible. A summary of the simulation's capabilities and the test results is presented next. This is then followed by a more detailed description of the full test plan and a discussion of some of the more interesting results.

7.1 SUMMARY

The capabilities of the simulation which are relevant to this project are listed in Table 7-1. The simulation is based on the 6 degree of freedom equations of motion for a rigid body driven by aerodynamic, propulsive, and gravity forces. The aerodynamic model is nonlinear and, for this project, could not be altered. Full independent control authority is available and realistic actuator models including rate and travel limits are employed. The control system described in subsection 6.2 was implemented with the capability to change the control gains and the nominal "trim" values at any preselected

TABLE 7-1. CAPABILITIES OF NASA's MODIFIED B-737 SIMULATION

6 DOF Rigid body Equations
Nonlinear Aerodynamic Model
Independent Control Authority
Actuator Models (Rate and Travel Limits)
Control System
Command Generation
Sensor Noise
Wind Gusts
Failures

times during the simulation. All control redesign and trim calculations were made off-line for the selected failure cases. A command generator which provided steps and ramps of commanded pitch angle, bank angle, sideslip, and longitudinal velocity was also made implemented. Finally, the simulation had the capability to simulate stuck (at last value) and hard-over (runaway) failures including engine out conditions.

There were three important general results that were observed. First, the nontraditional use of traditional control surfaces in a nominal feedback control system to spread control authority amongst many redundant (in terms of the forces and moments which can be produced) control elements provided a significant amount of fault tolerance without any use of restructuring techniques. In most single element failures, "recovery" was automatically achieved and little loss in command response performance was observed. A stuck rudder failure provided the most challenging single element failure

situation since it is used extensively for damping the dutch roll mode and since generation of side force is generally not possible with the other control elements.

Secondly, the use of new feedback gains (provided by the feedback control redesign procedure) following a failure, alone can provide significantly improved recovery as long as the control elements remain within their travel limits and as long as uncertainty about the failure identity is properly handled. This effect is particularly evident in the stuck rudder failure case. When control elements reach their travel limits during a failure, performance generally degrades as expected. In failure cases where the nominal control system performed well by itself, the application of redesigned feedback gains resulted in little, if any improvement. However, when a failure is misclassified and feedback control redesign is based on the incorrect control element, potentially severe performance degradation can take place. By embedding FDI uncertainty in the redesign procedure, significantly better performance is achieved (over the misclassified failure case) although it is clear that correct failure identification (and subsequent application of redesigned feedback gains) provides the best performance during failures.

Finally, the use of the feedforward trim solution in conjunction with redesigned feedback gains, allows recovery to take place in most cases, even when significant control saturation occurs. This is generally due to the fact that any servo errors resulting from a failure are quickly reduced by application of the feedforward trim solution. Since the redesigned control system stabilizes the aircraft and the servo errors remain small due to the feedforward trim, recovery is generally achieved even when many control elements reach and remain at their travel limits.

7.2 IMPLEMENTATION AND TEST PLAN DETAILS

In all of the results to be subsequently presented, the following assumptions were made.

1. All simulation runs were begun in the nominal configuration defined in subsection 6.1. The nominal trim values (x_o, u_o) initially applied to the aircraft are given by Eqs. 6-74 and 6-75.

2. In order to handle windup of the integrator states during control saturation, Eqs. 6-70 and 6-71 are modified to:

$$\dot{x}_I = G_I (y - y_o - r) \tag{7-1}$$

$$u = u_o - G_r x_r - G_y(y - y_o - r) - x_I \tag{7-2}$$

   Since there is, now, one integrator state per control element, when a particular control reaches its travel limit, the corresponding integrator state is held at its last value until the corresponding control comes out of saturation.

3. In most cases (except where noted in subsection 7.3) the travel limits on each control element are given by their allowable perturbations from trim and take the following values.

Stabilator limits	(-9 to 8 degrees)
Elevator limits	(±20 degrees)
Aileron limits	(±10 degrees)
Rudder limits	(±10 degrees)
Spoiler limits	(0 to 40 degrees)
Throttle limits	(-10 to 40 degrees)

4. All applications of the redesign technique (except where noted) were implemented by setting the column of the B matrix defined in Eq. 6-5 corresponding to the failed control element equal to zero.

5. Finally, the definitions and values used in solving the trim problem are (except where noted) given by Eqs. 6-82 through 6-87.

The overall test plan was designed to demonstrate the ability of the aircraft to recover from a failure and follow subsequent commands under the following conditions.

1. No redesign (nominal feedback system only),
2. Gains only (application of redesigned feedback gains at the time of failure),
3. Gains and Trim (application of redesigned feedback gains and feedforward trim values at the time of failure),
4. FDI delay (application of gains and trim at seledcted times following a failure),
5. FDI misclassification (application of redesigned control gains for an unfailed control at the time of failure and use of uncertainty in the redesign technique),
6. Spoilers (use of spoilers in the solution of the trim problem and application of gains and trim values at the time of failure.

Each of these "test cases" were examined for a variety of failure modes including:

1. Individual stuck surfaces (left or right stabilator, elevator, aileron and rudder),
2. Stabilator runaway (runaway up and runaway down),
3. Engine out,
4. Combinations of stuck failures.

In the next subsection, we present some of the more interesting results which provide substantiation for the conclusions drawn in subsection 7.1.

7.3 DETAILED RESULTS

For single element stuck failures (including the engine out failure), the nominal LQ control system performed quite well, both in terms of recovery and subsequent command following.

Figure 7-1 shows the command responses for a bank-sideslip-pitch maneuver for the unfailed aircraft (7-1a) and with the left elevator stuck at 3.6 degrees at t = 4 seconds (7-1b). We notice very little effect in the bank response (ϕ) during the bank maneuver in which the failure occurred or in the subsequent sideslip response. The pitch response with the left elevator failure shows slightly greater coupling during these lateral maneuvers but follows the pitch command nearly as well as with no failure. Surprisingly, little coupling in the lateral axis occurs during the pitch maneuver with the stuck elevator failure. Figures 7-2 and 7-3 show the control usage for the no-failure and left elevator stuck failure cases, respectively. Notice that the disturbance caused by the stuck off-centered elevator is compensated by a small amount of differential stabilator which is not present when there is no failure.

Figures 7-4 through 7-7 examine the impact of a stuck rudder failure occurring during a sideslip maneuver. Figure 7-4 shows the unfailed responses to the baseline sideslip-bank-pitch maneuver sequence. Figure 7-5 and 7-6 show the sideslip (β) and bank (ϕ) responses for a stuck rudder failure occurring at about t = 3 seconds (stuck off-center at about 7 degrees) for a variety of test cases. With no reconfiguration, we see signficant dutch roll oscillations as expected from the linear analyses of Section 6. Significant residual sideslip is still present at t = 60 secs. (about 55 secs. following the β = 0 command). The bank maneuver is performed with some loss in performance due to the fact that the ailerons become saturated. This occurs because of the significant use of ailerons to counteract the rolling moment of the stuck rudder. A roll command in the opposite direction, would, of course, not cause aileron

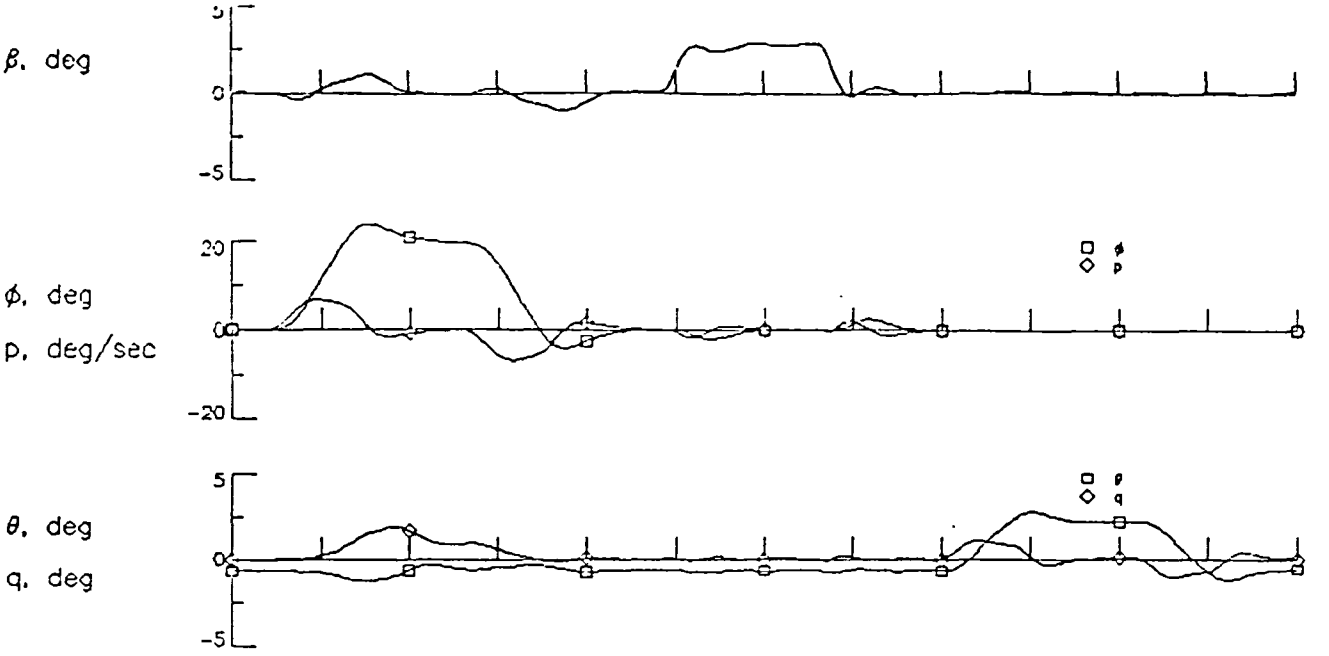

Figure 7-1a. No Failure Response

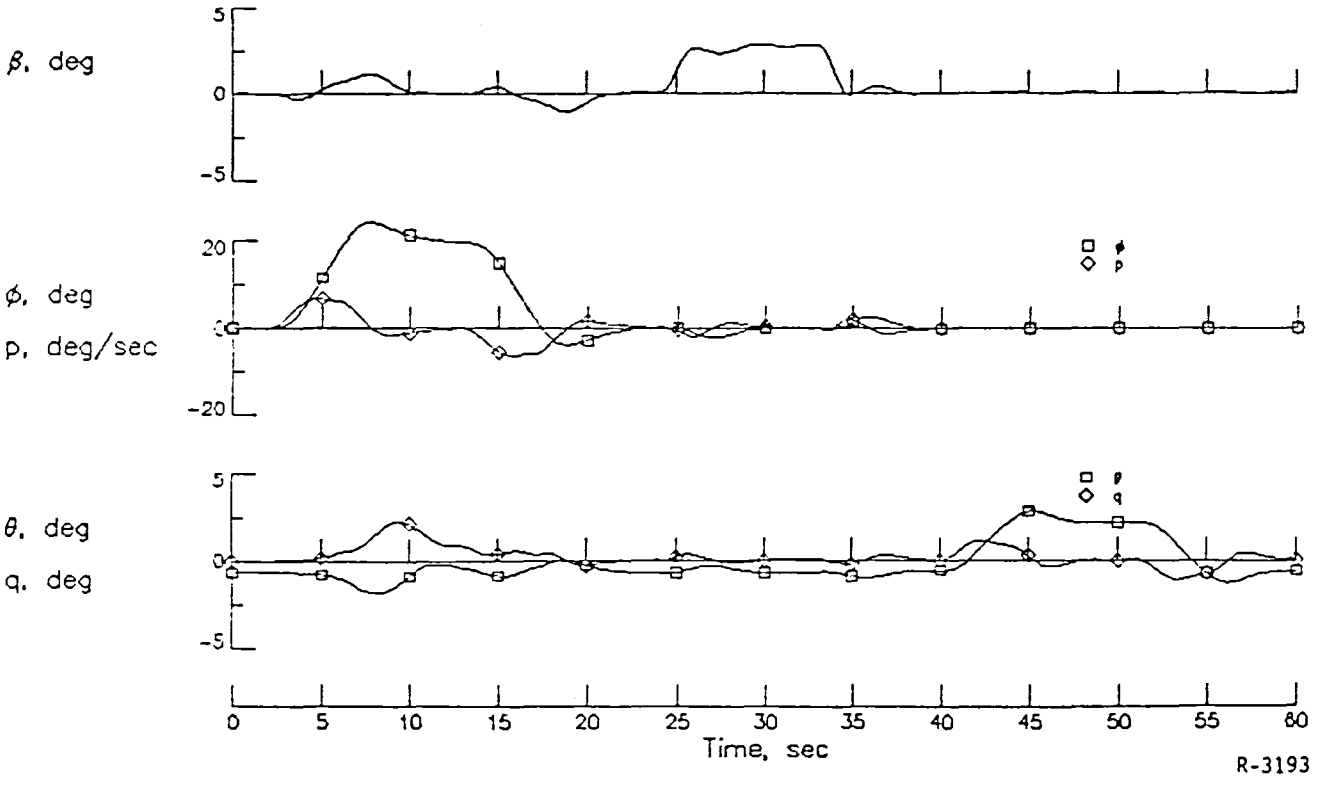

Figure 7-1b. LE Failure (No Recon) Response

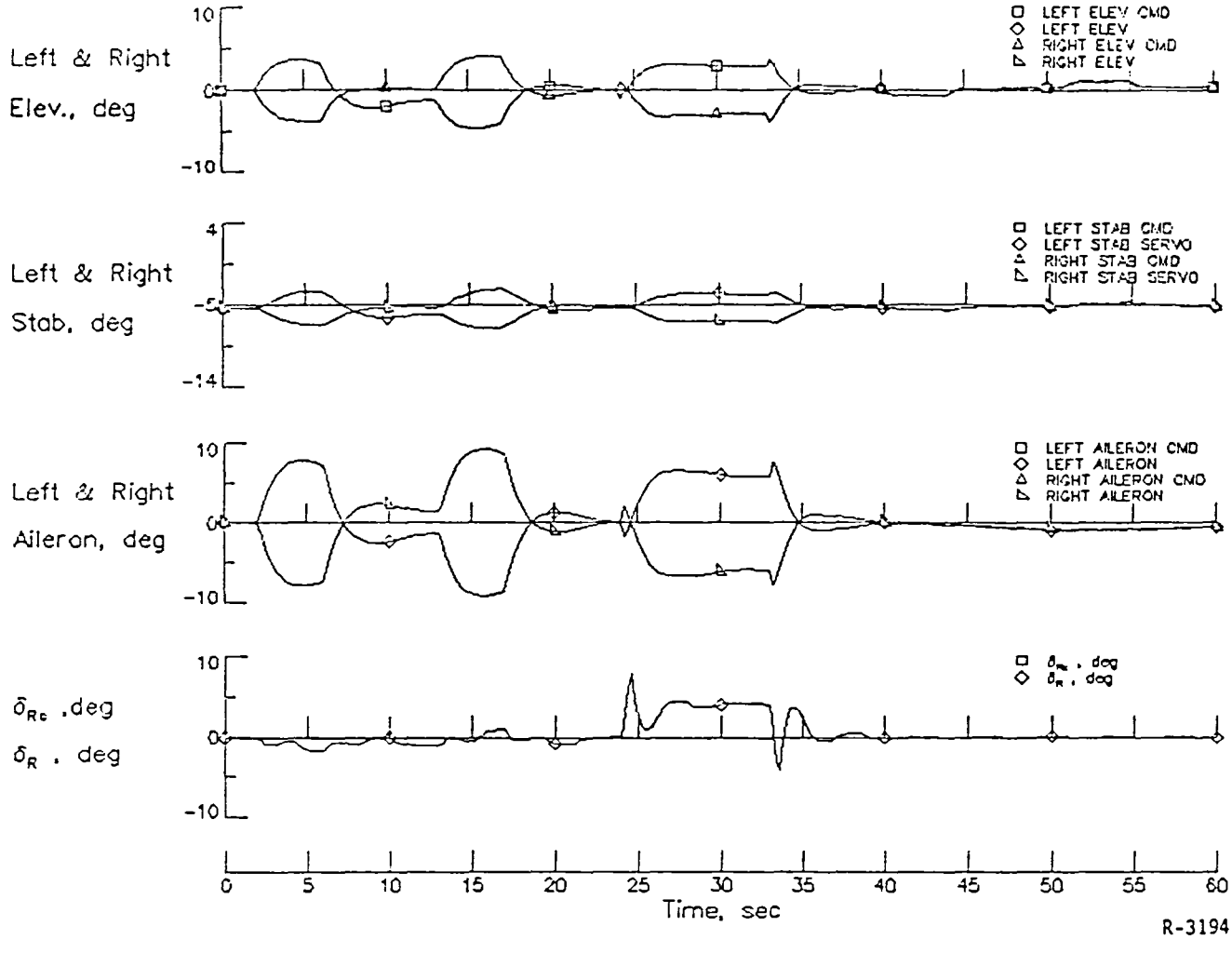

Figure 7-2. Control Usage for No Failure

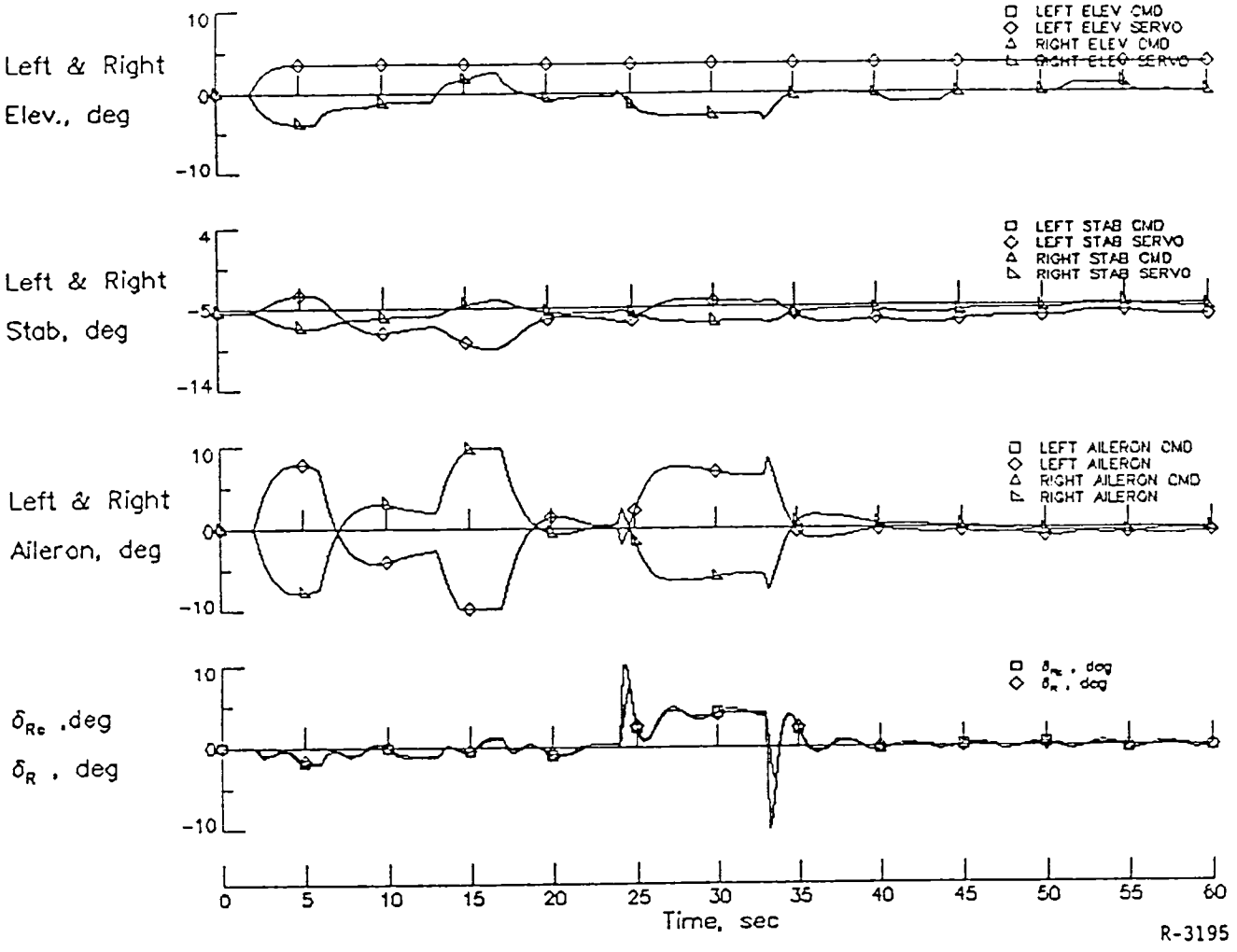

Figure 7-3. Control Usage for LE Failure (No Recon)

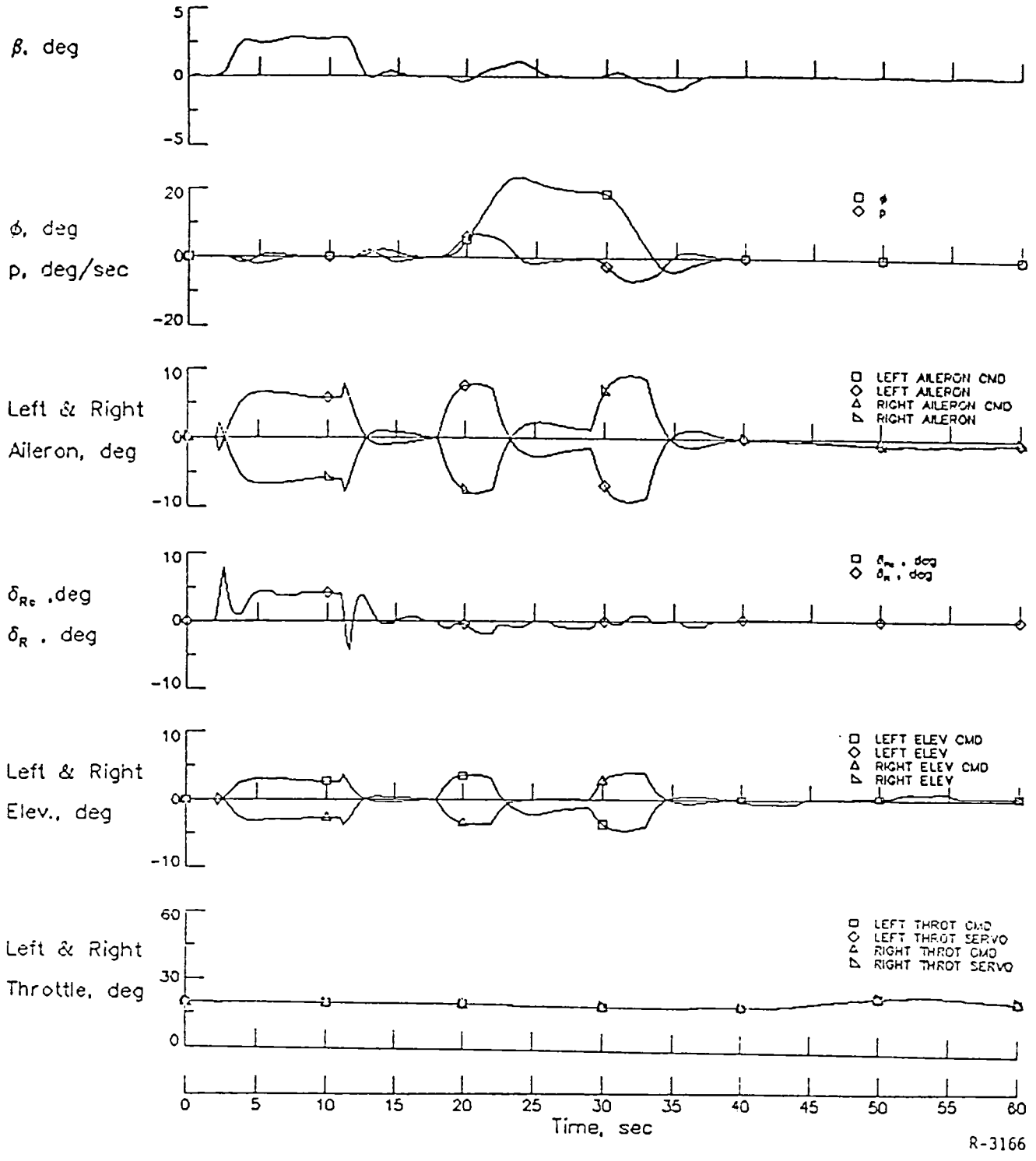

Figure 7-4. Normal Response

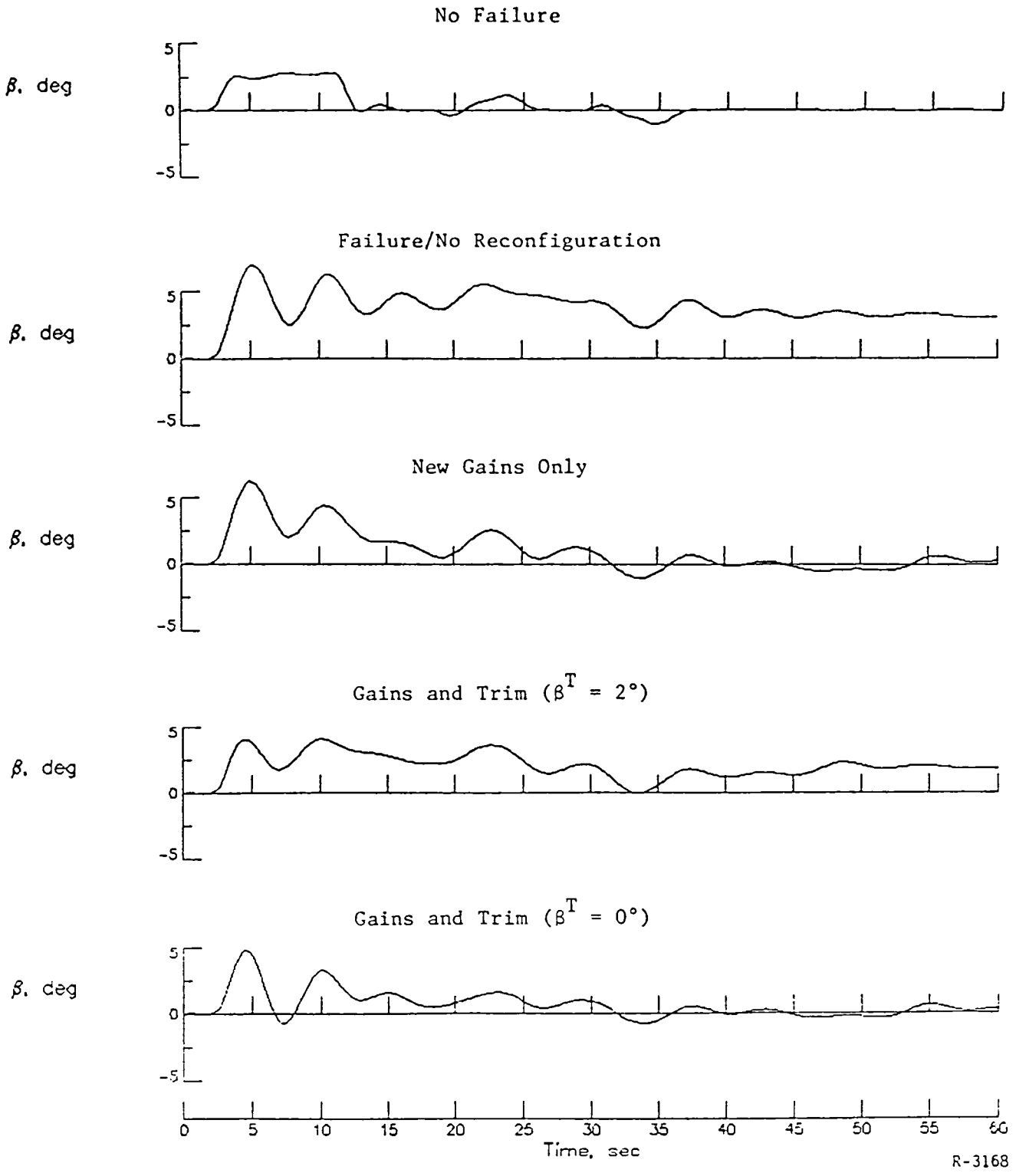

Figure 7-5. Rudder Stuck at 7 Degrees - β Responses

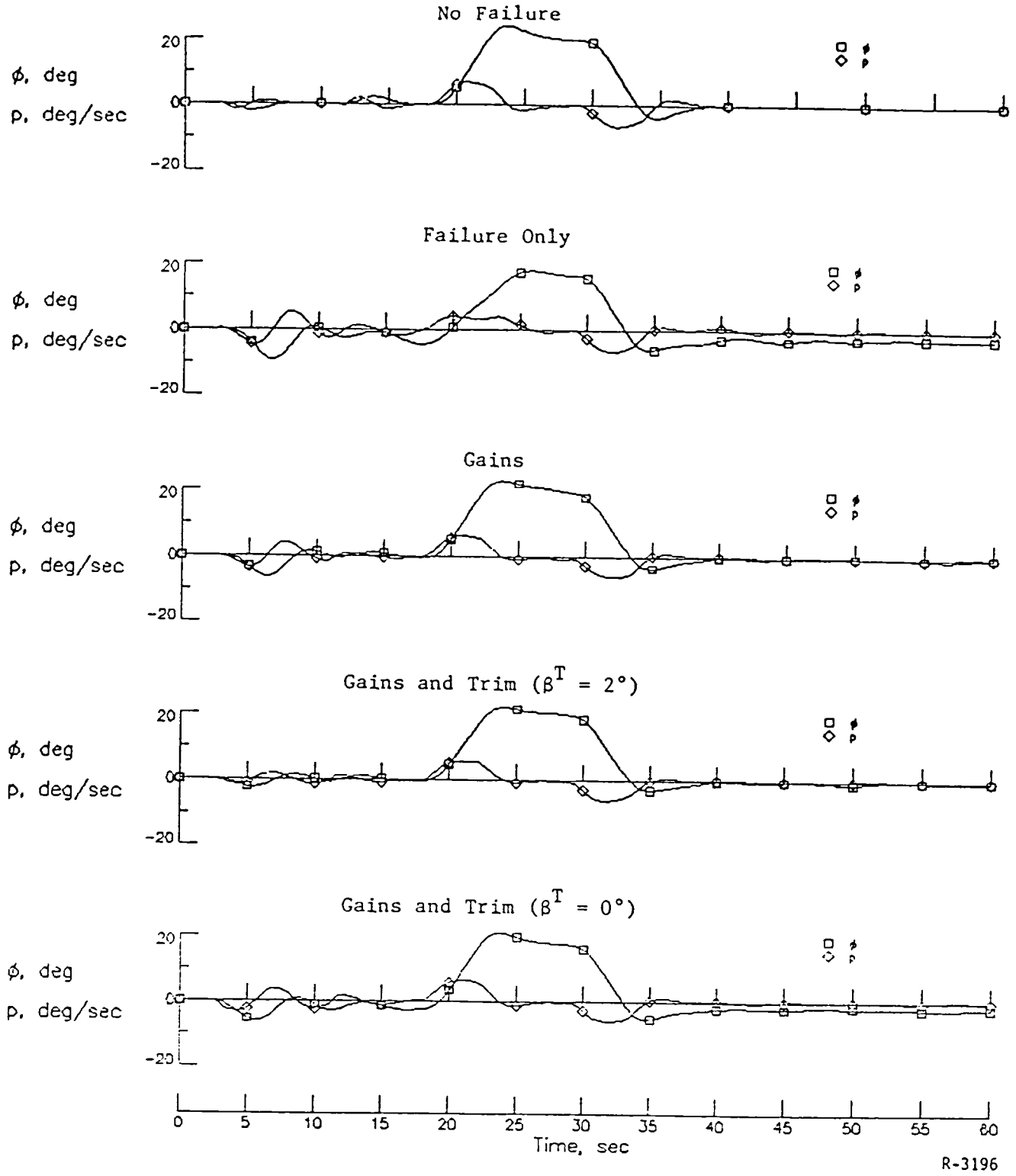

Figure 7-6. Rudder Stuck at 7 Degrees - Bank Responses

saturation and presumably result in much improved performance. When the redesigned feedback control gains are employed, we see that, although the dutch roll oscillations are still not adequately damped (as expected from Section 6 analyses), β is eventually reduced to near zero. During the bank maneuver, coordination is not maintained as desired, but the roll response is much improved due to the fact that the ailerons no longer saturate. This is because the redesigned control law makes greater use of differential elevator and stabilator in rolling the aircraft to compensate for the lost rudder. When we employ a feedforward trim (implemented at the time of failure assuming perfect FDI) we see small changes in the β and ϕ responses. However, the control usage is drastically altered, in general, keeping the stabilators and elevators further from their limits and making more use of differential throttle to compensate for the yawing moment induced by the stuck rudder. Note that two trim cases were examined. In the first case, β was constrained as described in subsection 6.3 whereas in the second case, $\beta = 0$ was added as a condition for feasible trim. The trim solution in both cases was feasible (zero error) however, it is clear that the control usage is drastically different in these two cases. Finally, Fig. 7-7 shows the throttle responses for the various test cases. From this figure it is clear that the (steady state) reduction in β error following a failure is due to the increased use of differential throttle controls in the reconfigured cases.

Figure 7-8 through 7-13 deal with a stabilator runaway failure occurring during the normal landing approach (no command generation). In each of these cases, both stabilator panels are slewed to their negative limits (trailing edge up) at about $t = 3$ seconds. Also, we employed elevator travel limits of ± 15 degrees (instead of ± 20 degree limits assumed in other runs). Figure 7-8

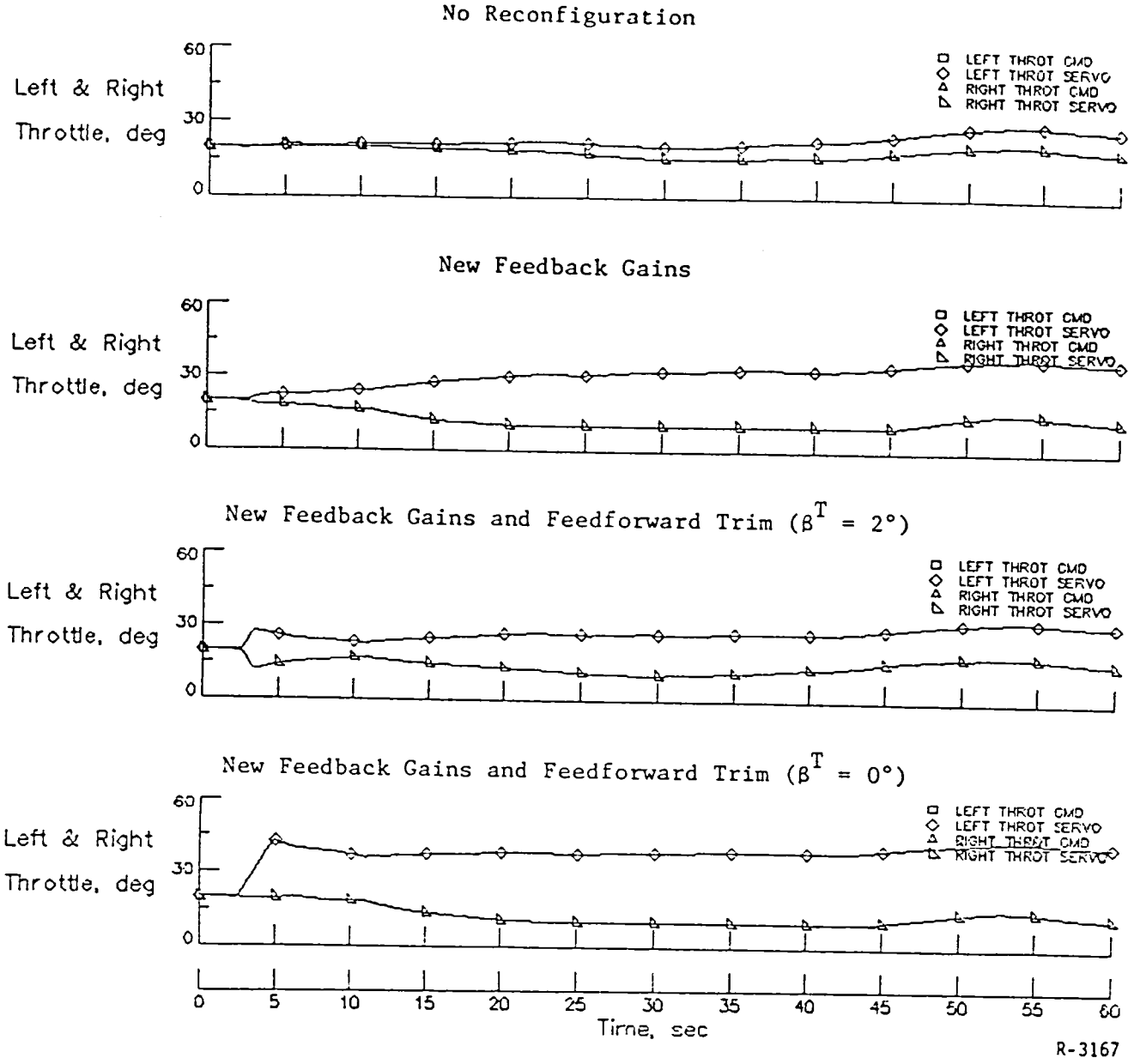

Figure 7-7. Rudder Stuck at 7 Degrees - Throttle Responses

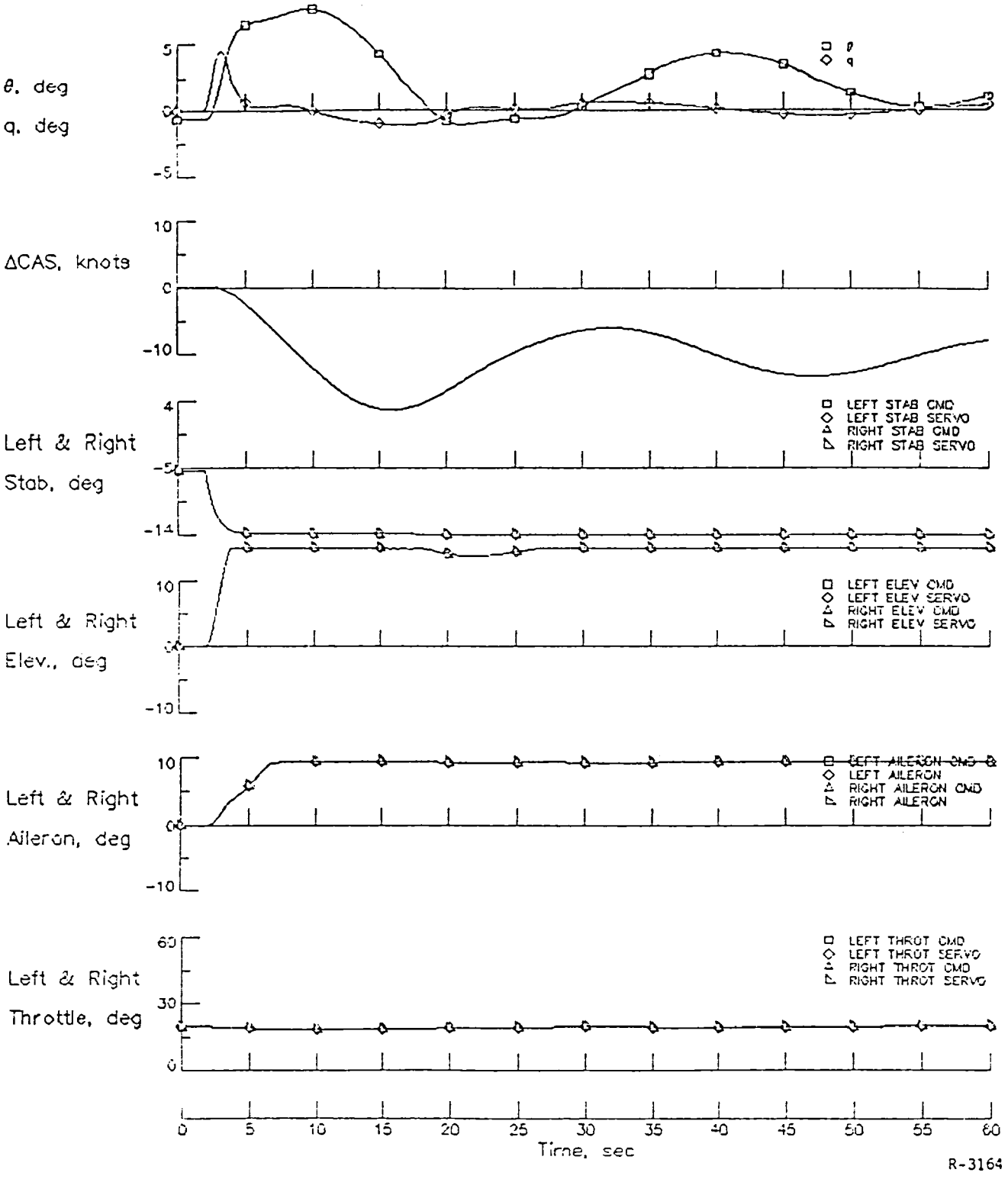

Figure 7-8. Stabilator Runaway - No Reconfiguration

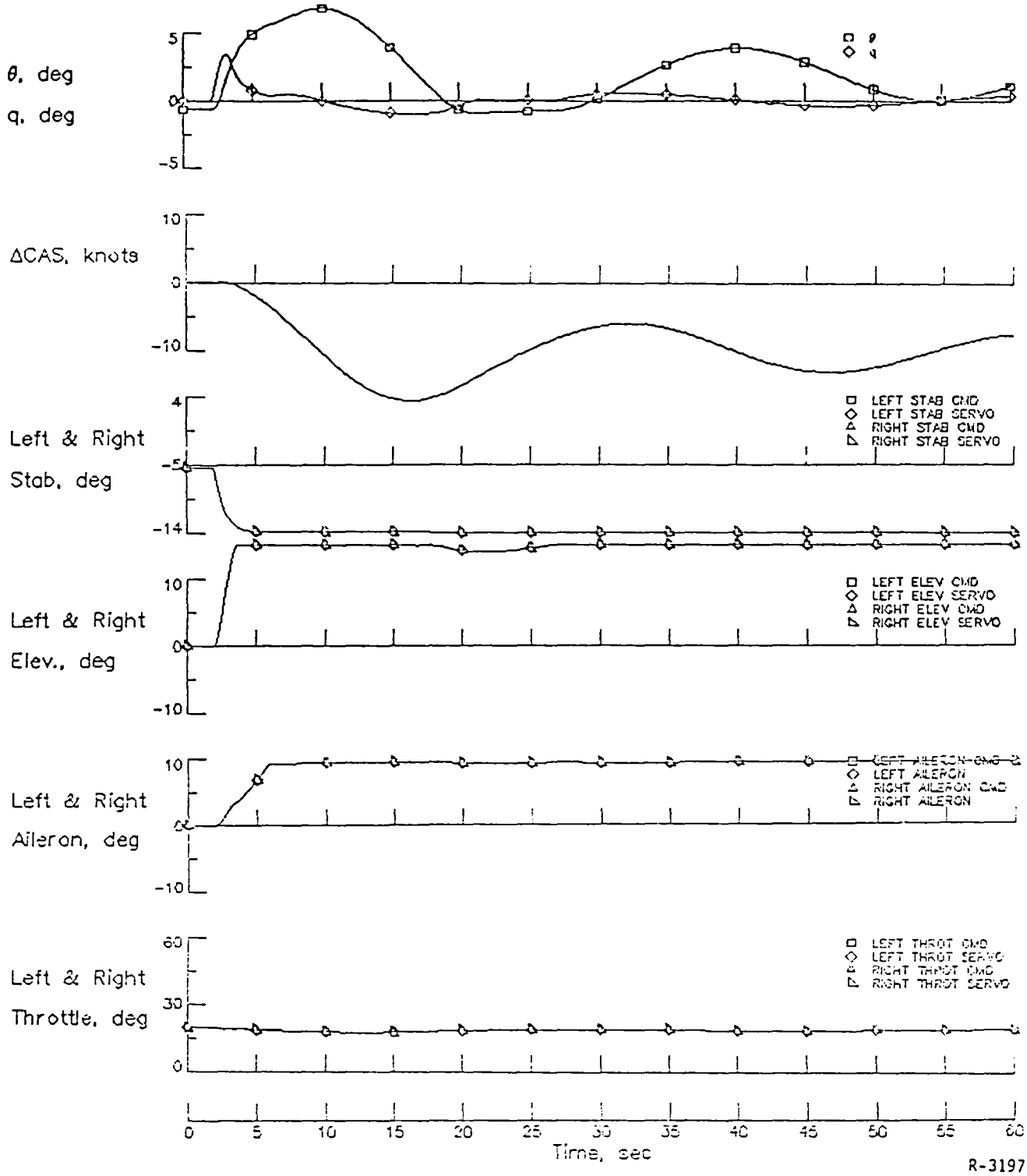

Figure 7-9. Stabilator Runaway - Gains Only

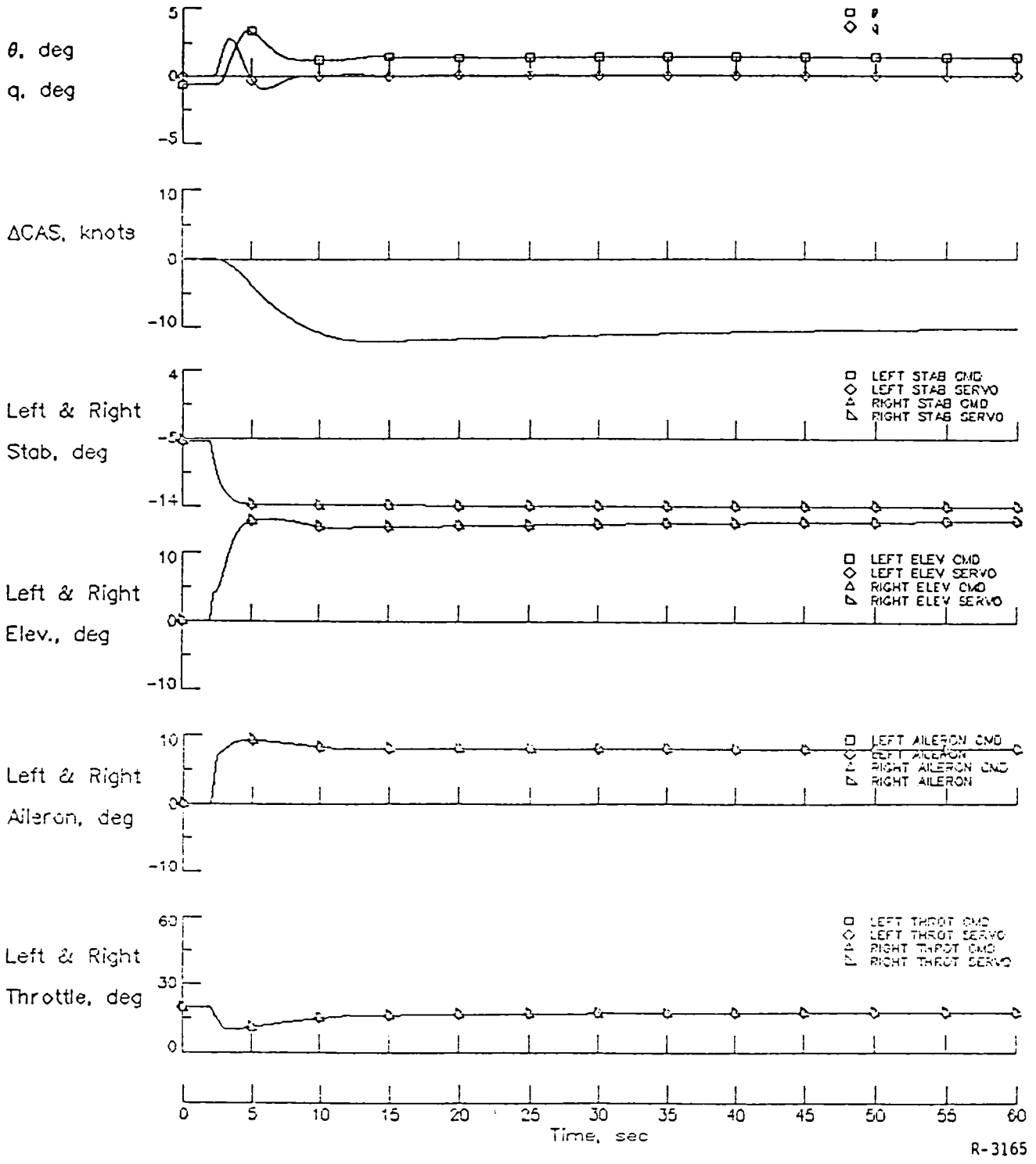

Figure 7-10. Stabilator Runaway - Gains and Trim

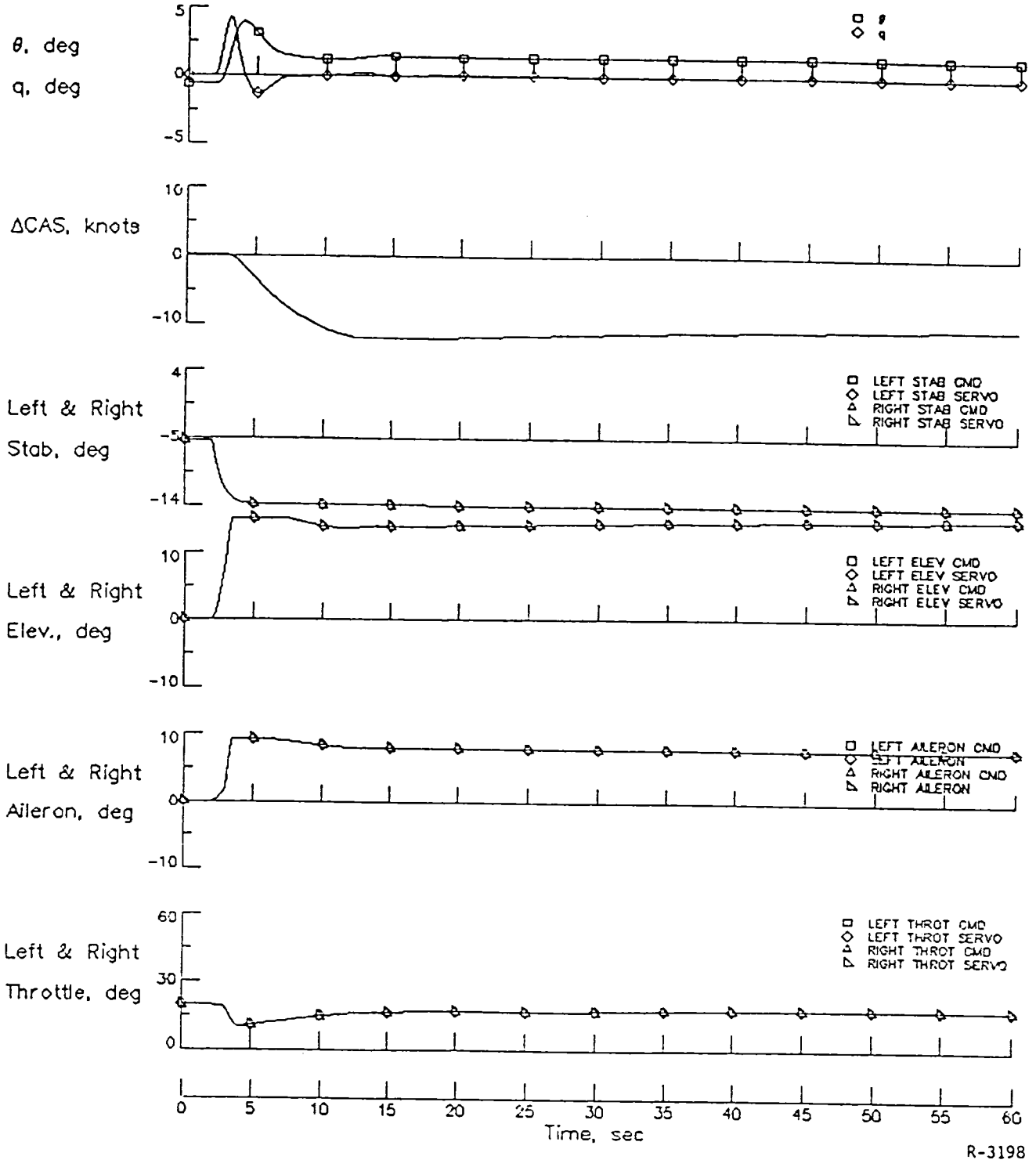

Figure 7-11. Stabilator Runaway - Gains and Trim Delayed by 1 Sec

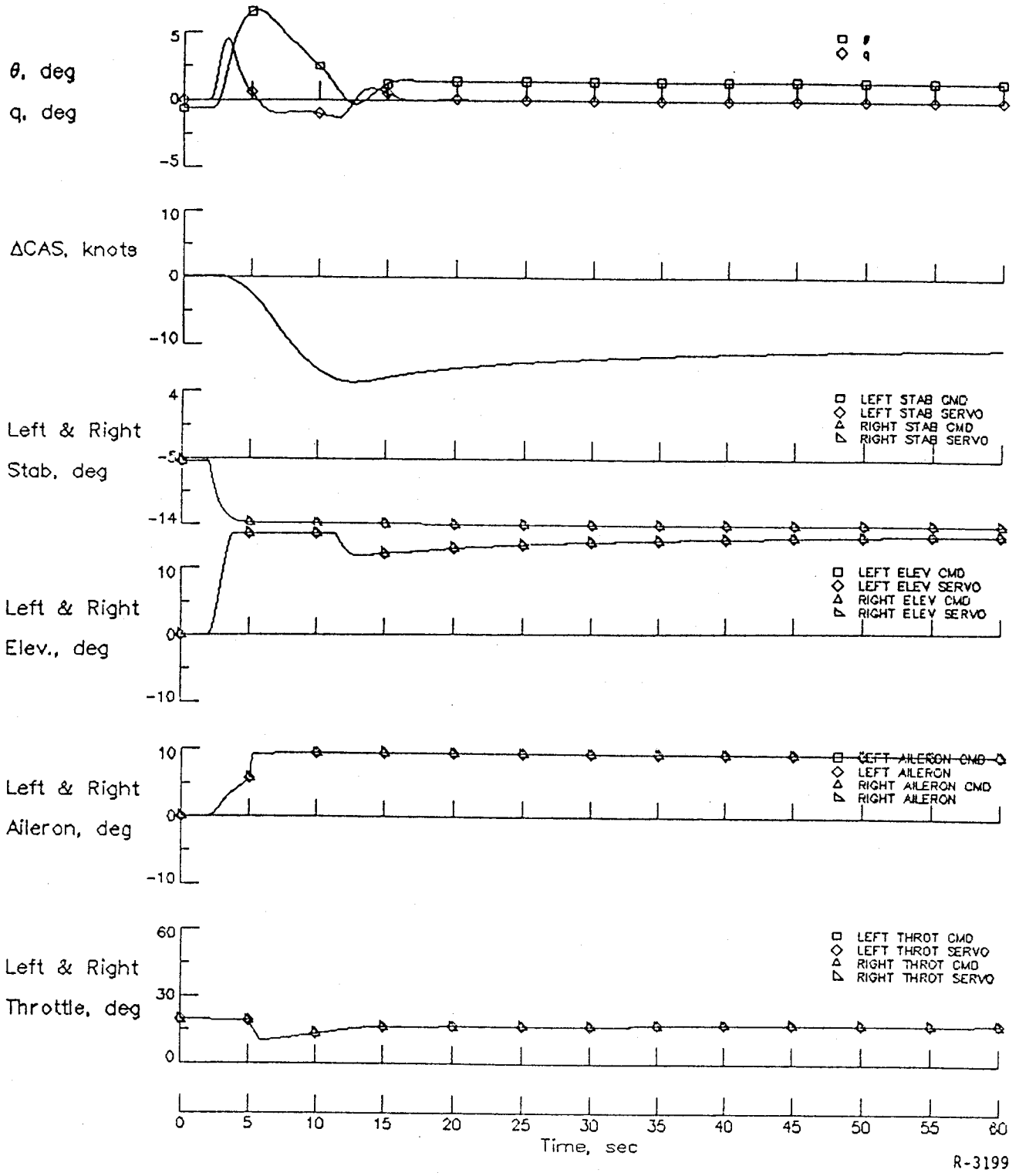

Figure 7-12. Stabilator Runaway - Gains and Trim Delayed by 3 Sec

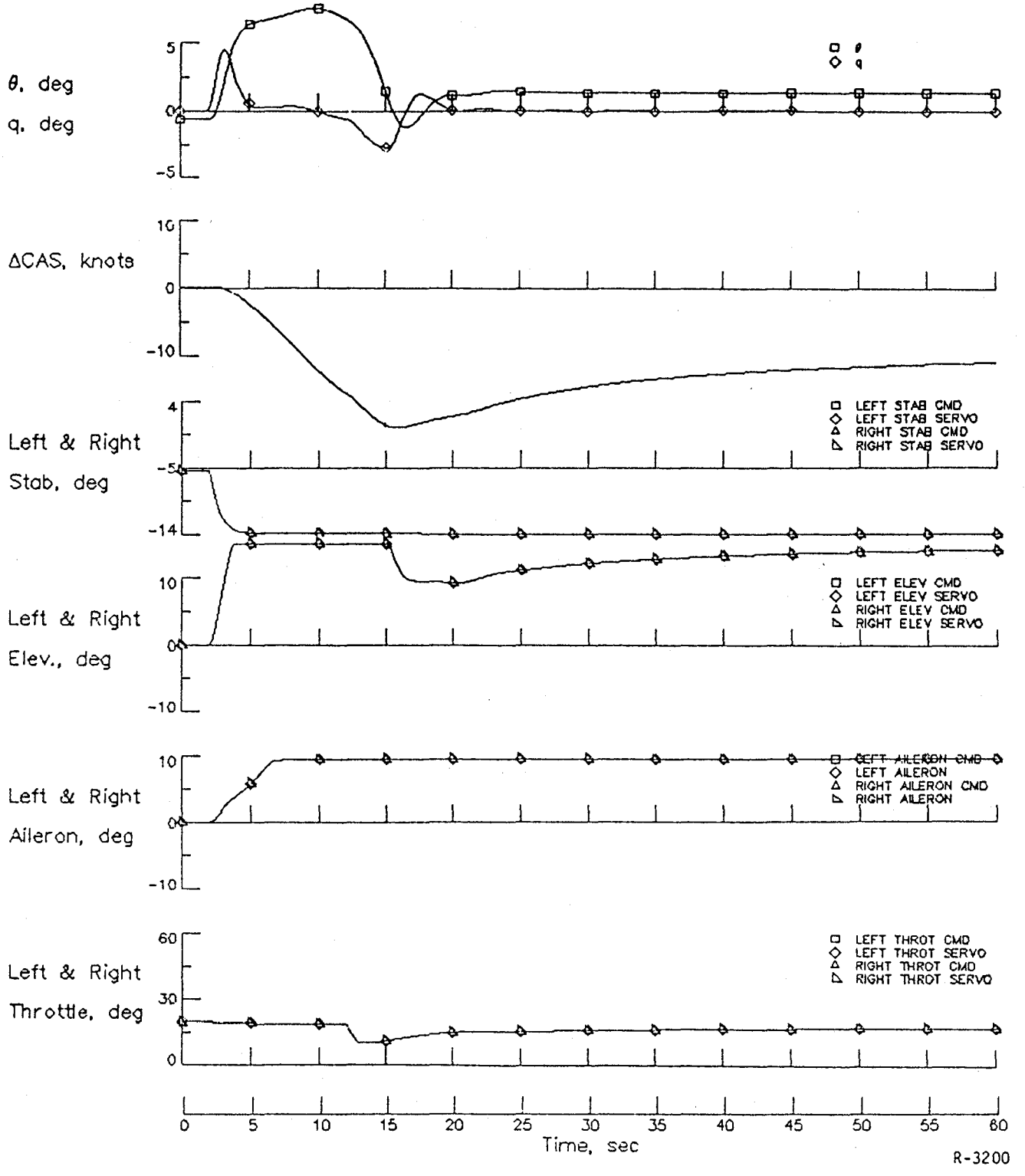

Figure 7-13. Stabilator Runaway - Gains and Trim Delayed by 10 Sec

shows various responses to the failure with no reconfiguration. A very high pitch attitude (θ) is reached before it begins decreasing with what appears to be a stable phugoid oscillation. The high pitch attitude is accompanied by a reduction of almost 20 knots in airspeed. This reduction comes very close to the stall speed of the aircraft and at that time both elevators and both ailerons are at their travel limits. No use of throttle is made because of the "conflicting" (at least in terms of throttle usage in the nominal control system) elements of positive pitch error and negative airspeed error. The use of redesigned feedback control gains by themselves provides little help in this case as shown in Fig. 7-9. The problem is that, by design, we can expect no faster responses from the redesigned control law (the bandwidth limits of the original design are maintained) and all control elements, except the throttle, reach their saturation limits fairly quickly. The throttle cannot, of course, be used alone to recover from the dangerous near stall condition and is therefore not used in the redesigned control law. When we add the feedforward trim to the RFCS solution, a very reasonable recovery is achieved. This is shown in Fig. 7-10. Notice that while the elevators saturate in this case too (the trim solution is infeasible), the increased use of elevators, ailerons and a throttle reduction, keeps the pitch attitude error from getting very large. The velocity is kept large enough to easily avoid a stall by its regulation to a new trim value of -11.8 knots below the old trim value. Notice that the steady-state pitch attitude and velocity are different than the unfailed trim case but that the flight path angle (γ = -3) degrees) is maintained reasonably well.

In Figs. 7-11 through 7-12, we investigated the effect of FDI delay by varying the time at which reconfiguration (application of redesigned feedback

control gains and feedforward trim) takes place. Figure 7-11 contains a 1 second delay (before any of the control elements saturate), Fig. 7-12 contains a 3 second delay (after the elevators but before the ailerons saturate) and Fig. 7-13 contains a 10 second delay (after both ailerons and elevators). As expected, recovery performance degrades with increasing FDI delay, however, in all cases, performance is better than without reconfiguration. Even with a 10 second delay (Fig. 7-13), application of the feedforward trim solution causes the throttle to be initially reduced which results in reduction of the pitch error before the airspeed is decreased too much. The change of sign in the pitch error then causes the elevator to come out of saturation to recover the new pitch trim while the throttle is being increased to recover the new airspeed trim. This nonstandard combination of control use to avoid stalling the aircraft during a stabilator runaway, may be an obvious solution in retrospect. However, the ability to have this solution available, automatically, to any pilot is an exciting advance in the potential for increased aviation safety.

In the last set of tests, we examined the impact of uncertainty in the FDI algorithm. Figure 7-14 shows various responses to a left elevator failure (see Figs. 7-1 through 7-3 for baseline cases) for three different "uncertainty" cases. The first plot in each series corresponds to an FDI misclassification in which the left and right ailerons are declared failed instead of the left elevator. We then implement only the feedback control gains corresponding to a left and right aileron failure. In the second plot of each series we assume a naive method of accounting for FDI uncertainty. In this case, since there is, by assumption, confusion between three possible failure modes (left elevator and left and right aileron) we use the feedback gains corresponding to

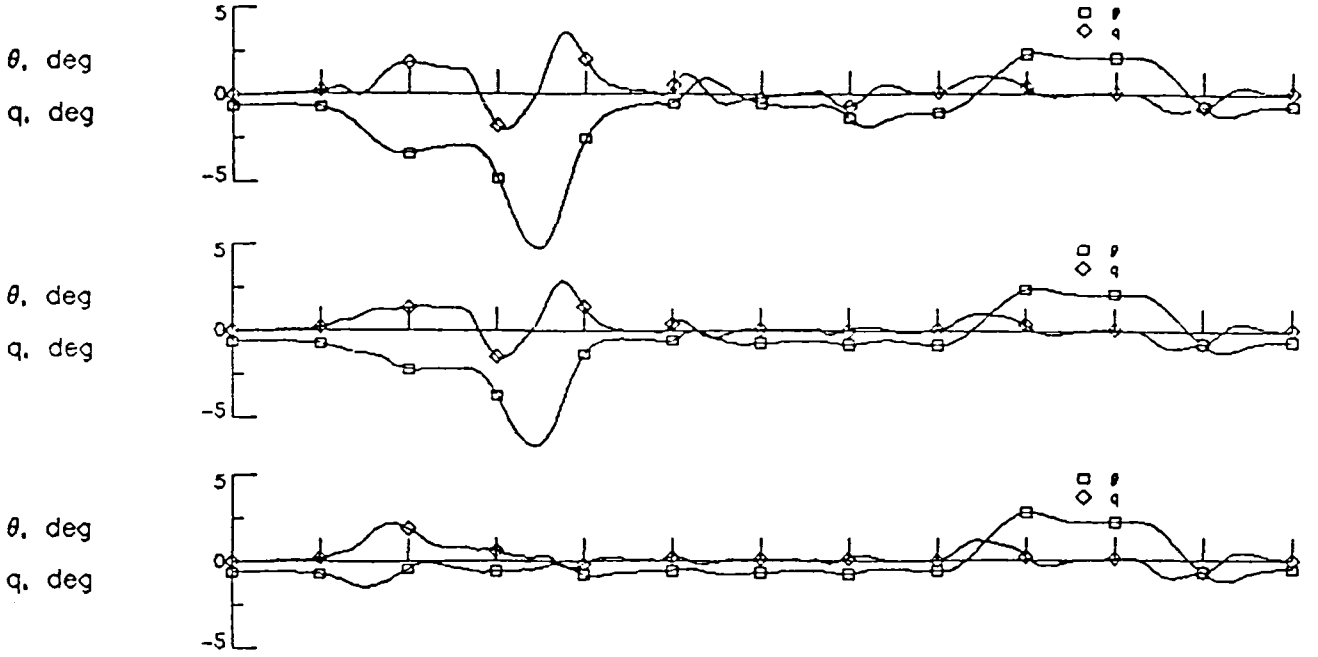

Figure 7-14a. Pitch Responses - Uncertain FDI

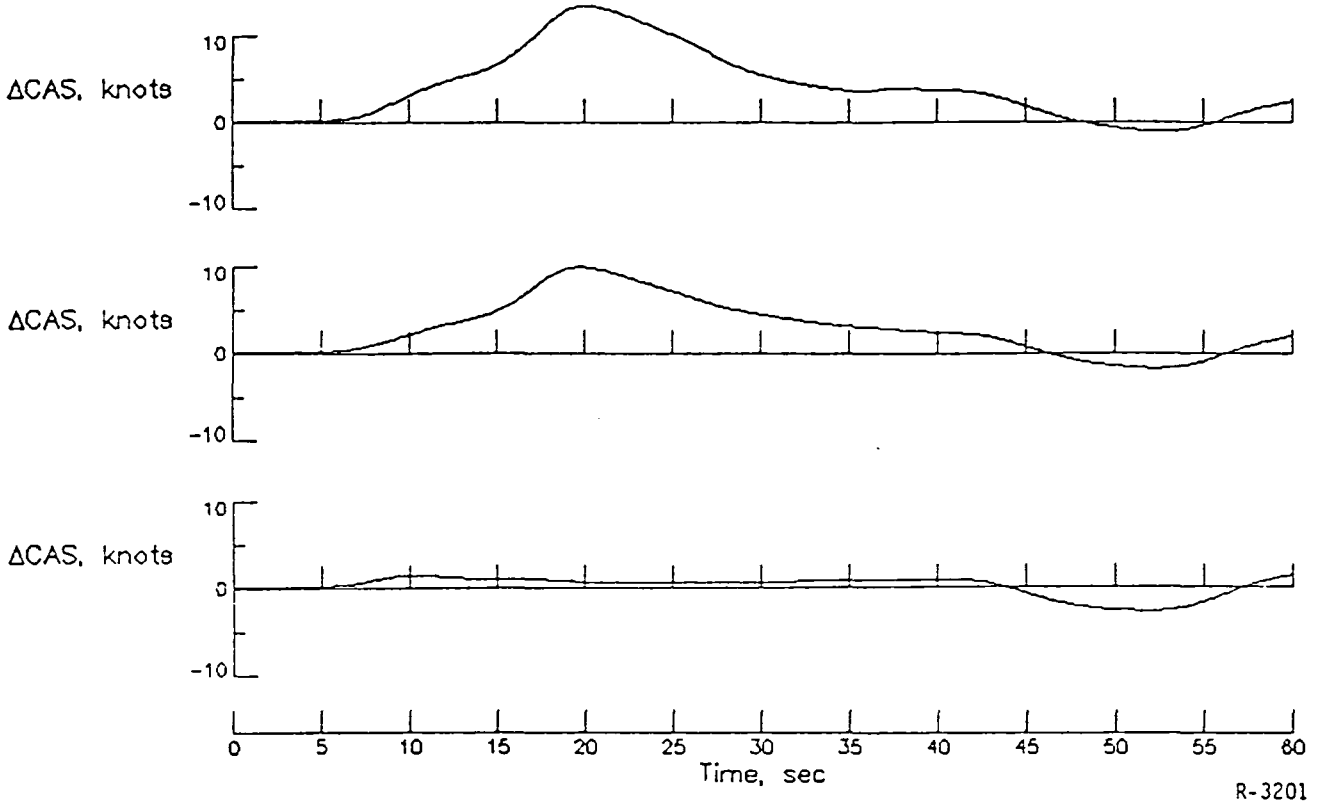

Figure 7-14b. ΔCAS Responses - Uncertain FDI

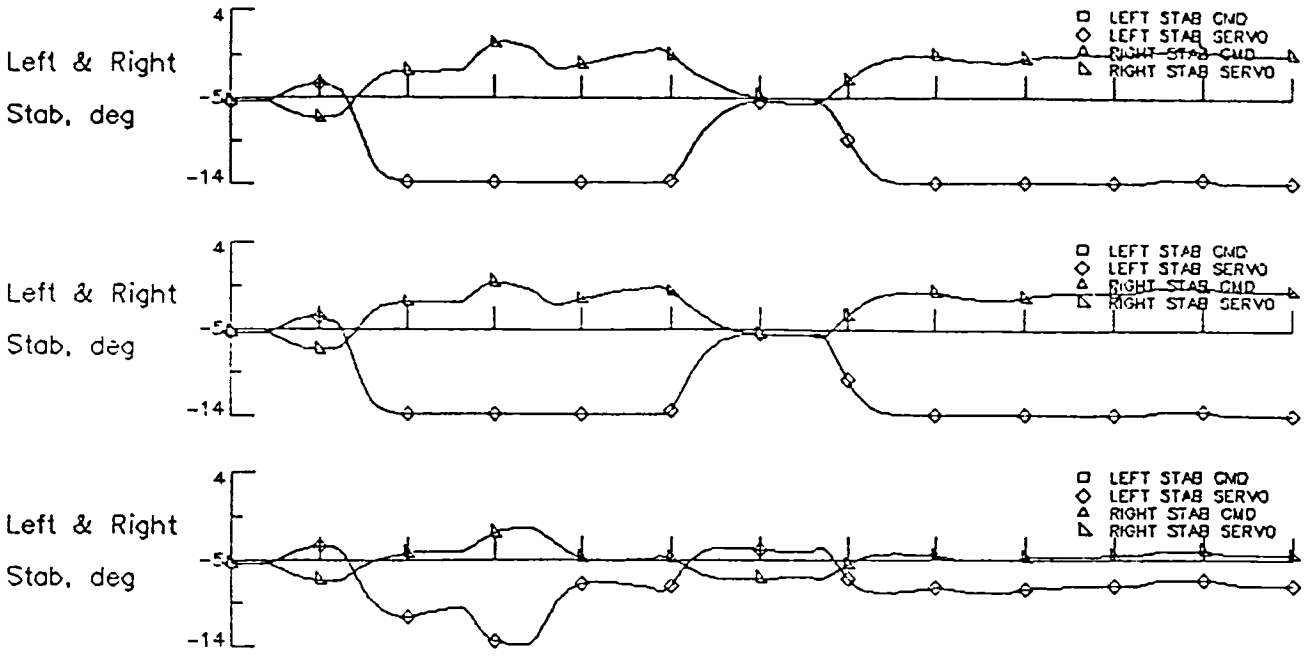

Figure 7-14c. Stabilator Responses - Uncertain FDI

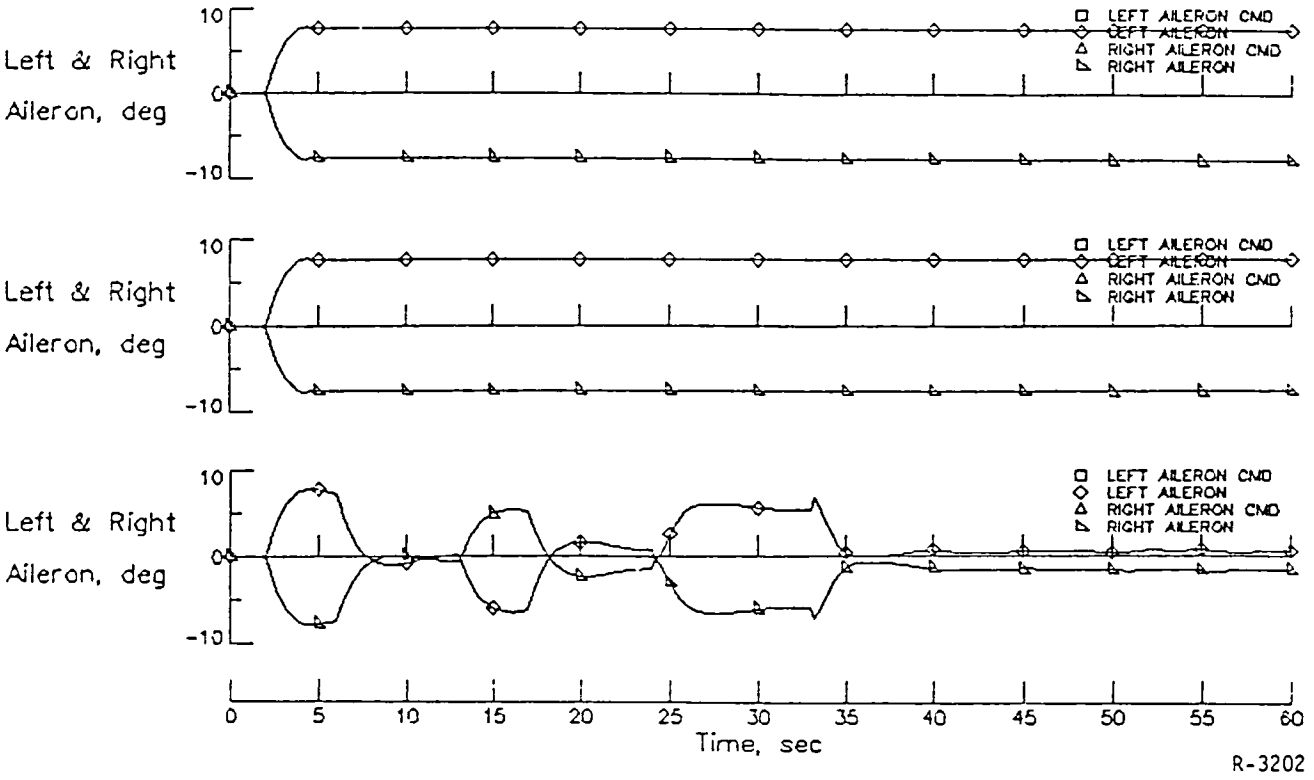

Figure 7-14d. Aileron Responses - Uncertain FDI

failure of all three surfaces. Finally, in the last plot of each series, we examine the efficacy of utilizing knowledge of uncertainty in the redesign method (see Section 4). In the first two cases, the important responses are fairly wild. This is, in part, due to the fact that we have three surfaces which are not being used for both of these cases. In the last case, we assumed the following:

1. The probability that the left elevator is failed (stuck) p_6, is .5,

2. The probability that the left or right ailerons are failed (stuck), p_7 and p_8, are .25,

3. The expected value of the true B matrix is B_o (the unfailed B matrix; note that this is formally inconsistent with the assumptions 1 and 2, but can be justified on other grounds). These three assumptions allow us to form the required statistics described in Section 4 for computing a redesigned control law. In particular, we have (see Eqs. 4-17 and 4-19),

$$B_f = B_o$$

$$\beta_{kilj} = \begin{cases} 0 & \text{for } j \neq i \\ \alpha_j^2 \cdot B_o{}^{lj} \cdot B_o{}^{kj} & \text{otherwise} \end{cases}$$

$$\alpha_j = p_j(1-p_j)$$

where j is the index corresponding to the potentially failed surfaces.

The resulting performance in the last case is clearly superior to either of the previous cases. This is due to that fact that all potentially failed surfaces have nonzero gains (as expected). Comparing this case to Figs. 7-1 and 7-3, we see that the command responses are virtually the same as when no redesign takes place, however, the control use in achieving these responses

is quite different. It is anticipated that in more severe cases (e.g., for unstable aircraft) that the use of the knowledge about FDI uncertainty in the control redesign algorithm would show more dramatic performance improvements as compared to the no-redesign case as well as in comparison to FDI misclassification cases.

SECTION 8

CONCLUSIONS

This report has presented the results of the last year in a two-year effort to develop an automatic control redesign procedure for restructurable aircraft control. During the first year of the project, a redesign technique was developed for the feedback portion of the flight control system. During the second year, this system was tested and integrated with a feedforward system for automatically trimming the aircraft to remove the known portion of the failure-induced force and moment imbalances. The complete system was tested on a nonlinear simulation of a Boeing 737 aircraft that was modified to permit individual control surface motion.

Three important general results were observed. First, the nontraditional use of standard control surfaces in a nominal feedback control system to spread control authority amongst many redundant (in terms of the forces and moments which can be produced) control elements provided a significant amount of fault tolerance without any use of restructuring techniques. In most single element failures, "recovery" was automatically achieved and little loss in command response performance was observed. A stuck rudder failure provided the most challenging single element failure situation since it is used extensively for damping the dutch roll mode and since only weak side forces are produced by the other control elements.

Secondly, the use of new feedback gains alone (from the feedback control redesign procedure but without retrimming) following a failure can provide significantly improved recovery as long as the control elements remain within their travel limits and as long as uncertainty about the failure identity is properly handled. This effect is particularly evident in the stuck rudder failure case. When control elements reach their travel limits during a failure, performance generally degrades as expected. In failure cases where the nominal control system performed well by itself, the application of redesigned feedback gains resulted in little, if any, improvement.

Finally, the use of the feedforward trim solution, in conjunction with redesigned feedback gains, allows recovery to take place even when significant control saturation occurs. This is generally due to the fact that servo errors resulting from a failure are quickly reduced by application of the feedforward trim solution. Since the redesigned control system stabilizes the aircraft and the servo errors remain small due to the feedforward trim, recovery is generally achieved even when many control elements reach and remain at their travel limits.

In summary, the results to date indicate that the combination of a robust nominal controller with an on-line redesign system can accommodate a variety of failures and result in a safe stable aircraft. The major program objective of developing the control design components of a restructurable control system have been met.

8.1 RECOMMENDATIONS FOR FUTURE WORK

Several steps remain, however, before a complete restructuring system can be implemented. The first is the integration of the redesign system with

a Failure Detection and Identification (FDI) system. This integration is the subject of the next phase of this project.

Other issues which need to be addressed in the future include

1. The need to model the post-failure aircraft,
2. The need to design the nominal controller, the FDI system, and the redesign sysem as a coordinated, fault tolerant whole,
3. The need to integrate the fault tolerant control system (including redesign components) with the rest of the aircraft design process, and
4. The need to verify emergency performance.

The first issue refers to the need for post-failure aircraft models in the redesign system. Although this system is designed to work with uncertain aircraft models, and could therefore use stored approximate models for a variety of anticipated failures, it can also take advantage of the better information which might be available after failure from the use of parameter identification procedures. The concepts used to detect and identify the failures, explicitly address many problems which are inherent to identification procedures. These procedures should also be useful for estimating the failure effects as well.

The second issue results from the differing abilities of each part of the fault tolerant control system for handling different failures. For example, those failures which can be handled by passive robustness are likely to be the hardest to detect and identify, since the aircraft performance will not be seriously affected. Conversely, those failures which result in serious performance degradation are also the easiest to find quickly. Such concerns point to the need to develop a methodology for designing all the fault tolerant controller components in a coordinated manner, so that failures not covered by one part of the system can be accommodated by another.

Third, the incorporation of a restructurable control system in an aircraft must be integrated with the rest of the aircraft design. For example, if differential elevator control is incorporated in an aircraft design for emergency use in restructuring, then the aircraft structure must be designed to accommodate it. This leads to a conflict between designing for normal operation and building in margins for emergency use. Although our restructuring system can accommodate limits on control authority (much as it handles bandwidth or travel limitations), the aircraft designer will need to trade off the cost of such limits in terms of failure coverage against the cost in structure. Tools to accomplish this multidisciplinary trade-off will be needed.

Finally, the restructurable control system will need to be flight tested to investigate its performance under real-world conditions. An important issue in such testing (and in subsequent validation of production designs) is the simulation of failures and their effects. Such testing under realistic conditions is essential to demonstrate the technology and bring it out of the research stage.

REFERENCES

1. Looze, D.P., S. Krolewski, J.L. Weiss, N.M. Barrett, and J.S. Eterno, "Automatic Control Design Procedures for Restructurable Aircraft Control," NASA CR-172489, Contract NAS1-17411, January 1985.

2. McMahan, J., "Flight 1080," Air Line Pilot, July 1978.

3. "National Transportation Safety Board Accident Report of the American Airlines DC10 Crash at Chicago - O'Hare International Airport, May 25, 1979, NTSB-AAR-79-17, December 21, 1979.

4. Weiss, J.L., "A Decentralized Approach to Design of Robust Failure Detection and Isolation (FDI) Algorithms," ALPHATECH Technical Memorandum TM-186, July 1985.

5. Weiss, J.L., J.M. Stifel, and K.S. Govindaraj, "Flight Test Results of a Control Element FDI Algorithm," Presented at NAECON '86, Dayton, OH.

6. Deckert, J.C., M.N. Desai, J.J. Deyst, and A.S. Willsky, "F8-DFBW Failure Identification Using Analytic Redundancy," IEEE Transactions on Automatic Control, Vol. AC-22, No. 5, October 1977, pp. 795-803.

7. Deckert, J.C., "Flight Tests Results for the F-8 Digital Fly-by-Wire Aircraft Control Sensor Analytic Redundancy Management Technique," Proceedings of the AIAA Guidance and Control Conference, Albuquerque, New Mexico, August 1981, pp. 491-499.

8. Pattipati, K.R., A.S. Willsky, J.C. Deckert, J.S. Eterno, and J.L. Weiss, "A Design Methodology for Robust Failure Detection and Isolation," 1984 American Control Conference, San Diego, CA, June 1984.

9. Weiss, J.L., A.S. Willsky, K.R. Pattipati, and J.S. Eterno, "Application of FDI Metrics to Detection and Isolation of Sensor Failures in Turbine Engines," 1985 American Control Conference, San Diego, CA, June 1984.

10. Willsky, A.S., "A Survey of Design Methods for Failure Detection in Dynamic Systems," Automatica, Vol. 12, 1976, pp. 601-611; also in AGARDograph No. 224 on "Integrity in Electronic Flight Control Systems."

11. Lou, X.-C., A.S. Willsky, and G.C. Verghese, "Failure Detection with Uncertain Models," Preprint Sept. 1982, invited paper for 1983 American Control Conference, June 1983.

12. Weiss, J.L., A.S. Willsky, D.P. Looze, J.T. Crawford, and R.R. Huber, "Detection and Isolation of Control Surface Effectiveness Failures in High Performance Aircraft," in IEEE Proceedings of NAECON, May 1985.

13. Gilmore, J.P., and R.A. McKern, "A Redundant Strapdown Inertial Reference Unit (SIRU)," J. Spacecr. Rockets, January 1972.

14. Daly, K., et al., "Generalized Likelihood Test for FDI in Redundant Sensor Configurations," J. Guidance and Control, Vol. 2, No. 1, January - February 1979.

15. Eterno, J.S., J.L. Weiss, D.P. Looze, and A.S. Willsky, "Design Issues for Fault Tolerant-Restructurable Aircraft Control," ALPHATECH Technical Paper TP-225, presented at the 1985 Conference on Decision and Control, Fort Lauderdale, FL, August 1985.

16. Eterno, J.S., J.L. Weiss, D.P. Looze, and A.S. Willsky, "Restructurable Control of High Performance Aircraft," ALPHATECH Technical Paper TP-227, Presented at the 1985 AIAA Guidance and Control Conference, Snowmass, CO, August 1985.

17. Looze, D.P., J.L. Weiss, J.S. Eterno, and N.M. Barrett, "An Automatic Redesign Approach for Restructurable Control Systems," ALPHATECH Technical Paper TP-205-1, IEEE Control Systems Magazine, May 1985.

18. Weiss, J.L. and D.P. Looze, "Further Development of an Automatic Control Design Procedure for Restructurable Aircraft Control, ALPHATECH Technical Report TR-249, Second Quarterly Report, June 1985.

19. Gill, P. et al., Practical Optimization, Academic Press, New York, 1981.

20. Luenberger, D., Introduction to Linear and Nonlinear Programming, Addison-Wesley, Reading, MA, 1973.

21. Huber, R. and B. McCullough, "Self-Repairing Flight Control Systems, Society of Automotive Engineers, Paper #SAE-841552, presented at Aerospace Congress and Exposition, Long Beach, CA., October 1984.

22. "Self-Repairing Digital Flight Control System, Contract F33615-80-C-3100, Final Report, General Electric, July 1984.

23. Athans, M., "The Role and Use of the Stochastic Linear-Quadratic-Gaussian Problem in Control System Design," IEEE Transactions on Automatic Control, Vol. AC-16, December 1971, pp. 529-552.

24. Doyle, J.C. and G. Stein, "Multivariable Feedback Design: Concepts for a Classical/Modern Synthesis," IEEE Transactions on Automatic Control, Vol. AC-26, No. 1, February 1981.

25. Stein, G. and M. Athans, "The LQG/LTR Procedure for Multivariable Feedback Control Design," submitted to IEEE Transactions on Automatic Control.

26. Kalman, R.E., "When is a Linear Control System Optimal?" Journal of Basic Engineering, Transactions of ASME, Series D, Vol. 86, March 1984.

27. Horowitz, I.M., Synthesis of Feedback Systems, Academic Press, New York, 1963.

28. Cruz, J.B., J.S. Freudenberg, and D.P. Looze, "A Relationship Between Sensitivity and Stability for Multivariable Feedback Systems," IEEE Transactions on Automatic Control, Vol. AC-26, No. 1, February 1981.

29. Safonov, M.G., A.J. Laub, and G.L. Hartman, "Feedback Properties of Multivariable Systems: The Role and Use of the Return Difference Matrix," IEEE Transactions on Automatic Control, Vol. AC-26, No. 1, February 1981.

30. Bode, H.W., Network Analysis and Feedback Amplifier Design, Van Nostrand, Princeton, NJ, 1945.

31. Horowitz, I.M., Synthesis of Feedback Systems, Academic Press, New York, 1963.

32. Ryneski, E.G. and K.S. Govindaraj, "Control Concepts for the Alleviation of Wind Gusts," NASA CR-166022, Contract NAS1-16691, July 1982.

33. Etkin, B., Dynamics of Atmospheric Flight, Wiley and Sons, Inc., New York, 1947.

34. Klema, V.C. and A.J. Laub, "The Singular Value Decomposition: Its Computation and Some Applications," IEEE.

Standard Bibliographic Page

1. Report No.	2. Government Accession No.	3. Recipient's Catalog No.
NASA CR-178064		

4. Title and Subtitle	5. Report Date
Initial Design and Evaluation of Automatic Restructurable Flight Control System Concepts	June 1986
	6. Performing Organization Code
7. Author(s)	8. Performing Organization Report No.
J.L. Weiss, D.P. Looze, J.S. Eterno, D.B. Grunberg	TR-269-1
9. Performing Organization Name and Address	10. Work Unit No.
ALPHATECH, Inc. 2 Burlington Executive Center 111 Middlesex Turnpike Burlington, MA 01803	11. Contract or Grant No. NAS1-17411
12. Sponsoring Agency Name and Address	13. Type of Report and Period Covered
NASA-Langley Research Center Hampton, VA 23665	Contractor Rpt 11/85-11/86
	14. Sponsoring Agency Code

15. Supplementary Notes

Annual Report

16. Abstract

This report presents the results of a two-year effort sponsored by the NASA Langley Research Center under contract NAS1-17411 to develop automatic control design procedures for restructurable aircraft control systems. The restructurable aircraft control problem involves designing a fault tolerant control system which can accommodate a wide variety of unanticipated aircraft failures. Under NASA sponsorship, sorship, ALPHATECH has been developing and testing many of the technologies which make such a system possible. Future work under this contract will focus on developing a methodology for integrating these technologies and demonstration of a complete system.

17. Key Words (Suggested by Authors(s))	18. Distribution Statement
Fault Tolerant Control Reconfiguration	Unclassified-Unlimited

19. Security Classif.(of this report)	20. Security Classif.(of this page)	21. No. of Pages	22. Price
Unclassified	Unclassified	162	

For sale by the National Technical Information Service, Springfield, Virginia 22161

NASA Langley Form 63 (June 1985)